FINAL REPORT

DEVELOPMENT OF A PROTOTYPE OF AN ICE THERMAL ENERGY STORAGE WITH DIRECT CONTACT EVAPORATOR

TANONGKIAT KIATSIRIROAT

MAY 2001

FINAL REPORT

DEVELOPMENT OF A PROTOTYPE OF AN ICE THERMAL ENERGY STORAGE WITH DIRECT CONTACT EVAPORATOR

TANONGKIAT KIATSIRIROAT

MAY 2001

สำนักงานกองทุนสนับสนุนการวิจัย (สกว.)
ชั้น 14 อาคารเอสเอ็ม ทาวเวอร์
เลขที่ 979/17-21 ถนนพหลโยธิน แขวงสามเสนใน
เขตพญาไท กรุงเทพฯ 10400
โทร.298-0455 โทรสาร 298-0476
Home page : http://www.trf.or.th
E-mail : trf-info@trf.or.th

สัญญาเลขที่ BRG/5/2542

FINAL REPORT

DEVELOPMENT OF A PROTOTYPE OF AN ICE THERMAL ENERGY STORAGE WITH DIRECT CONTACT EVAPORATOR

Prof. Dr. TANONGKIAT KIATSIRIROAT,

DEPARTMENT OF MECHANICAL ENGINEERING

CHIANGMAI UNIVERSITY

Dr. ATIPOANG NUNTAPHAN,

SOUTH EAST ASIA CENTER FOR TRAINING IN ENERGY FOR DEVELOPMENT

ELECTRICITY GENERATING AUTHORITY OF THAILAND

THE THAILAND RESEARCH FUND

การพัฒนาต้นแบบระบบเก็บรักษาพลังงานในรูปน้ำแข็งโดยใช้อีวาปอเรเตอร์แบบสัมผัสโดยตรง

โดย ศาสตราจารย์ ทนงเกียรติ เกียรติศิริโรจน์
ภาควิชาวิศวกรรมเครื่องกล คณะวิศวกรรมศาสตร์ มหาวิทยาลัยเชียงใหม่

บทคัดย่อ

ในงานวิจัยนี้ ได้ทำการพัฒนาและสร้างชุดระบบเก็บรักษาพลังงานในรูปน้ำแข็งที่มีอีวาปอเรเตอร์แบบสัมผัสโดยตรง และใช้จริงในสำนักงานแห่งหนึ่งที่มหาวิทยาลัยเชียงใหม่ ระบบจะมีวงจรการทำงาน 2 ชุด ชุดหนึ่งคือวงจรทำน้ำเย็น และอีกชุดหนึ่งเป็นวงจรในการทำน้ำแข็ง การศึกษาจะดำเนินทำแบบจำลองของอุปกรณ์ต่างๆ ได้แก่ คอมเพรสเซอร์ คอนเดนเซอร์ วาล์วขยายตัว ชุดน้ำเย็น และอีวาปเรเตอร์แบบสัมผัสโดยตรง จากนั้นจะมีการจำลองการทำงานของระบบ ผลที่ได้พบว่าใกล้เคียงกับการทดลอง โดยมีความผิดพลาดไม่เกิน 5%

ผลจากการจำลองสถานการณ์การทำงาน พบว่าเงื่อนไขการทำงานที่เหมาะสมของวงจรทำน้ำเย็น ควรใช้อัตราการไหลของสารทำความเย็น 0.06 – 0.08 kg/s ที่ความเร็วรอบเต็มกำลังของคอมเพรสเซอร์ และในวงจรทำน้ำแข็ง อัตราการไหลจะเป็น 0.08 – 0.09 kg/s โดยความเร็วรอบคอมเพรสเซอร์ 9.5 rps ค่าสัมประสิทธิ์สมรรถนะของแต่ละวงจรจะมีค่าประมาณ 3.1

นอกจากนี้เพื่อนำไปประยุกต์ใช้ในระบบแบบ partial storage พบว่าขนาดของแต่ละงวดที่เหมาะสมในการใช้งาน ในแต่ละวงจรจะมีค่าเป็น 3.5 ใหม่ ของวงจรทำน้ำเย็น และ 14 kW ของระบบผลิตน้ำแข็ง 39.2% หาค่าความต้องการกำลังไฟฟ้าสูงสุดในช่วง on-peak สามารถลดลง และสามารถเลื่อนไปอยู่ในช่วง off-peak ค่าไฟฟ้า 32% สามารถประหยัดได้ เมื่อเทียบกับระบบทำน้ำเย็นทั่วไปในการปรับอากาศที่ไม่มีชุดทำน้ำแข็ง

คำสำคัญ ระบบเก็บรักษาพลังงานในรูปน้ำแข็ง การถ่ายเทความร้อนแบบสัมผัสโดยตรง
โมเดลคณิตศาสตร์ การจำลองการทำงานของระบบ

Development of a Prototype of an Ice Thermal Energy Storage with Direct Contact Evaporator

T. Kiatsiriroat

Department of Mechanical Engineering, Chiang Mai University

Abstract

In this research, an ice thermal energy storage with direct contact evaporator was built and has been studied by applying to an office located in Chiang Mai University, Chiang Mai, Thailand. The system consists of two cycles, basic chilled water cycle and ice storage cycle. From the collected experimental data, the mathematical models for main components composing of compressor, condenser, expansion valve, water chiller and direct contact evaporator are developed and the system simulation is created. Evidently from the results, the simulation agrees well with the experiment with 5% error.

The simulation shows the suitable conditions for operating the system at 0.06-0.08 kg/s of the refrigerant mass flow rate with full compressor speed for chilled water cycle and at 0.08-0.09 kg/s of the refrigerant mass flow rate at compressor speed of 9.5 rps. for ice storage cycle. The coefficient of performance (COP) of both cycles on these conditions is approximately 3.1.

The simulation also indicates that the partial storage design system that consists of 3.5 kW of chilled water system capacity and 14 kW of ice storage system capacity is the best combination. Under this appropriate operating condition, the system can shift 39.2% of peak electricity demand from on-peak to off-peak period. Therefore, 32% of electricity charge are saved comparing to those of the conventional system.

Keywords: Ice thermal energy storage system, direct contact heat transfer, mathematical model, system simulation

Executive Summary

A prototype of an air-conditioner with an ice thermal energy storage (ITES) has been designed and used to support the cooling load requirement about (18 kW max) of a selected office in Chiang Mai University. The unit consists of two main cycles, the chilled water cycle and the ITES cycle. The characteristics of the components for the chilled water cycle and the ITES cycle are as follows.

Characteristic of the components in the chilled water cycle.

Component	Characteristic
Compressor	Semi-hermetic reciprocating compressor for 5 TR air-conditioning system
Condenser	Shell and tube water cooled condenser for 5 TR air-conditioning system
Expansion valve	Manual control expansion valve for 5 TR air-conditioning system
Chiller	Shell and tube, water chiller for 5 TR air-conditioning system
Chilled water pump	Max. head: 40 m., Q_{max}. 40 L/min.0.37 kW
Filter dryer	Shell type for 5 TR air-conditioning system
Receiver	Liquid receiver for use with R12 for 5 TR air-conditioning system
Fan-coil unit	18 kW.

Characteristic of the components in the ice storage cycle.

Component	Characteristic
Compressor	Reciprocating compressor; open type for 2 TR air-conditioning system
Motor	Three phase induction motor, 5 HP, 4 Poles
Inverter	For use with 5 HP motor
Condenser	Air cool condenser, 7 kW
Expansion valve	Manual control expansion valve for 2 TR air-conditioning system
Direct contact evaporator	1000 liters. Steel cylinder tank
Accumulator	R12 accumulator for 2 TR air-conditioning system

Filter Dryer	Dryer for 7TR refrigeration system, steel take apart, shell type
Oil separator	For use with R12, for 2 TR air-conditioning system
Receiver	R12 liquid receiver, max. pressure 3.445 kPa., for 2 TR air-conditioning system

A direct contact evaporator-ice storage tank is used in the ITES cycle which is designed as a partial storage types. At the evaporator, R12 is injected into the water and ice could be generated in the tank. The R12 vapor leaves the tank to the compressor – evaporator part of the cycle.

The chilled water cycle is designed to supply the base load of the office. The cooled water from the chiller is fed through the fan-coil unit to extract heat from the space and turns back to the chiller. If the cooling load required is too high than the set limit the chilled water from the fan coil will pass through the ice storage tank to lower the water temperature before returning back to the chiller.

The mathematical models of all the main components of the chilled water cycle and the ITES cycle are developed and the system simulation is performed to find out the suitable operation of both cycles.

The simulation shows that the refrigerant mass flow rate with full compressor speed for chilled water cycle should be 0.06 – 0.08 kg/s and that for the ITES cycle should be 0.08 – 0.09 kg/s at the compressor speed of 9.5 rps. The coefficient of each cycle under these conditions is found to be about 3.1.

From the system simulation, it is found that as the cooling load is highly supported by the ITES, peak energy demand during the on-peak period decreases significantly. The appropriate size of the storage capacity is about 14 kW. The base chilled water system capacity then is about 3.5 kW. With this condition, the system can shift 39.2% of peak electricity demand from the on-peak to the off-peak then 32% of the electric charge could be saved compared to the stand-alone 18 kW conventional chilled water system.

The total period of the study is 2 years With a total budget of 1,411,200 Baht.

ACKNOWLEDGEMENT

The anther could like to appreciate the Thailand Research Fund for the financial support. The author is grateful thank to the Department of Mechanical Engineering, Chiang Mai University for all facilities and accommodations and the helpful of all students in Thermal System Research Unit, CMU are also appreciated.

CONTENTS

LIST OF TABLES

LIST OF FIGURES

NOMENCLATURES

A	heat transfer area (m^2)
C_P	specific heat capacity (kJ/kgK)
CLF	cooling load factor for glass
$CLTD_c$	cooling load temperature difference (°C)
D	diameter (m)
DC	demand charge (Baht/kW)
DT	actual condenser inlet temperature (°C)
EC	energy charge (Baht/unit)
h	specific enthalpy (kJ/kg)
k	polytropic index
L	latent heat (kJ/kgK)
m	mass flow rate (kg/s)
M	mass (kg)
N	compressor speed (rps)
n	number of people
OC	overall charge (Baht))
P	pressure (MPa)
Q	heat transfer rate (kW)
SC	shading coefficient
SCT	saturated condensing temperature (°C)
SDT	saturated discharge temperature (°C)
SET	saturated evaporator temperature (°C)
$SHFG$	maximum solar heat gain factor (W/m^2)

SST	saturated suction temperature (°C)
T	temperature (°C)
Δt	period of time (s)
TD	temperature difference through thing of which heat flow from higher temperature to lower temperature (°C)
U	average of the overall heat transfer coefficient (kW/m^2K)
UA	overall heat transfer coefficient (kW/K)
W	total lighting capacity (watts)

Subscripts

a	air
amb	ambient
avg	average
cd	condenser
ch	chiller
cp	compressor
d	discharge
ev	evaporator
ex	expansion valve
i	inlet
o	outlet
r	refrigerant
s	suction
w	water

Abbreviation

EGAT	Electricity Generating Authority of Thailand
ITES	Ice Thermal Energy Storage
TES	Thermal Energy Storage
TOD	Time-of-day electricity tariff
TOU	Time-of-use electricity tariff
TR	Ton of refrigerant (equal to 3.516 kW)

CHAPTER 1
INTRODUCTION

1.1 Introduction

At present, high electrical energy consumption is consumed every year especially during the peak demand period. The electricity demand, for example in Thailand, is annually increased by 12% [1]. To support the increment, the Electricity Generating Authority of Thailand (EGAT) has to construct new power plants or buy electricity from neighboring countries. However, to create a new power plant for serving the peak demand which occurs in a short duration is not appropriate. A lot of money, land and available energy resources have to be invested. The demand-side management policy has been pointed out by charging the consumers high premium rate for the energy consumed during the peak period and low rate during the off-peak hours. Thus, uniform load factor and reduction of the peak demand will be achieved. In Thailand, EGAT has set two electricity tariffs named Time-of-day (TOD) and Time-of-use (TOU) rate. Both tariffs are used for the buildings that consumed high electrical energy during on-peak period. The difference between TOD and TOU rate is time schedule. The time schedules of TOD and TOU rate are as following.

Table 1.1 Time schedule of electricity tariffs.

Period	Time-of-day (TOD)	Time-of-use (TOD)
On peak	Monday – Sunday 18.30 – 21.30	Monday – Saturday 09.00 – 22.00
Partial peak	Monday – Sunday 08.00 – 18.30	Monday – Saturday 22.00 – 09.00
Off peak	Monday – Sunday 21.30 – 08.00	Sunday 00.00 – 24.00

The electricity cost charged by TOD rate consists of demand charge and energy charge. The demand charge is counted on the average maximum electricity used in kW over 15 minutes in each month. The energy charge is based on the total amount of power consumed in kW-hr (unit) during each month. For TOU rate, it consists of the monthly service charge besides the demand charge and the energy charge. The examples of the TOD and TOU rates are shown in Tables 1.2 and 1.3

Table 1.2 Electricity costs (TOD Rate) for commercial building.

Voltage	Demand charge (Baht/kW)			Energy charge (Baht/unit)
	1*	2*	3*	
> 69 kV	224.30	29.91	0	1.0208
22 – 33 kV	285.05	58.88	0	1.0582
< 22 kV	332.71	68.22	0	1.0862

1* Monday – Sunday 18.30 –21.30

2* Monday – Sunday 08.00 – 18.30 charge only the excess of the peak

3* Monday – Sunday 21.30 – 08.00

Table 1.3 Electricity costs (TOU Rate) for commercial building.

Voltage	Demand Charge (Baht/kW)	Energy Charge (Baht/unit)			Service Charge (Baht/month)
	1*	1*	2*	3*	
> 115 kV	102.80	1.5349	0.6671	0.6062	400.00
69 kV	158.88	1.6292	0.6769	0.6153	400.00
22 – 33 kV	200.93	1.7736	0.6861	0.6236	850.00
< 22 kV	214.95	1.8891	0.7283	0.6616	850.00

1* Monday – Saturday 09.00 – 22.00

2* Monday – Saturday 22.00 – 09.00

3* Sunday 00.00 – 24.00

For commercial building, it is found that the main electricity consumption is mainly caused by air conditioning system. Then, thermal energy storage (TES) system is one concept that is becoming more attractive to reduce the large peak demand especially for the commercial buildings which have already employed a conventional chilled water system. Moreover, the operating cost is consequently decreased.

Thermal energy storage (TES) is the energy management technique. In the case of cooling purpose, the system with TES shifts all or part of the electricity

requirement from the peak period to off-peak hour. The compressor sizing of the system is designed to meet the average load rather than the peak load. From the application of the TES, the electricity is used to charge a storage tank when it is cheapest and then the energy stored in the storage tank is used to cool the building during the time when the electricity is expensive.

TES system are often classified according to the storage medium used, the storage technology and the model of operation

1.1.1 Thermal storage media classification

The most common storage media for cooling purpose are water, ice and other phase-change materials, known as eutectic salts. The differences among these media are the amount of the energy stored per unit volume, the temperatures at which they store cooling and the physical requirements of storing energy.

(a) Chilled water storage system

Chilled water storage system uses the sensible heat capacity of water (4.184 kJ/kg-K) to store cooling. The chilled water is generally stored at temperature between 4 and 6 °C.

(b) Ice storage system

Ice storage system uses the latent heat of fusion of water (335 kJ/kg). The energy is stored in ice at the freezing point of water (0°C). To store this energy, refrigeration equipment must provide charging fluid at temperature of –9 to –3°C.

(c) Eutectic salts system

Eutectic salt phase change materials are available in various formulations to melt and freeze at selected temperatures. The most common formulation for cool storage applications is a mixture of inorganic salts, water and nucleating and stabilizing agents, which melts and freezes at 8.3 °C. This temperature is higher than the supply temperatures of most conventional cooling system, so operating strategies may be limited.

1.1.2 Storage technology classification

Thermal energy storage technologies in cooling purpose can be divided into the following categories:

(a) Chilled water storage

Chilled water is stored in tanks, using natural stratification or other techniques to separate cold water from warm return water.

(b) Ice harvesting

Ice is formed on an evaporator surface and periodically released into water filled in storage tank.

(c) Ice-on-coil

- External melt ice-on-coil

Ice is formed on submerged pipes or tubes through which a refrigerant or secondary coolant is circulated. Cooling is discharged by circulating the water that surrounds the ice pipes, melting the ice from the outside.

- Internal melt ice-on-coil

Ice is formed on submerged pipes or tubes, similar to those of the external melt system. Cooling is discharge by circulating warm coolant through the pipes, melting the ice from inside.

(d) Encapsulated ice

Water inside submerged plastic container freezes and thaws as cold or warm coolant is circulated through the tank holding the containers.

(e) Phase-change materials

A eutectic salt phase-change material freezes and thaws in response to circulated cold or warm water. The most common approach has the phase-change material in submerged containers similar to those in the encapsulated ice technology.

1.1.3 Operation model classification

Most of the storage installations use one of the three basic operational models, which are full, partial and demand-limited storage. These models are shown in Fig. 1.1 along with a conventional cooling system which operates during the occupied hours of the building to satisfy the occupants comfort level.

(a) Full storage

Full storage minimizes the cost of a building by shifting the use of the energy from on-peak to off-peak hours. In full storage system, the size of the chiller and storage tank are depended on the time-of-use rate schedule of the building. Under this rate, the primary cooling equipment does not operate during on-peak period so that the entire cooling requirement for the building is supplied from the storage. Since the daily cooling load of the building must be met by using the available off-peak hours for charging of the storage, full storage requires larger storage volume than the other storage strategies.

(b) Partial storage

With partial storage, the chiller is downsized compared to a conventional cooling system and runs at steady rate over 24 hours. Compared with a conventional system, it is observed that, for a given design day, building peak load is significantly reduced with the use of partial storage strategy. Although the system operates continuously all day, the storage does not meet peak demand but supplements the full output of the chiller.

(c) Demand-limited storage

A demand-limited storage is variation of partial storage such that the chiller runs during all day except hours of maximum non-cooling demand. This strategy requires complicated control system, since the peak demand must be met through the storage. A demand-limited strategy is most applicable to the building with significant demand charges and short occupancy periods that allows greater storage charging time.

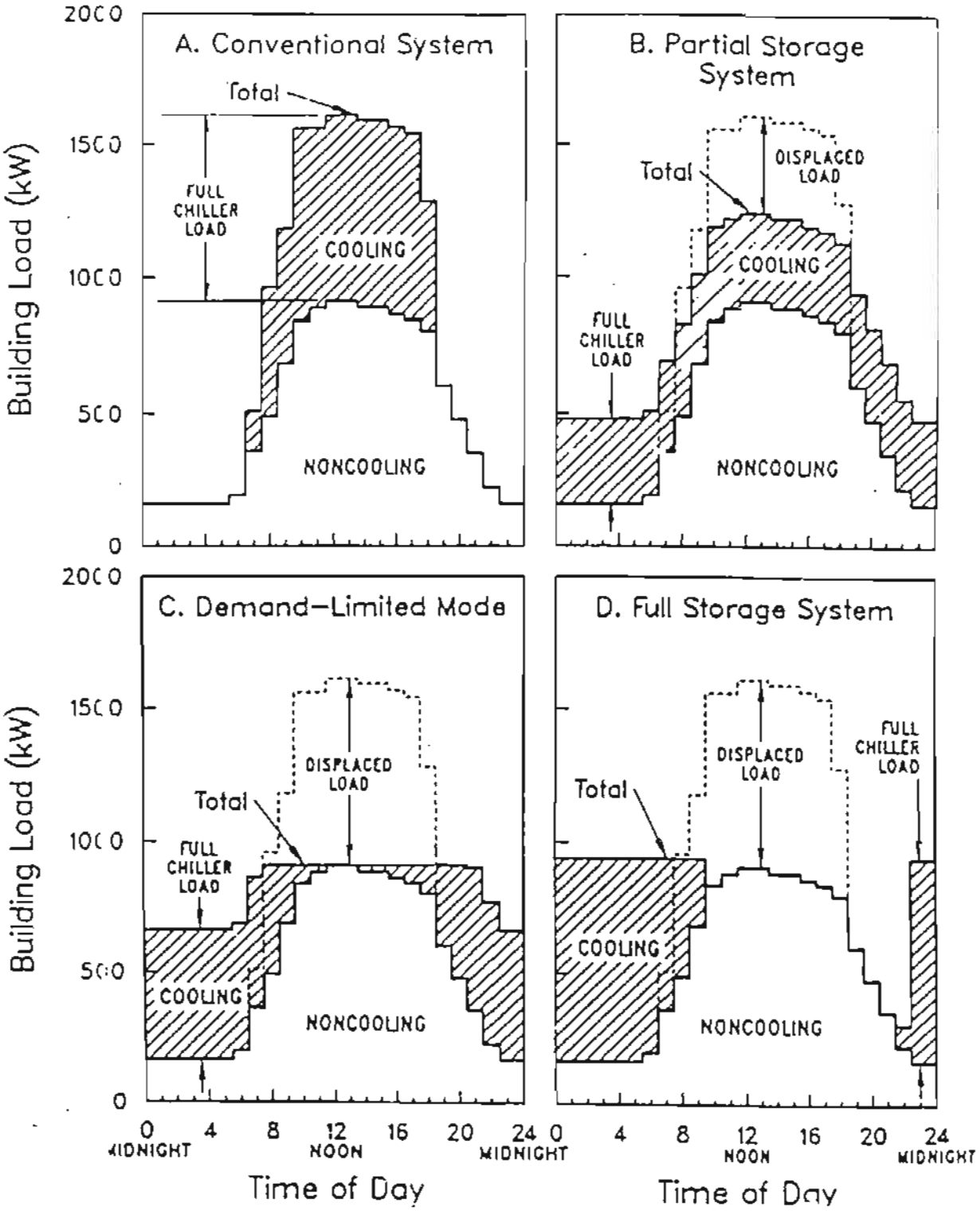

Fig. 1.1 Hourly load profile for a building with a conventional air conditioning system on design day compared with three thermal energy storage operational model [2].

At present, the most commonly used of TES system is the ice thermal energy storage (ITES) system especially ice-on-coil type using water as a storage medium. A simple schematic circuit diagram for the ice-on-coil thermal energy storage system is shown in Fig. 1.2.

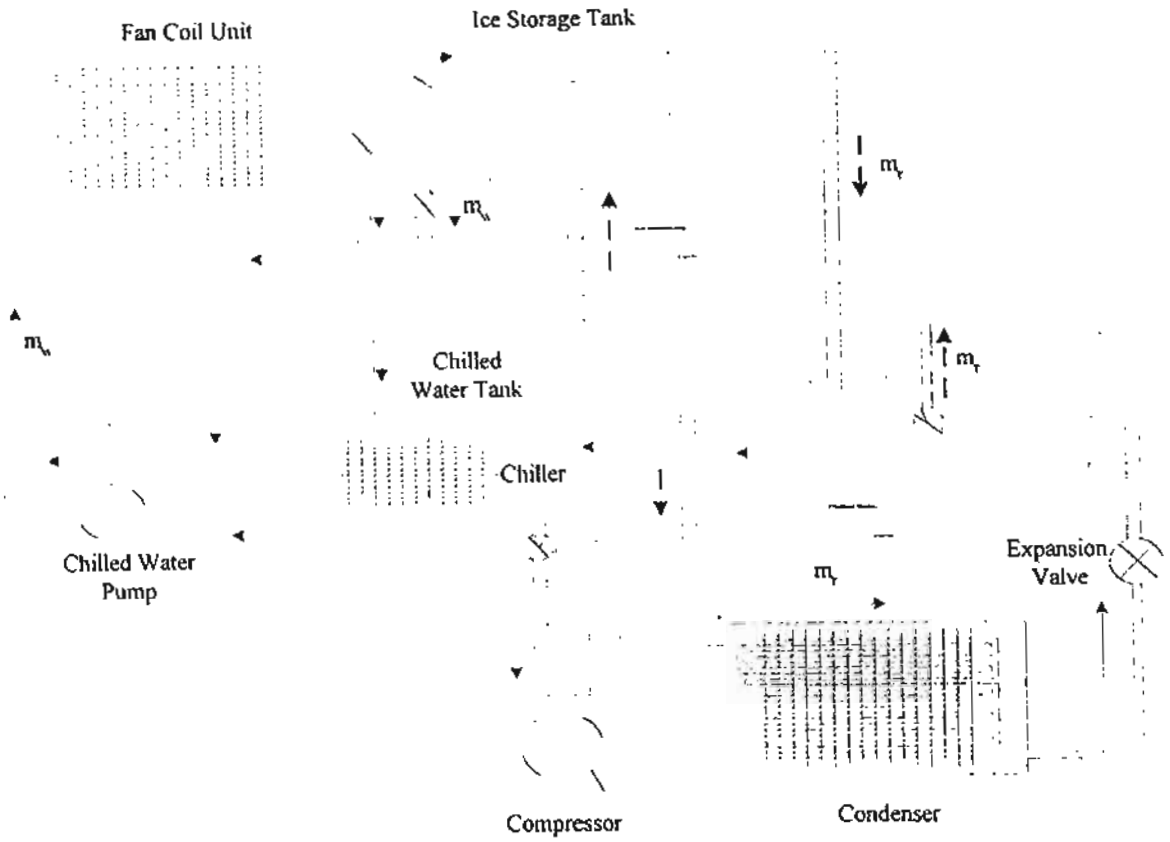

Fig. 1.2 Schematic diagram of building circuit for ice thermal energy storage.

The system consists of 2 cycles, chilled water cycle and ice producing cycle. During the chilled water producing process, the refrigeration system consisting of the compressor, the condenser and the expansion valve is operated to run the refrigerant passing through the chiller to extract heat. Then during the ice producing process, the same system is operated to produce the ice by bypass the refrigerant from the chiller to the cooling coil submerged in the storage tank.

As the ice is formed directly on the coils submerged in the water in the storage tank [3], this system has two main problems, big space for handling the evaporator coil is needed and high thermal resistance is obtained due to the low thermal conductivity of the ice when it is formed on the coil [4,5]. During the ice formation process, as the ice thickness is increased, the rate of heat extraction

decreases. Thus, to overcome these problems, the direct contact heat transfer technique has been much interest in recent years through its application [6,7].

Direct contact heat transfer is a fundamental process by which heat transfer occurs in nature.

The major advantages of the direct contact heat transfer are

(1) High heat transfer rates associated with intimate mixing of the two fluids. This is mainly due to the very large interfacial surface area in dispersed particulate systems and to the high level of turbulence produced by the mixing process.

(2) Much simplified construction and capital cost reduction due to elimination of the relatively complex tube or plate arrays.

(3) Elimination of metal walls which impose thermal resistance.

(4) The feasibility of using low temperature fluid without introducing the thermal stress problems that are met in metal wall heat exchangers.

As shown in Fig. 1.3, the storage tank in ITES system acts as the evaporating unit. There is no cooling coil in the storage tank.

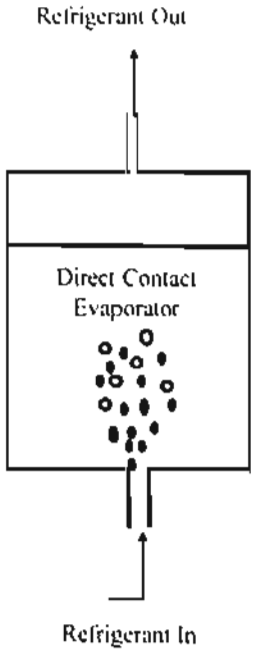

Fig. 1.3 Schematic of direct contact evaporator tank.

The refrigerant is injected through the expansion valve where the pressure and temperature of the refrigerant decrease. The low temperature refrigerant exchanges heat with water in the storage tank directly and then leaves the tank and returns back to the condensing unit. During the refrigerant passes through the water, the water temperature decreases. The ice is formed.

In this research work, the study of an ice thermal energy storage with the direct contact evaporator system for air conditioning system of an office in Chiang Mai province, Thailand has been carried out.

1.2 Literature Review

1.2.1 Direct contact heat transfer technique

Subbaiyer et al. [6] showed a simulated result of a refrigeration unit with a direct contact evaporator. The unit required only 50 – 60 % of electrical energy consumption per ton of refrigerant compared with a cooling coil ice generator.

Nuntaphan [8] studied the parameters affecting thermal performance of a direct contact evaporator. It was found that rapid sensible heat cooling of water in the evaporator was obtained with a high value of Stanton number of the refrigerant. It's also found that the performance of the system was about 3.4 – 3.6 at the compressor speed of 8 – 10 rps. and for a refrigerant mass flow rate of 0.04 – 0.06 kg/s.

Kiatsiriroat and Maneechote [9] studied about the ice formation and melting process in the direct contact evaporator. The researchers injected the low temperature oil into the water in the tank. It was found that the ice formation depended on 4 main factors i.e., oil flow rate, oil temperature, number of nozzle, and water volume in the tank. It's also found that the ice melting process depends on the oil temperature.

Chatakanonda and Na Bangchang [10] studied the performance of a refrigeration cycle utilizing a direct contact evaporator with R22 refrigerant as a working fluid. The performance of the system is about 3.5 – 4.0 which is higher than the conventional system. It is found that R22 dissolves in water. The R22-and-water solution shows high acidity and causes a problem of corrosion.

Hence, in conclusion, the ice thermal energy storage with direct contact evaporator has higher performance than the ice-on-coil ITES system. From recent research work, it can be further concluded that R12 is appropriate for the direct contact heat transfer technique more than R22 [8,10].

1.2.2 The feasibility of using ice thermal energy storage system

Crane and Dunlop [4] studied the economic feasibility of the external-ice-melt thermal energy storage system in a department store located in London. The ITES system can provide 50% of the store's required cooling load and results to the significant saving. However, a problem of low thermal conductivity of ice still persists.

Simmonds [11] indicated that the chiller system incorporating with the ice thermal energy storage system consumed less energy than that of the conventional chiller system. The electrical energy consumption of the storage system and conventional system of the selected building were 8,795 and 10,219 kW-hr, respectively.

Ritthi [12] presented the effectiveness of the ice storage system in a case study of Thai Rath Press. The electricity charge of TOD rate is reduced from 305 Baht/kW and 1.07 Baht/kW-hr to 285.08 Baht/kW and 1.0528 Baht/kW-hr, respectively by using the ice thermal energy storage. While the COP of water chiller system was 2.64 and the COP of ice storage system was 1.90.

Therefore, the ITES system could decrease the energy consumption and also the electricity charge.

1.2.3 Heat transfer analysis of ice thermal energy storage

Knebel [13] studied the model for the ice harvesting thermal energy storage system. The model for each main component is shown as the following:

Compressor model

$$Q_{comp} = f(SST, SDT, subcooling, superheat) \qquad (1.1)$$

where SST = saturated suction temperature

SDT = saturated discharge temperature

subcooling = external subcooling obtain in the condense liquid

superheat = heat addition to the suction gas that contributes to the useful refrigerant effect

Condenser model

$$Q_{cond} = f(SCT,\ DT,\ subcooling\ ,T_{amb}) \tag{1.2}$$

where SCT = saturated condensing temperature

DT = actual condenser inlet temperature

subcooling = external subcooling obtain in the condense liquid

T_{amb} = ambient temperature

Evaporator model

$$Q_{evap} = U_{avg} A(EWT - SET) \tag{1.3}$$

where U_{avg} = average of the overall heat transfer coefficient

A = heat transfer area of the evaporator

EWT = evaporator entering water temperature

SET = saturated evaporator temperature

Stoecker [14] formulated a mathematical modeling for a various kind of turbomachines such as fans, pumps, compressor and turbines. Performance of these equipment is expressed in dimensionless group. In the case of a centrifugal compressor, the ratio of the discharge pressure to the suction pressure, P_d/P_s, can be expressed as

$$\frac{P_d}{P_s} = f\left[\frac{m_r(C_p T_s)^{0.5}}{D^2 P_s}, \frac{ND}{(C_p T_s)^{0.5}}\right] \tag{1.4}$$

where P_d = discharge pressure (MPa)

P_s = suction pressure (MPa)

m_r = refrigerant mass rate of flow (kg/s)

N = rotative speed (rps)

D = wheel diameter (m.)

C_p = specific heat of fluid (kJ/kg-K)

T_s = suction temperature (K)

Kiatsiriroat, et al [15] offered mathematical modelings for three main components of the refrigeration system: compressor, condenser, and evaporator. These can be shown in the followings:

Compressor modeling

$$\frac{P_{cp,i}}{P_{cp,o}} = f\left[\frac{m_r T_{cp,o}^{0.5}}{P_{cp,o}}, N\right] \tag{1.5}$$

where $P_{cp,i}$ = inlet pressure of compressor (MPa)

$P_{cp,o}$ = outlet pressure of compressor (MPa)

N = compressor speed (rps)

m_r = refrigerant mass flow rate (kg/s)

$T_{cp,o}$ = outlet temperature of compressor (K)

Condenser modeling

$$\frac{(T_w - T_o)}{(T_{cd,i} - T_a)} = f\left[\frac{(UA)_{cd}}{m_w C_{pw}}\right] \tag{1.6}$$

where T_w = water temperature (°C)

T_o = ambient temperature (°C)

$T_{cd,i}$ = inlet temperature of condenser (°C)

$(UA)_{cd}$ = product of heat transfer coefficient and the heat transfer area of the condenser (kW)

m_w = water mass flow rate (kg/s)

C_{pw} = specific heat of the water (kJ/kg-K)

Evaporator modeling

$$\frac{T_{ev}}{(T_L - T_{ev})} = f\left[\frac{(UA)_{ev}}{m_r}, T_{cd}\right] \qquad (1.7)$$

where T_{ev} = evaporating temperature (°C)

T_{cd} = condensing temperature (°C)

T_L = temperature of the water in the tank which evaporator coil is submerged (°C)

$(UA)_{ev}$ = product of the overall heat transfer coefficient of the fluid in the evaporator unit and the heat transfer rate area (kW)

Hence, it could be found that the compressor work and the heat transfer rate at the heat exchanger are related to the actual inlet and outlet temperatures and pressures of the components, heat loss, and heat gain [13]. This shows that the experimental data should be collected at the actual inlet and outlet port of the components. Moreover, as the characteristic models of the reciprocating compressor, the condenser and the evaporator have been generated into a mathematical function [15], the system simulation in this current work will be developed by the list of the characteristic function.

1.3 Research Objectives

1. To design the ice producing system with the direct contact evaporator.
2. To construct and test the ITES unit with direct contact evaporator for selected office.
3. To study the performance of the system.
4. To study the parameters affecting the system performance.
5. To study the economic feasibility in operating the system for the selected office.

1.4 Scopes of Research Work

1. The experimental unit consists of two cycles, the chilled water cycle and the ice storage cycle. The capacity of refrigeration cycles for the chilled water system and the ice storage system are 17500 kW (5 TR) and 7000 kW (2TR), respectively.
2. The unit is operated for the selected office in Chiang Mai University, Chiang Mai, Thailand.
3. The chiller load is assumed to be equal to the cooling load of the selected office.
4. The electricity charge is calculated under TOU tariff.

1.5 Expected Benefit

The ice thermal energy storage using direct contact evaporator could be developed for more practical work and could be expanded for big scale commercial buildings.

CHAPTER 2
THEORY

2.1. Theoretical Background

2.1.1 Cooling load calculation [14, 16, 17]

Since living spaces of the building gain heat from a number of sources, if the temperature and humidity of air in room have to be maintained at a comfortable level, heat must be extracted to offset these heat gains. The net amount of the heat removed is called the cooling load arising from conduction through external structure, conduction through internal structure, solar radiation through glass, lighting, people, equipment, and heat from infiltration of outside air through openings. The calculation of the cooling load can be derived based on the heat transfer principle consisting of these modes: conduction, convection, and radiation. The detail of each formulation is presented below.

(a) Conduction through external walls, roof, ceiling, and floors

The conduction heat gains through the external roof, walls and glass are each found from the following equation

$$Q = U \cdot A \cdot CLTD_c, \qquad (2.1)$$

where Q = net room conduction heat gain through roof, wall, or glass (W)

U = overall heat transfer coefficient for roof, wall, or glass (W/m^2-°C)

A = area of roof, wall, or glass (m^2)

$CLTD_c$ = cooling load temperature difference (°C)

$CLTD_c$ is the temperature difference between the temperature of the outer surface of the sunlit exterior wall or roof and the room temperature.

(b) Conduction through internal partitions, ceiling, and floors

The heat that flows from internal unconditioned spaces to the conditioned spaces through partitions, ceiling, and floors can be found from

$$Q = U \cdot A \cdot TD, \qquad (2.2)$$

where Q = heat transfer rate through partition, floor, or ceiling (W)

U = overall heat transfer coefficient for partition, floor, or ceiling (W/m^2-°C)

A = area of partition, floor, or ceiling (m^2)

TD = Temperature difference between the temperature of the adjacent area that is unconditioned and the room temperature (°C)

If the temperature of the unconditioned space is not known, an approximation often used is to assume that it is at 5°C less than the outdoor temperature. Space with heat sources, such as boiler room, may be at a much higher temperature.

(c) Solar radiation through glass

Radiant energy from the sun passes through transparent materials such as glass and becomes a heat gain to the room. Its value varies with time, orientation, shading, and storage effect. The net heat gain can be found from the following equation

$$Q = SHFG \cdot A \cdot SC \cdot CLF, \qquad (2.3)$$

where Q = net solar radiation heat gain through glass (W)

$SHFG$ = maximum solar heat gain factor (W/m^2)

A = area of glass (m^2)

SC = shading factor

CLF = cooling load factor for glass

The maximum solar heat gain factor (*SHGF*) is the maximum solar heat gain through 0.32 cm. (1/8 inch) single clear glass at a given month, orientation, and latitude. To account for heat gains with different condition arrangement, the shading coefficient *SC* is introduced. The *SC* is the proportional amount of maximum heat gain through arrangements other than 0.32 cm. (1/8 inch). single clear glass.

(d) Lighting

The equation for determining heat gain from lighting is

$$Q = W, \tag{2.4}$$

where Q = net heat gain from lighting (W)

W = total lighting capacity (W)

(e) People

The heat gain from people is composed of two parts, sensible heat and the latent heat resulting from perspiration. Some of the sensible heat may be absorbed by the heat storage effect, but not the latent heat. The equations for sensible and latent heat gains from people are

$$Q_s = q_s \cdot n \cdot CLF, \tag{2.5}$$

and

$$Q_l = q_l \cdot n, \tag{2.6}$$

where Q_s = sensible heat gain (W)

Q_l = latent heat gain (W)

q_s = sensible heat gain per person (W/person)

q_l = latent heat gains per person (W/person)

n = number of people

CLF = cooling factor for people

The rate of heat gain from people depends of their physical activity.

(f) Equipment

The heat gain from equipment may sometimes be found directly from the manufacturer or the nameplate data, allowing for intermittent use. Some equipment produces both sensible and latent heat.

(g) Infiltration

The infiltration of air through cracks around windows or doors in both a sensible heat and latent heat gain to the rooms. Most summer air conditioning systems have mechanical ventilation using some outside air, which reduces or eliminates infiltration by creating a positive air pressure within the building. In this case the ventilation air is not a load on the room, but is a load on the central cooling equipment. Many modern buildings have sealed windows and therefore have no infiltration loss, except for entrances.

2.1.2 Direct contact heat transfer technique

From the preliminary experiments, it is found that the temperature of water is uniform during an injection of the refrigerant into water due to the high turbulence. The refrigerant temperature existed from the storage tank is also close to water temperature. Moreover, it is assumed that the refrigerant is not soluble in water and there is no water mass transfer to the refrigerant in the evaporator tank. Then, the thermal characteristic of water in the storage tank can be analyzed under the application of an energy balance. The equation can be expressed as

$$\frac{d}{dt}\left(M_w h_w\right) + M_t C_t \frac{dT}{dt} = m_r\left(h_{ev,i} - h_{ev,o}\right) + \left(UA\right)_{ev}\left(T_{amb} - T_w\right), \quad (2.7)$$

where M_w = mass of water in the storage tank (kg)

h_w = enthalpy of water in the storage tank (kJ/kg)

M_t = mass of direct contact evaporator (kg)

C_t = specific heat of direct contact evaporator (kJ/kg-K)

m_r = refrigerant mass flow rate (kg/s)

$h_{ev,i}$ = inlet refrigerant enthalpy (kJ/kg)

$h_{ev,o}$ = outlet refrigerant enthalpy (kJ/kg)

$(UA)_{ev}$ = total heat transfer coefficient of the tank (kW/K)

T_{amb} = ambient temperature (°C)

T_w = water temperature (°C)

The left-hand terms of the equation refer to the enthalpy change rates of water in the storage tank and the evaporator unit while the right-hand terms are the enthalpy change rate of the refrigerant and the external heat gain from the surrounding ambient.

For the numerical analysis the characteristic equation can be written as

$$h_w^{t+\Delta t} = h_w^t + \frac{m_r \Delta t}{M_w}\left(h_{ev,i} - h_{ev,o}\right) + \frac{(UA)_{ev}\,\Delta t}{M_w}\left(T_{amb} - T_w\right), \qquad (2.8)$$

where Δt = time lapses (s)

2.2. Mathematical Model

2.2.1 Compressor modeling

For a centrifugal compressor [14], the pressure ratio can be performed in dimensionless group as

$$\frac{P_d}{P_s} = f\left(\frac{m_r\left(C_p T_s\right)^{0.5}}{D^2 P_s}, \frac{ND}{\left(C_p T_s\right)^{0.5}}\right), \qquad (2.9)$$

where P_s = suction pressure of compressor (MPa)

P_d = discharge pressure of compressor (MPa)

m_r = refrigerant mass flow rate (kg/s)

C_p = specific heat of working fluid (kJ/kg-°C)

T_s = suction temperature of compressor (°C)

D = wheel diameter (m.)

N = rotative speed (rps).

Then, in the case of using a reciprocating compressor [15], as D is a constant parameter and the working fluid used in the system is R12 which has nearly constant specific heat, the characteristic function can be expressed as

$$\frac{P_{cp,i}}{P_{cp,o}} = f\left[\frac{m_r T_{cp,i}^{0.5}}{P_{cp,i}}, N\right], \tag{2.10}$$

and

$$\frac{P_{cp,i}}{P_{cp,o}} = f\left[\frac{m_r T_{cp,o}^{0.5}}{P_{cp,o}}, N\right], \tag{2.11}$$

where $P_{cp,i}$ = inlet compressor pressure or suction pressure (MPa)

$P_{cp,o}$ = outlet compressor pressure or discharge pressure (MPa)

$T_{cp,i}$ = inlet temperature (°C)

$T_{cp,o}$ = outlet temperature (°C)

N = compressor speed (rps).

The work input into the compressor can be calculated from

$$W_{cp} = m_r\left(h_{cp,o} - h_{cp,i}\right). \tag{2.12}$$

where W_{cp} = compressor work (kW)

$h_{cp,i}$ = inlet enthalpy of compressor (kJ/kg)

$h_{cp,o}$ = outlet enthalpy of compressor (kJ/kg).

2.2.2 Condenser modeling

The condenser could be classified due to the secondary working fluid. The common used type is air-cool condenser and water-cool condenser. The mathematical modeling of both types can be modified from

$$\frac{\left(T_{a,o} - T_a\right)}{\left(T_{cd,i} - T_a\right)} = f\left[\frac{(UA)_{cd}}{m_a C_{pa}}\right], \tag{2.13}$$

and

$$\frac{\left(T_{w,o} - T_{w,i}\right)}{\left(T_{cd,i} - T_{w,i}\right)} = f\left[\frac{(UA)_{cd}}{m_w C_{pw}}\right], \tag{2.14}$$

where C_{pw} = specific heat of water (kJ/kg.K)

C_{pa} = specific heat of air (kJ/kg.K)

T_a = ambient temperature (°C)

$T_{a,o}$ = outlet air temperature (°C)

$T_{w,i}$ = inlet water temperature (°C)

$T_{w,o}$ = outlet water temperature (°C)

$T_{cd,i}$ = inlet refrigerant temperature (°C)

$(UA)_{cd}$ = overall heat transfer coefficient of condenser (kW/K).

The heat transfer rate at the condenser can be calculated from

$$Q_{cd} = m_r\left(h_{cd,i} - h_{cd,o}\right), \tag{2.15}$$

where Q_{cd} = heat transfer rate at condenser (kW)

$h_{cd,i}$ = inlet enthalpy of condenser (kJ/kg)

$h_{cd,o}$ = outlet enthalpy of condenser (kJ/kg).

2.2.3 Expansion valve modeling

For expansion valve [8], the mathematical modeling can be modified as from

$$\frac{P_{exo}}{P_{exi}} = f\left(m_r, N\right). \tag{2.16}$$

2.2.4 Chiller modeling

For chiller using water as a secondary working fluid [15], the mathematical modeling can be modified from

$$\frac{T_{ch}}{\left(T_w - T_{ch}\right)} = f\left[\frac{\left(UA\right)_{ch}}{m_r}, T_{cd}\right], \tag{2.17}$$

where T_{ch} = evaporating temperature of the chiller (K)

T_{cd} = condensing temperature (K)

T_w = water temperature (K)

$(UA)_{ev}$ = overall heat transfer coefficient (kW/K).

The heat transfer rate at chiller can be calculated from

$$Q_{ch} = m_r\left(h_{ch,o} - h_{ch,i}\right), \tag{2.18}$$

where $h_{ch,i}$ = inlet enthalpy of chiller (kJ/kg)

$h_{ch,o}$ = outlet enthalpy of chiller (kJ/kg).

2.2.5 Direct contact evaporator modeling

To create the evaporator modeling, the experiment is divided into 2 processes, sensible heat process and ice forming process.

During the sensible heat process, the tank temperature is assumed to be the same as that of the water inside. From energy balance the characteristic modeling can be expressed as

$$\left(M_w C_{pw} + M_t C_{pt}\right)\left(\Delta T_w\right) = m_r\left(h_{ev,i} - h_{ev,o}\right)\Delta t\,, \tag{2.19}$$

where M_t = mass of direct contact evaporator (kg)

C_{pw} = specific heat of water (kJ/kg-°C)

C_{pt} = specific heat of direct contact evaporator (kJ/kg-°C)

ΔT_w = water temperature difference during the period of time Δt (°C)

During the ice formation process, the temperature is constant at about 0.01°C. The mass of the ice forming during a period of time Δt can be found as

$$M_w L = m_r\left(h_{ev,i} - h_{ev,o}\right)\Delta t\,, \tag{2.20}$$

where L = latent heat of water (kJ/kg).

CHAPTER 3
EXPERIMENTAL SET-UP AND SYSTEM MODELING

3.1 Experimental Set-up

In this research work, the experimental unit of an air-conditioner with an ice thermal energy storage (ITES) system is designed to support the cooling requirement of a selected office in Chiang Mai University. The schematic diagram of the experimental set-up with the pressure, the temperature and mass flow rate measurement positions are illustrated in Fig. 3.1.

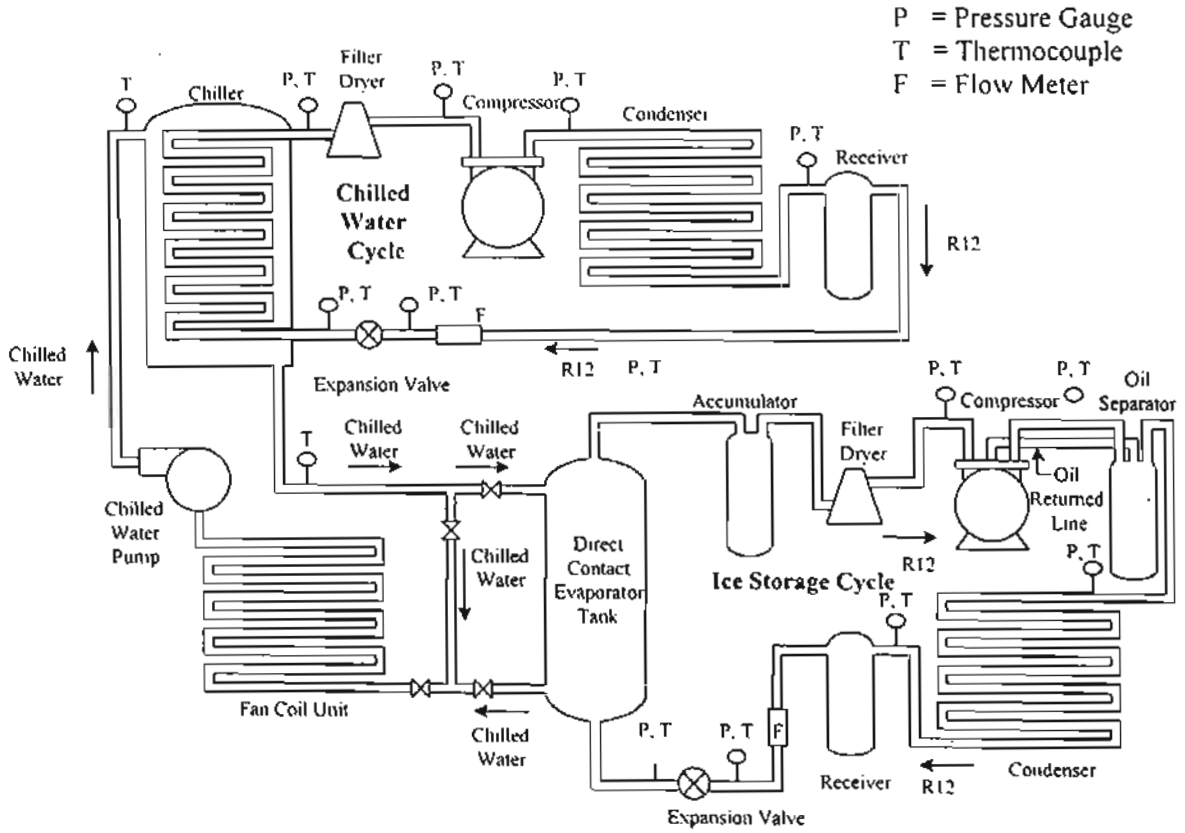

Fig. 3.1. Schematic diagram of the experimental set-up.

The system consists of two main cycles, chilled water cycle and ice thermal energy storage (ITES) cycle. The ITES is designed as a partial storage type and the whole system uses R12 refrigerant as the working fluid. During the off-peak period, the low temperature R12 in the ITES cycle is injected through an expansion valve into the water in the storage tank to exchange heat directly. The water temperature in the storage tank is decreased to the freezing point. The ice is formed

and stored in the tank. During the on-peak period, the chilled water cycle is operated to produce the cooled water to achieve the cooling requirement. The cooled water passes from the chiller to the fan-coil unit to exchange heat and then turns back to the chiller. If the required cooling load is higher than the capacity of the chiller, the chilled water from the fan-coil unit controlled by a two-way valve will pass through the ice storage tank to lower the chilled water temperature before going back to the chiller.

3.1.1 Chilled water system

The chilled water system in this research work consists of the components for the standard 5 TR (18 kW) vapor-compression refrigeration system. The characteristic of each component is shown in Table 3.1.

Table 3.1 Characteristic of the components in the chilled water cycle.

Component	Characteristic
Compressor	Semi-hermetic reciprocating compressor for 5 TR air-conditioning system
Condenser	Shell and tube water cooled condenser for 5 TR air-conditioning system
Expansion valve	Manual control expansion valve for 5 TR air-conditioning system
Chiller	Shell and tube, water chiller for 5 TR air-conditioning system
Chilled water pump	Max. head: 40 m., Q_{max}. 40 L/min.0.37 kW
Filter dryer	Shell type for 5 TR air-conditioning system
Receiver	Liquid receiver for use with R12 for 5 TR air-conditioning system
Fan-coil unit	18 kW.

3.1.2 Ice storage system

The ice storage system used in this work is illustrated in Fig. 3.2. It has another vapor compression refrigerant cycle using R12 refrigerant separated from the chilled water system. The compressor, the condenser and the expansion valve are the standard-size components of the 2 TR (7 kW) refrigeration system. The ice storage tank works as the direct contact evaporator unit since R12 is injected through

the water to extract heat directly. The characteristic of each component is summarized in Table 3.2.

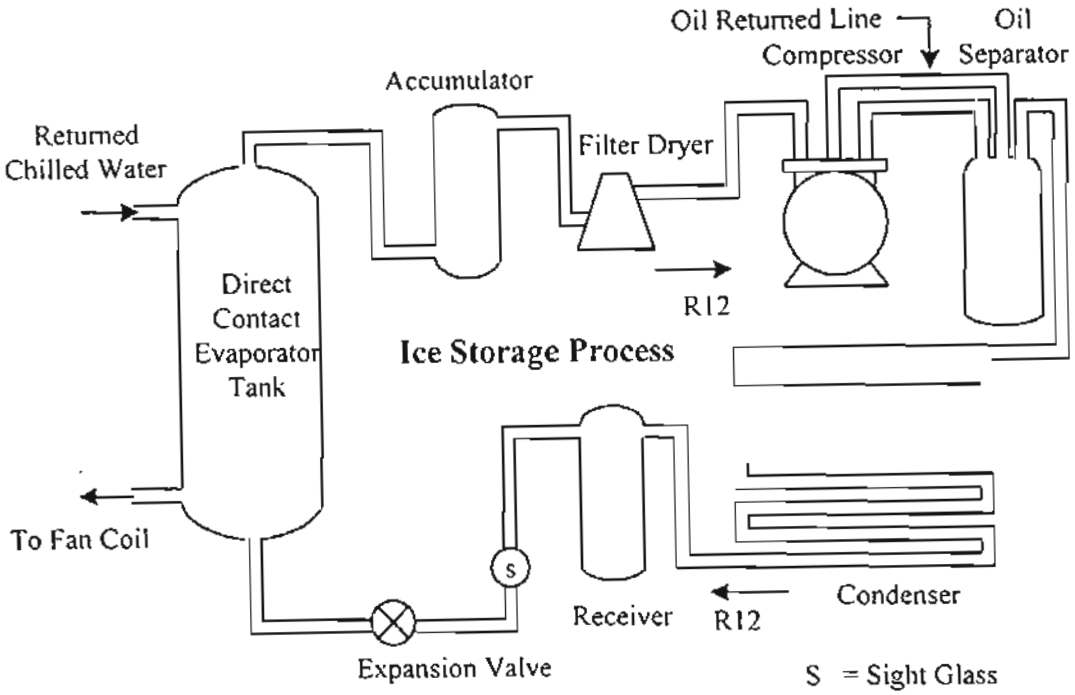

Fig. 3.2. Schematic diagram of the experimental set-up for the ice storage system.

Table 3.2 Characteristic of the components in the ice storage cycle.

Component	Characteristic
Compressor	Reciprocating compressor; open type for 2 TR air-conditioning system
Motor	Three phase induction motor, 5 HP, 4 Poles
Inverter	For use with 5 HP motor
Condenser	Air cool condenser, 7 kW
Expansion valve	Manual control expansion valve for 2 TR air-conditioning system
Direct contact evaporator	1000 liters. Steel cylinder tank
Accumulator	R12 accumulator for 2 TR air-conditioning system
Filter Dryer	Dryer for 7TR refrigeration system, steel take apart, shell type
Oil separator	For use with R12, for 2 TR air-conditioning system
Receiver	R12 liquid receiver, max. pressure 3.445 kPa., for 2 TR air-conditioning system

The system requires auxiliary refrigerant storage space when all of the refrigerant in the system cannot be condensed and stored in the condenser during the shutdown period. Receiver is a cylinder tank made of steel sheets used to serve this purpose. The top of the tank is connected to the liquid line from the condenser. It also has a liquid discharge line connected to the evaporator by a shutoff valve.

However, moisture and foreign objects from the refrigerant have to be removed during the period of operation. Therefore, filter dryer is used. It contains a molded, porous core made of material with high moisture affinity, such as alumina and acid-neutralizing agents. The core should be replaced after a certain period of time.

To observe the condition of refrigerant flow in the liquid line, a sight glass is used. The sight glass is located just before the expansion valve. Bubbles seen through the sight glass indicate the presence of flash gas instead of liquid refrigerant. The presence of flash gas always indicates that evaporator capacity is reduced because of a shortage of refrigerant or insufficient subcooling. A moisture chemical is built into the sight chamber behind the sight glass. If excessive moisture is present in R12, the chemical turns pink. If the moisture is below the safe limit, the color remains green.

3.2. System Modeling

In this section, the mathematical models of the main components for the air conditioner including the direct contact ITES are formulated as follows:

3.2.1 Chilled water system

For chilled water refrigeration cycle, a standard vapor-compression refrigeration system is simulated under steady-state conditions to produce the chilled water to support the cooling load. The system is operated with chiller priority strategy, in this research. The chiller is allowed to operate at full load during peak hours and the ice is only utilized to over the building load that exceeds the full load capacity of the chiller. The compressor in the system usually operates at constant full speed.

The refrigerant mass flow rate adjusted by the manual-controlled expansion valve is varied from 0.033 kg/s to 0.088 kg/s. At any given mass flow rate,

the pressure and the temperature of the refrigerant at the inlet and the outlet of each main component are measured. The mathematical modeling of each main component could be developed at various refrigerant mass flow rates.

(a) Compressor Modeling

Since the refrigerant mass flow rate in chilled water system is varied at full speed of the compressor, The pressure ratio of the compressor responds to the mass flow rate and also the temperature of the refrigerant. The correlation between these values can be deducted from the experimental results shown in Fig. 3.3 and 3.4 as

$$\frac{P_{cp,i}}{P_{cp,o}} = 0.0973\left(\frac{m_r T_{cp,i}^{0.5}}{P_{cp,i}}\right) + 0.0663. \tag{3.1}$$

and

$$\frac{P_{cp,i}}{P_{cp,o}} = 0.0873\left(\frac{m_r T_{cp,o}^{0.5}}{P_{cp,o}}\right) + 0.1088. \tag{3.2}$$

The pressure ratio of the compressor can be additionally calculated from

$$\frac{P_{cp,i}}{P_{cp,o}} = \left(\frac{T_{cp,i}}{T_{cp,o}}\right)^{k/(k-1)} \tag{3.3}$$

where k is the polytropic index. However, the index is not a constant value and depends on the refrigerant mass flow rate. When the flow rate increases, the index also increases. The relation between the flow rate and the index is shown in Fig. 3.5 from which the characteristic equation can be expressed as

$$k = -2.1397 m_r^2 + 0.4896 m_r + 1.1867. \tag{3.4}$$

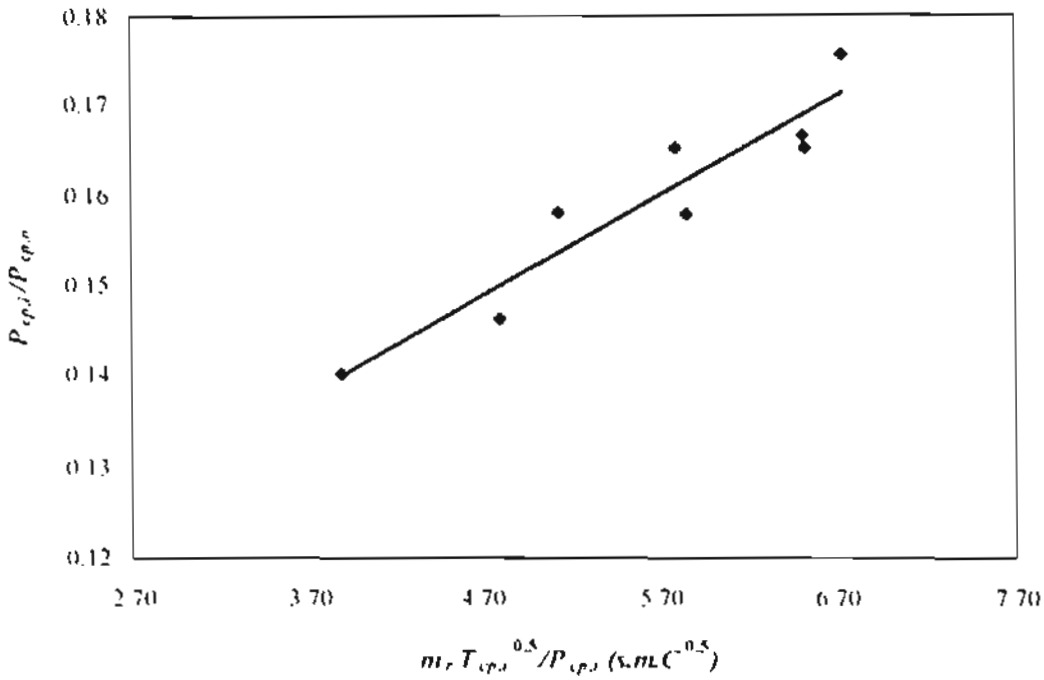

Fig.3.3. The relation between pressure ratio of the compressor and a function of $m_r T_{cp,o}^{0.5}/P_{cp,o}$

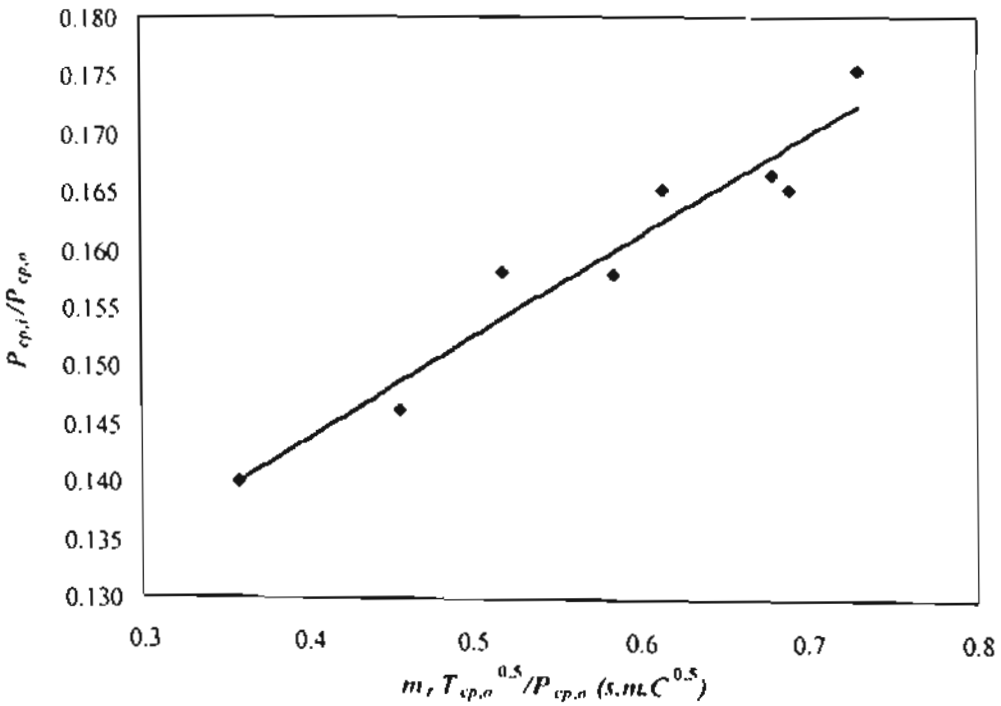

Fig.3.4. The relation between pressure ratio of the compressor and a function of $m_r T_{cp.o}^{0.5}/P_{cp.o}$

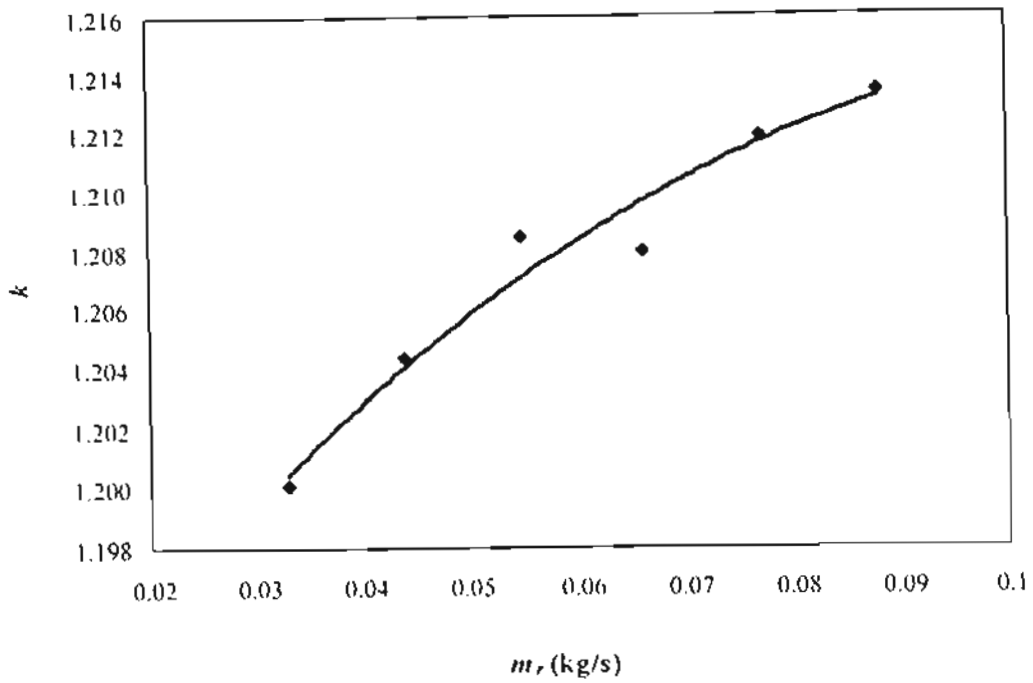

Fig.3.5. The relation between mass flow rate of the refrigerant and the polytropic index of the compressor in chilled water system.

(b) Condenser Modeling

A shell and tube heat exchanger having circulating water as a coolant is used as a condenser to extract heat from the refrigeration system. From the experiment, it could be found that the refrigerant becomes saturated liquid after passing the condenser from which the extracted heat is calculated from

$$Q_{cd} = m_r\left(h_{cd,i} - h_{cd,o}\right). \tag{3.5}$$

Q_{cd} is the rate of heat extraction, $h_{cd,i}$ and $h_{cd,o}$ are the enthalpies at the inlet and the outlet of the condenser, respectively.

(c) Expansion Valve Modeling

The expansion valve is operated manually to control the refrigerant mass flow and the pressure of the cycle. The results from the experiment are shown in Fig. 3.6. The pressure ratio at the inlet and outlet of the valve depends on the refrigerant mass flow rate. As the refrigerant mass flow rate increases, the pressure ratio is also increased. The characteristic equation of the valve is, hence, expressed as

$$\frac{P_{ex,o}}{P_{ex,i}} = -20.114m_r^2 + 3.5432m_r + 0.1291. \tag{3.6}$$

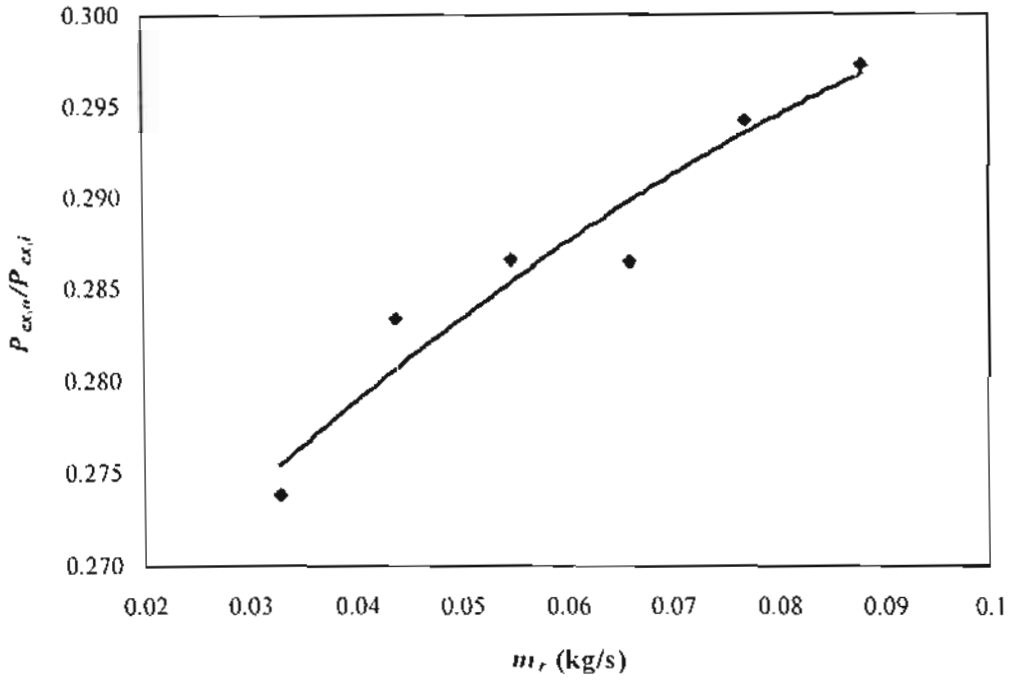

Fig.3.6. The relation between the pressure ratio in the chilled water system and the refrigerant mass flow rate.

(d) Chiller Modeling

The water chiller used in this case is a shell-and-tube flow type of which the relevant heat transfer rate is calculated from

$$Q_{ch} = m_r\left(h_{ch,o} - h_{ch,i}\right), \tag{3.7}$$

or

$$Q_{ch} = m_w C_{cpw}\left(T_{w,i} - T_{w,o}\right), \tag{3.8}$$

and

$$Q_{ch} = \left(UA\right)_{ch}\left[\frac{\left(T_{w,i} - T_{ch,o}\right) - \left(T_{w,o} - T_{ch,i}\right)}{\ln\left[\frac{T_{w,i} - T_{ch,o}}{T_{w,o} - T_{ch,i}}\right]}\right], \tag{3.9}$$

where $(UA)_{ch}$ is found out from the experiment data and Eqs. 3.8-3.9.

It is observed that there exists a pressure drop across the condenser and the chiller which can be expressed in terms of the pressure ratios at the expansion valve and compressor as

$$\frac{P_{cp,i}}{P_{cp,o}} = 0.7733\left[\frac{P_{ex,o}}{P_{ex,i}}\right] - 0.0194. \qquad (3.10)$$

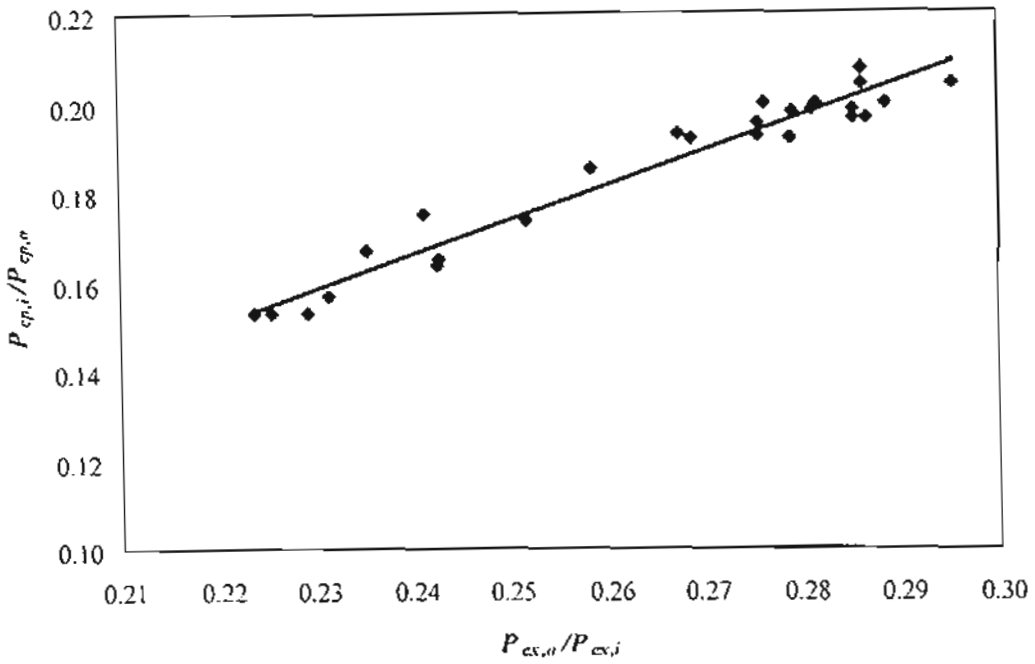

Fig. 3.7. The relation between the pressure ratio of the compressor and the pressure ratio of the expansion valve in the chilled water system.

3.2.2 Ice storage system

Standard vapor-compression refrigeration cycle is operated as the ice storage system. The system hosts two processes; the ice producing and the ice melting process. The ice producing process is operated during the nighttime or off-peak period. To formulate the mathematical models of the system, the refrigerant mass flow rate is varied from 0.033 kg/s to 0.088 kg/s similar to the chilled water system. The compressor in the system is an open-type. Its speed controlled by the inverter is varied from 7.1 rps to 11.8 rps. For this experiment, the mass of water in the storage tank is also varied from 200 kg to 400 kg. The experiment starts with adding water into the direct contact evaporator/storage tank in the required amount and then injecting R12 through the expansion valve into the water directly to extract heat. The

pressures and the temperatures of the refrigerant at the inlet and the outlet of each main component, and the temperature of the water in the storage tank are measured during the ice producing process..

After the ice is produced and stored in the storage tank, the compressor of the system is shut down. Then, when the chiller in chilled water system reaches its capacity, the chilled water is bypass through the ice in the storage tank. The ice is melted. Time taken during the ice melting process and the temperature of the water in the storage tank are recorded.

Hence, the characteristic models of main components in the system are created from the experimental data as followings:

(a) Compressor Modeling

During the ice producing, the compressor model could be characterized similar to that of the chilled water system. It is noted that the pressure ratio of the compressor depends on both of the refrigerant mass flow rate and the compressor speed. The pressure ratio is proportional to the function of $m_r T_{cp.o}^{0.5}/P_{cp.o}$. The pressure ratio is decreased when the compressor speed increases. However, the compressor speed does not affect on the polytropic index. The relation among these variables are illustrated in Figs. 3.8 and 3.9 from which the characteristic equations of the compressor can be expressed as

$$\frac{P_{cp.i}}{P_{cp.o}} = \left[\begin{array}{l} \left(-0.0015N^2 - 0.0087N + 0.3003\right)\left[\dfrac{m_r T_{cp.o}^{0.5}}{P_{cp.o}}\right] \\ + \left(0.0022N^2 - 0.0581N + 0.5824\right) \end{array} \right], \qquad (3.11)$$

and

$$k = 1.9584\, m_r + 1.1503\ . \qquad (3.12)$$

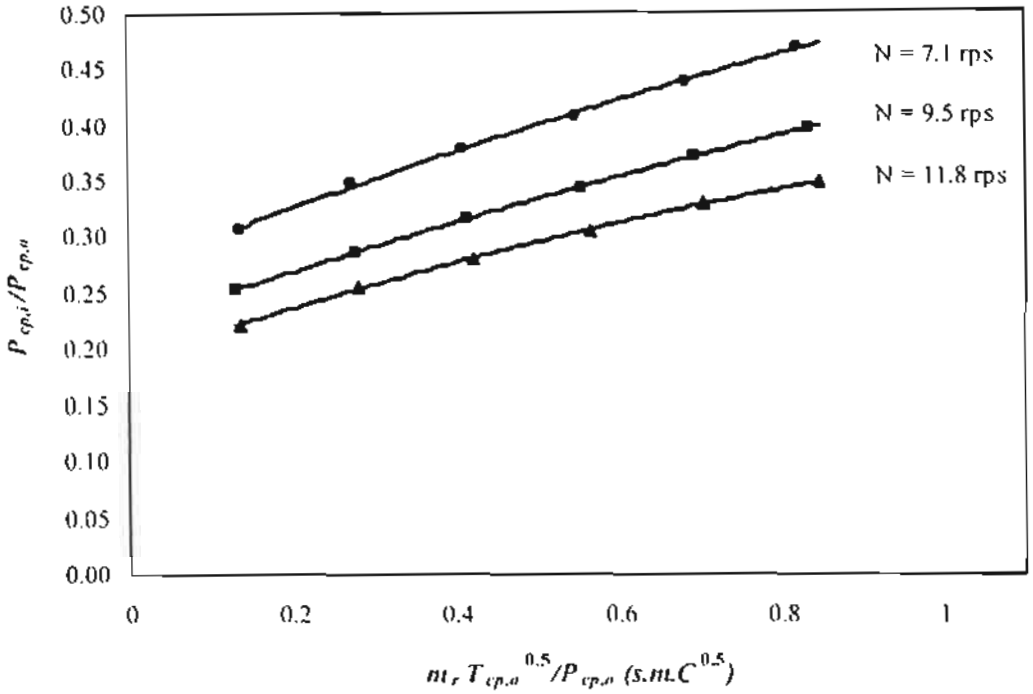

Fig.3.8. The relation between pressure ratio of the compressor in the ice storage system and a function of $m_r T_{cp,o}^{0.5}/P_{cp,o}$ and N.

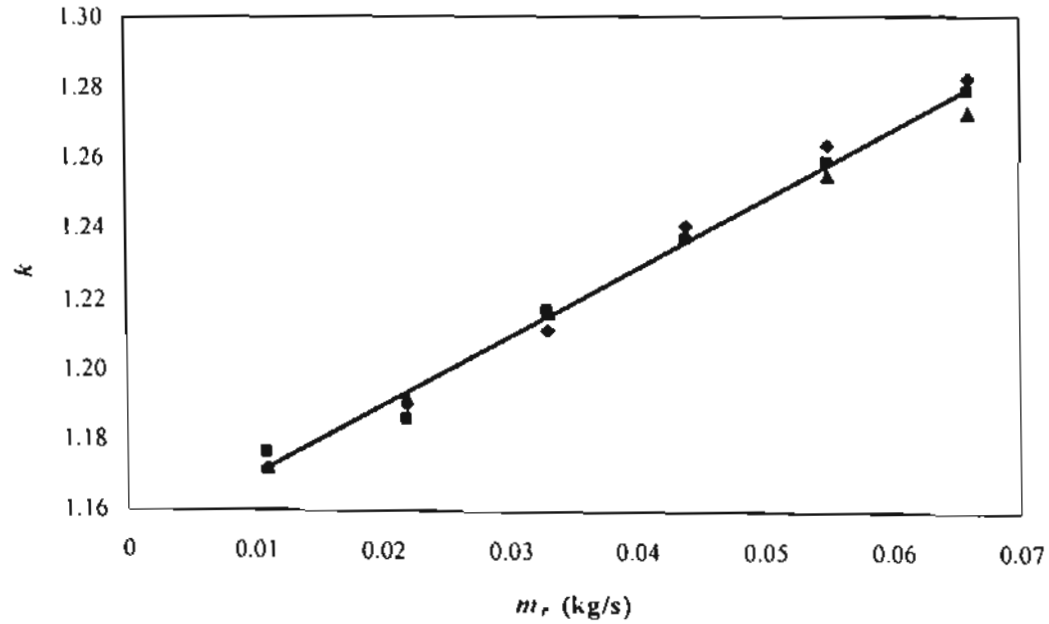

Fig.3.9. The relation between mass flow rate of refrigerant and the polytropic index of the compressor in ice storage system.

(b) Condenser Modeling

A cross flow heat exchanger using air as a coolant is used to extract heat from the refrigerant. The temperature ratio of the condenser is a function of a dimensionless group $(UA)_{cd}/m_aC_{pa}$. When the value of the dimensionless group increases, the temperature ratio also increases as shown in Fig. 3.10.

Deduction from the experiments, the characteristic equation of the condenser can be expressed as

$$\frac{T_{a,o}-T_a}{T_{cd,i}-T_a}=\frac{0.2723(UA)_{cd}}{m_aC_{pa}}+0.0107. \qquad (3.13)$$

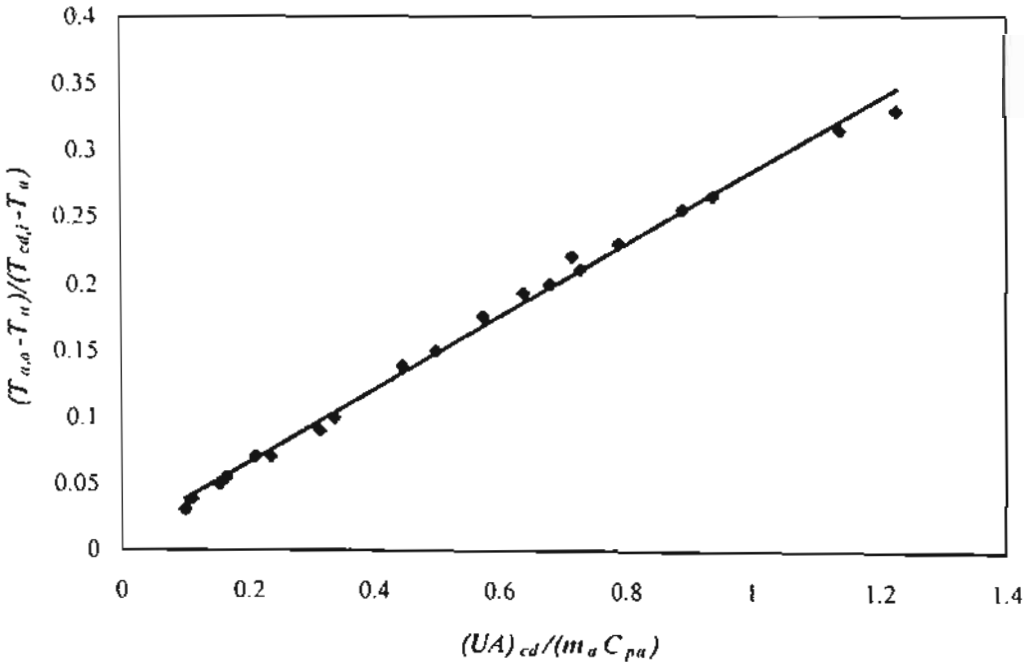

Fig.3.10. The effect of mass flow rate of air and total heat transfer coefficient to outlet temperature of air.

(c) Expansion Valve Modeling

The characteristic function of the expansion valve in this system is similar to that of the chilled water system. Both of the refrigerant mass flow rate and the compressor speed have the effects on the pressure ratio of the expansion valve. However, the pressure ratio is increased when the flow rate increases, it is decreased when the compressor speed increases. The correlation of the variables can be expressed as

$$\frac{P_{ex,o}}{P_{ex,i}} = \begin{bmatrix} \left(1.5134N^2 - 32.0125N + 148.8285\right)m_r^2 \\ +\left(-0.1020N^2 + 2.0160N - 5.8329\right)m_r \\ +\left(0.0032N^2 - 0.0824N + 0.7113\right) \end{bmatrix}. \quad (3.14)$$

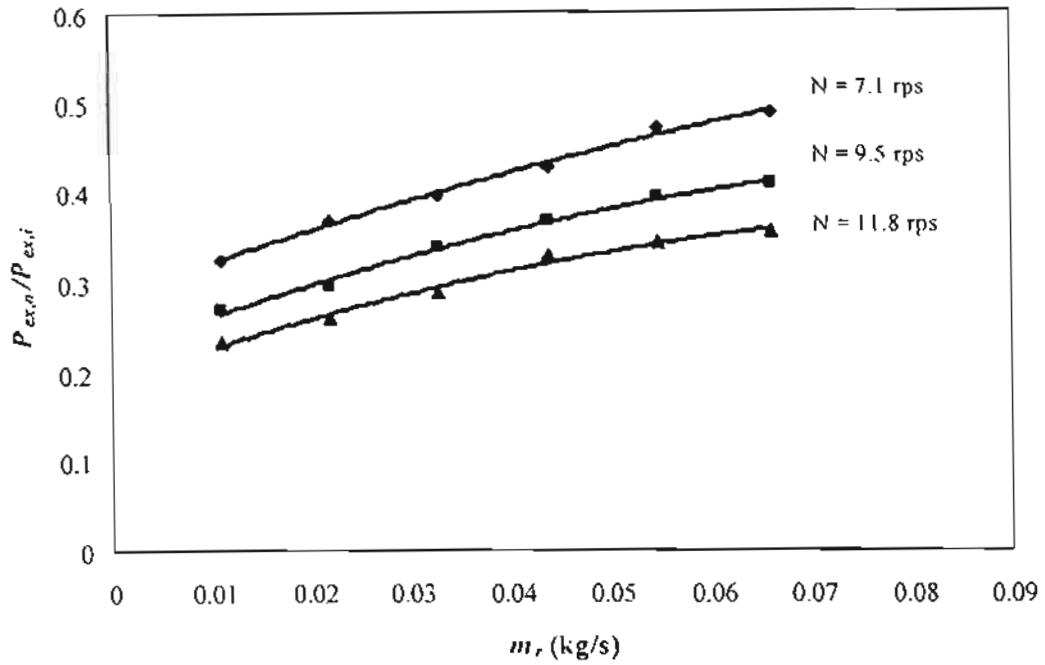

Fig.3.11. The relation between pressure ratio of the expansion valve in the ice storage system and mass flow rate of refrigerant at various compressor speeds.

As shown in Fig. 3.2, there are some accessory components in this system such as filter drier, accumulator and receiver. These components cause pressure drops as well as heat losses. The pressure drop is found to relate to the pressure ratio of the compressor and the expansion valve from which it can be concluded that

$$\frac{P_{cp,i}}{P_{cp,o}} = 0.954\left(\frac{P_{ex,o}}{P_{ex,i}}\right). \quad (3.15)$$

Observed from the results, there is a pressure drop across the condenser which can be expressed as

$$P_{cd,o} = P_{cd,i} - 0.034\,. \tag{3.16}$$

where $P_{cd,i}$ and $P_{cd,o}$ are in MPa.

(d) Direct Contact Evaporator Modeling

The mathematical model for the direct contact evaporator is formulated by lump model. Using the energy balance, the thermal characteristics of the water in the tank can be expressed as

$$\frac{d}{dt}(M_w h_w) + M_t C_t \frac{dT}{dt} = m_r (h_{ev,i} - h_{ev,o}) + (UA)(T_a - T_w). \tag{3.17}$$

As shown in the equation, the first three terms relate to the enthalpy change rates of the water, the container and the refrigerant, respectively. The last term relates to the external heat gain from the surrounding ambient. In this study, the direct contact evaporator is well insulated, the external heat gain then can be neglected. The water temperature of the water inside the tank changes in two steps according to two related processes, which are sensible heat process and ice formation process. The characteristic equations of the direct contact evaporator during the sensible heat process and the ice formation process can be expressed in the following equations, respectively as

$$T_w^{t+\Delta t} = T_w^t + \frac{m_r (h_{ev,i} - h_{ev,o})\Delta t}{M_t C_{pt} + M_w C_{pw}} \tag{3.18}$$

$$M_{ice} = \frac{m_r (h_{ev,o} - h_{ev,i})\Delta t}{L} \tag{3.19}$$

Due to the long length of the pipes between the evaporator unit, the compressor and the condenser in the direct contact experiment set-up, the heat gain and loss can not be ruled out. From the preliminary study, the heat gain between the low temperature refrigerant flowing inside the pipes from the evaporator to the compressor and the surrounding ambient can be characterized as

$$m_r C_{pr} (T_{cp,i} - T_{ev,o}) = f\left(T_a - \left(\frac{T_{ev,o} + T_{cp,i}}{2}\right), m_r\right) \tag{3.20}$$

The results of this part are shown in Fig. 3.12 from where the equation can be expressed as

$$m_r C_{pr}\left(T_{cp,i} - T_{ev,o}\right) = \left[\begin{array}{l} \left(-0.4132 m_r^2 + 0.0409 m_r - 0.0012\right)\left(T_a - \left(\frac{T_{ev,o} + T_{cp,i}}{2}\right)\right)^2 \\ + \left(6.0055 m_r^2 - 0.3648 m_r + 0.0448\right)\left(T_a - \left(\frac{T_{ev,o} + T_{cp,i}}{2}\right)\right) \\ + \left((-38.4022) m_r^2 + 6.243 m_r - 0.2699\right) \end{array}\right] \quad (3.21)$$

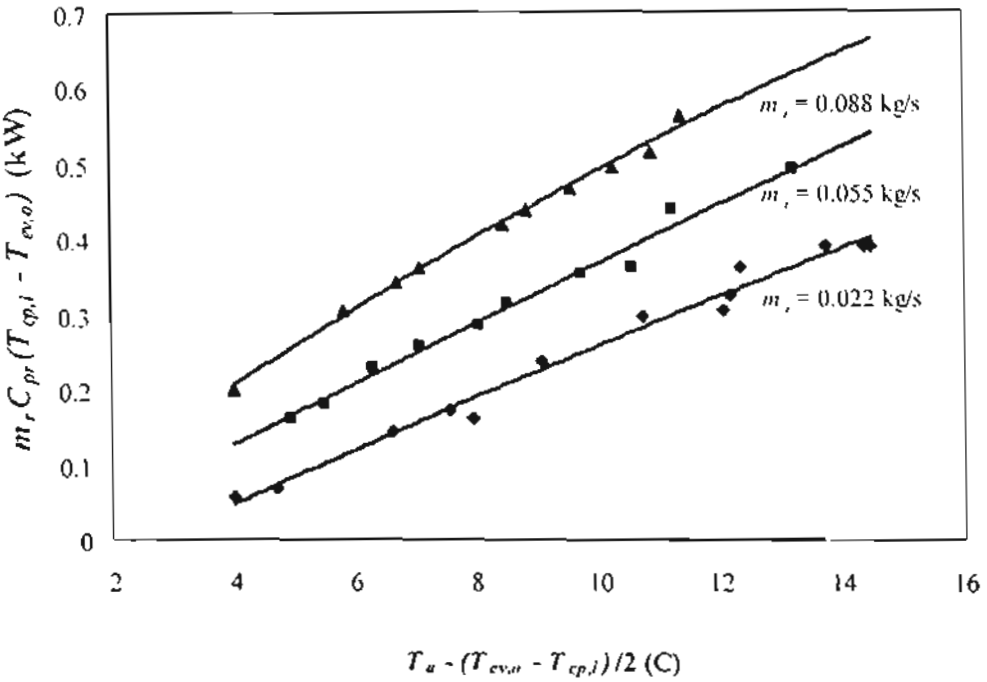

Fig. 3.12. The relation between heat gain through pipes from the evaporator to the compressor and a function of T_a-$(T_{ev,o}$-$T_{cp,i})/2$ (°C).

As the high temperature refrigerant flows through the pipe between the compressor and condenser, the heat loss occurs and can be characterized as

$$m_r C_{pr}\left(T_{cp,o} - T_{cd,i}\right) = f\left(\left(\frac{T_{cp,o} + T_{cd,i}}{2}\right) - T_a, m_r\right). \quad (3.22)$$

The heat loss characteristic is experimentally observed and plotted in Fig. 3.13. The empirical relation between this loss and aforementioned relevant parameters is deducted as

$$m_r C_{pr}\left(T_{cp,o}-T_{cd,i}\right)=\begin{bmatrix}(-0.0001)\left(\left(\frac{T_{cp,o}+T_{cd,i}}{2}\right)-T_a\right)^2\\ \left(1.607m_r^2-0.0298m_r-0.0146\right)\left(\left(\frac{T_{cp,o}+T_{cd,i}}{2}\right)-T_a\right)\\ +\left(-20.432m_r^2+1.9399m_r-0.293\right)\end{bmatrix}. \quad (3.23)$$

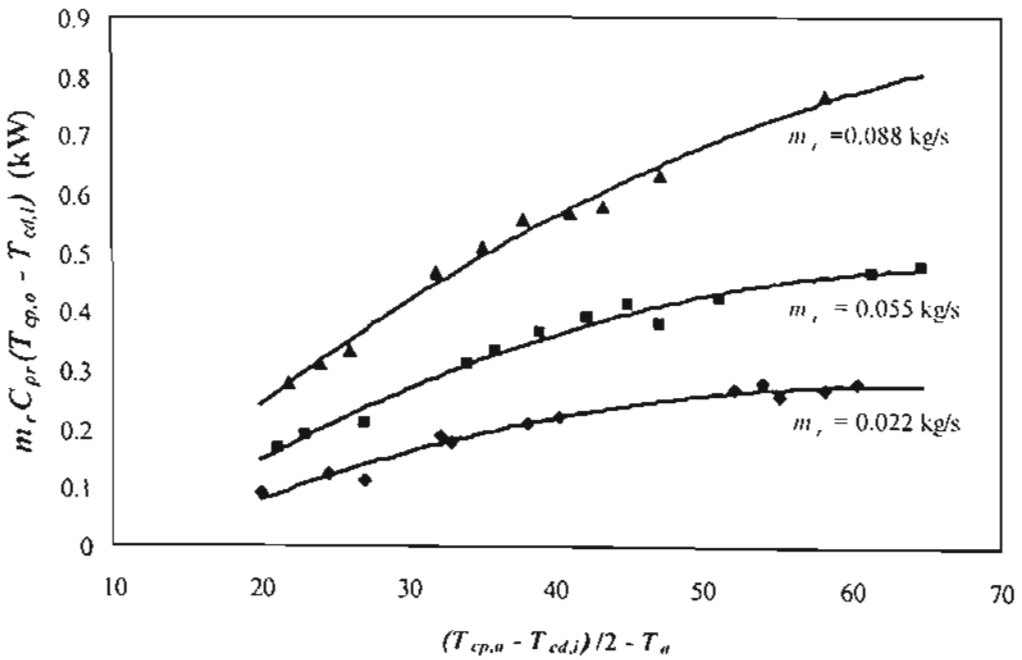

Fig. 3.13. The relation between heat loss through pipes from the compressor to the condenser and a function of $(T_{cp,o}+T_{cd,i})/2 - T_a$ (°C).

CHAPTER 4
SYSTEM SIMULATION

4.1 Simulation Program

With the mathematical modeling of each component in the system, the simulation is created to determine the energy consumption of the system at various possible combinations of the conventional chilled water system and the ice thermal energy storage (ITES) system. The computational steps are shown in Fig. 4.1.

As shown in Fig.4.1, the simulation consists of two parts, chilled water system and ice storage system. The input parameters of the simulation are the total cooling load, Q_{load}; the compressor speed of the ice storage system, N_{dc}; the mass flow rate of the refrigerant for the ice storage system, $m_{r,dc}$; the initial temperature of water in the storage tank, T_{wi}; the ambient temperature, T_{amb} and the properties of the system working fluid.

The cooling load is divided into two parts for chilled water system and ice storage system, $Q_{load,ac}$ and $Q_{load,dc}$. For the chilled water system, the trial and error has been done to find out the suitable mass flow rate of the refrigerant at the given cooling load and the power input of the compressor is also the output parameter. Starting with Eqs. 3.6 and 3.10 and guessing the initial value of mass flow rate of the refrigerant, the pressure ratio is calculated and transferred to the compressor modeling mode. The equations used to calculate the properties of R12 refrigerant or refrigerant equations are as followings [18]:

For the saturated conditions,

$$\ln(P_{sat} \times 10) = -15.6 + 8.96\left(\frac{T_{sat} + 273.15}{100}\right) - 1.038\left(\frac{T_{sat} + 273.15}{100}\right)^2 \qquad (4.1)$$

$$h_f = -239.8 + 100.6\left(\frac{T_{sat} + 273.15}{100}\right) \qquad (4.2)$$

$$h_g = 187.28 + 0.4722\left(T_{sat}\right) \qquad (4.3)$$

The suffixes "*f*" and "*g*" refer to saturated liquid and saturated gas conditions, respectively and the suffix "*sat*" refers to saturated condition.

For superheated conditions,

$$h = 173.52 + 13.01(\ln(P \times 10)) + (0.57 + 0.0826 \ln(P \times 10))(T - T_{sat}) \qquad (4.4)$$

P and T are pressure and temperature in MPa and K, respectively and h is the specific enthalpy in kJ/kg.

By using Eqs. 3.1 – 3.4 and Eqs. 4.1-4.4, the pressures and the temperatures at the inlet and the outlet of the compressor are calculated. The compressor work is also found out. The outlet pressure and temperature of the compressor are the input conditions for the condenser. Then, using Eq. 3.5 and Eqs. 4.1-4.4, the heat transfer rate of the condenser and the outlet pressure and the temperature of the condenser are calculated. These values are then transferred for the expansion valve. By assuming the isenthalpic process (enthalpy is assumed to be constant during a preocess), the outlet pressure and temperature of the expansion valve are evaluated and sent to the chiller. After that, the heat load of the chiller is calculated by using Eqs. 3.7 – 3.9 and the refrigerant equation. The heat load of the chiller is compared with the initial value of the input cooling load of the chilled water system. If the difference is not significant, the calculation will be stopped and the power input of the compressor, the heat transfer rates at the condenser and the chiller are the output results of the program. Otherwise, the program is calculated by using the new value of the mass flow rate of the refrigerant.

For the ice storage part, the method for transfer data through each component in this system is the same as the chilled water system. Note that, the leaving temperature of the refrigerant of the ice storage tank is equal to the temperature of the water in the tank because of high turbulence due to the refrigerant injection into the water tank. When the temperature of water is higher than 0.01°C, the calculation is in sensible heat mode. As the water temperature is lower than 0.01°C, the latent heat mode is applied. The outputs of this part are the power consumption at the compressor, the heat transfer rate of the direct contact evaporator and the time consumed for producing ice.

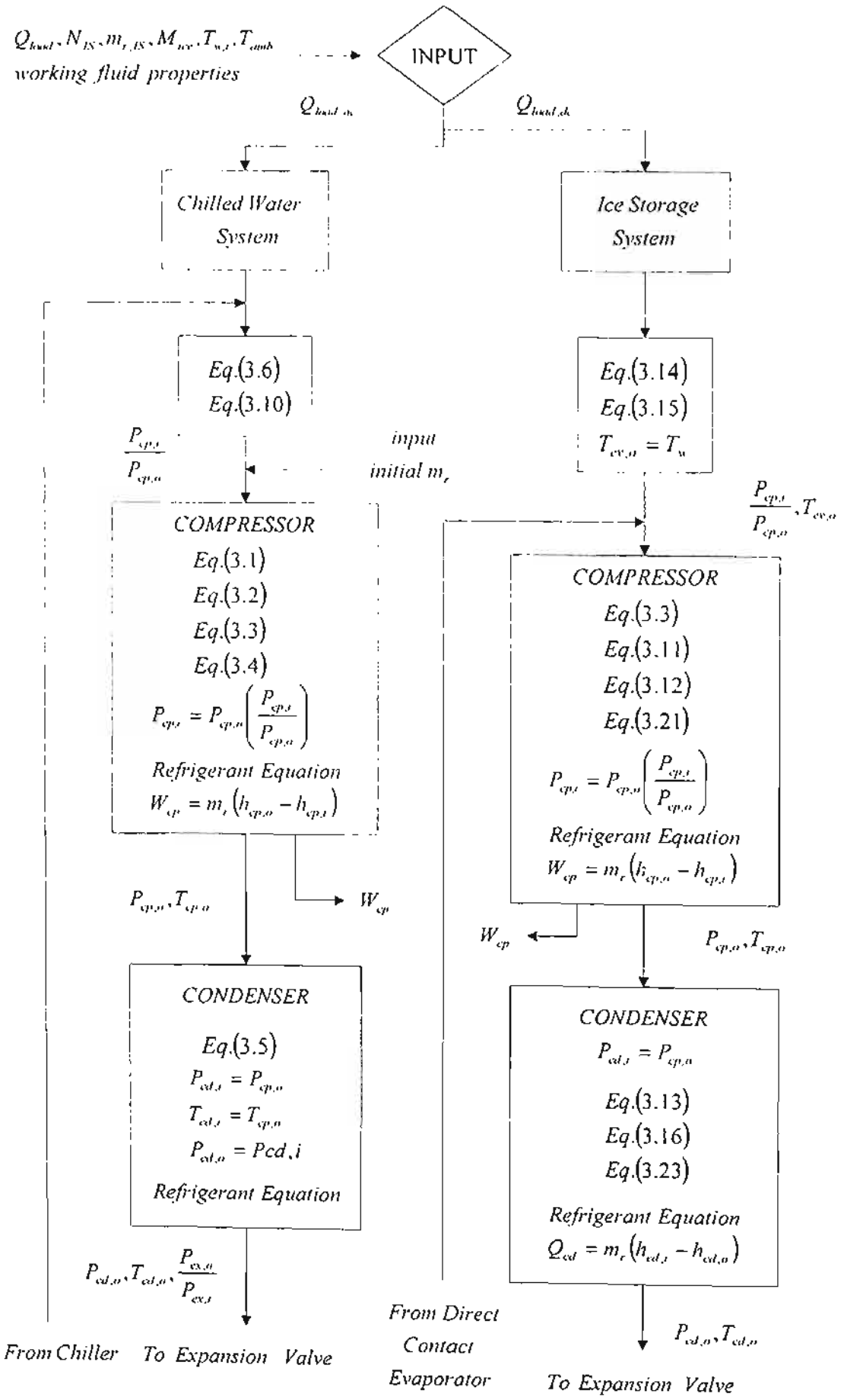

Fig. 4.1. Information flow diagram of the system simulation.

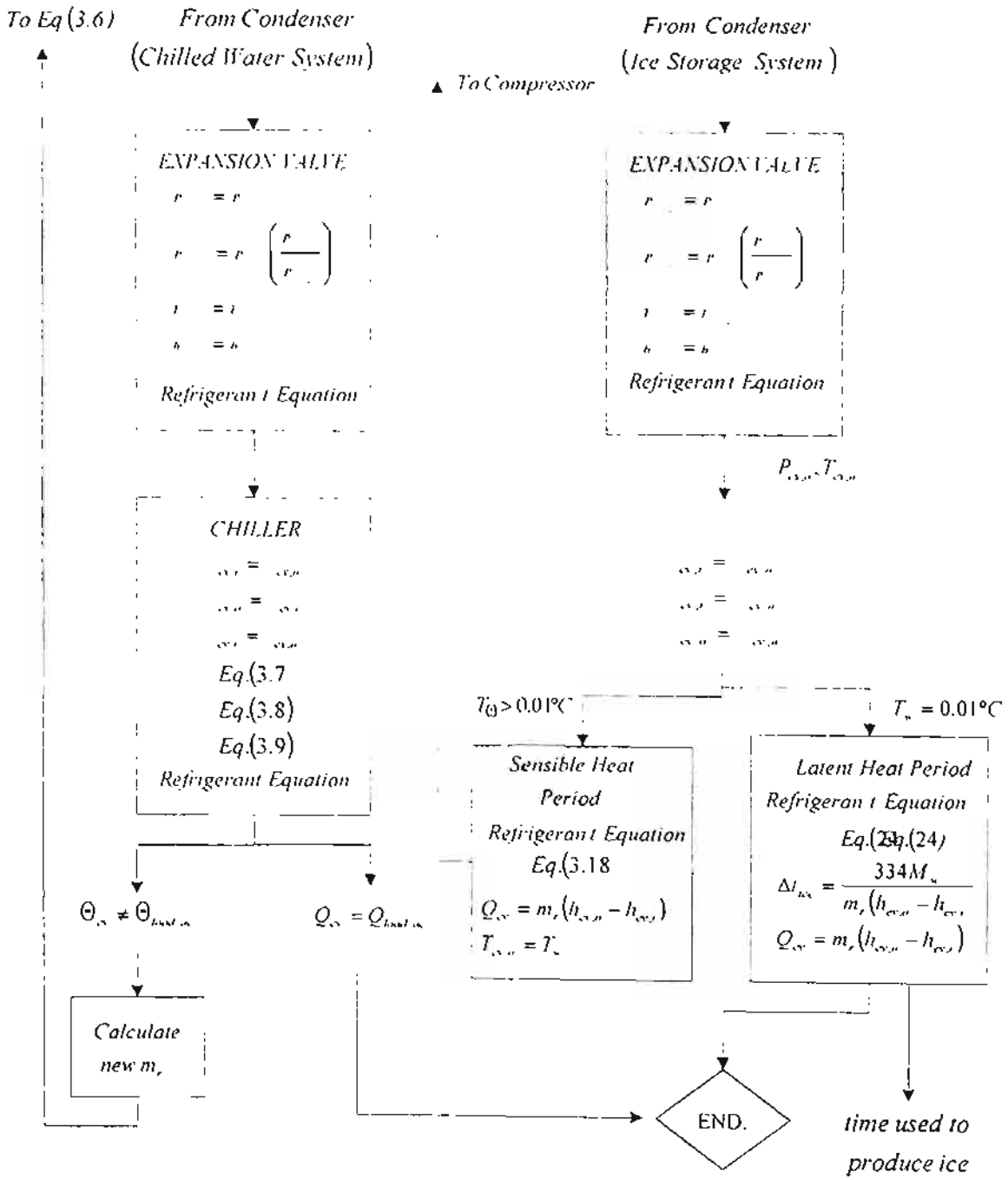

Fig. 4.1. Information flow diagram of the system simulation (continued).

4.2 Simulation Results

4.2.1 Chilled water system

In the chilled water system part of the simulation program, after input the initial values of the variables, which are cooling load, refrigerant mass flow rate and ambient temperature, the compressor work and the heat transfer rate at the chiller are evaluated. From the experiments, the pressures and the temperatures of the refrigerant are measured at the inlet and the outlet of the compressor and the chiller. Therefore, the compressor work and the heat transfer rate at the chiller can be found out from

$$W_{cp} = m_r \left(h_{cp,o} - h_{cp,i} \right) \tag{4.5}$$

and

$$Q_{ch} = m_r \left(h_{ch,o} - h_{ch,i} \right) \tag{4.6}$$

The results from the simulation are compared to those of the experiments. The results are illustrated in Figs. 4.2-4.3.

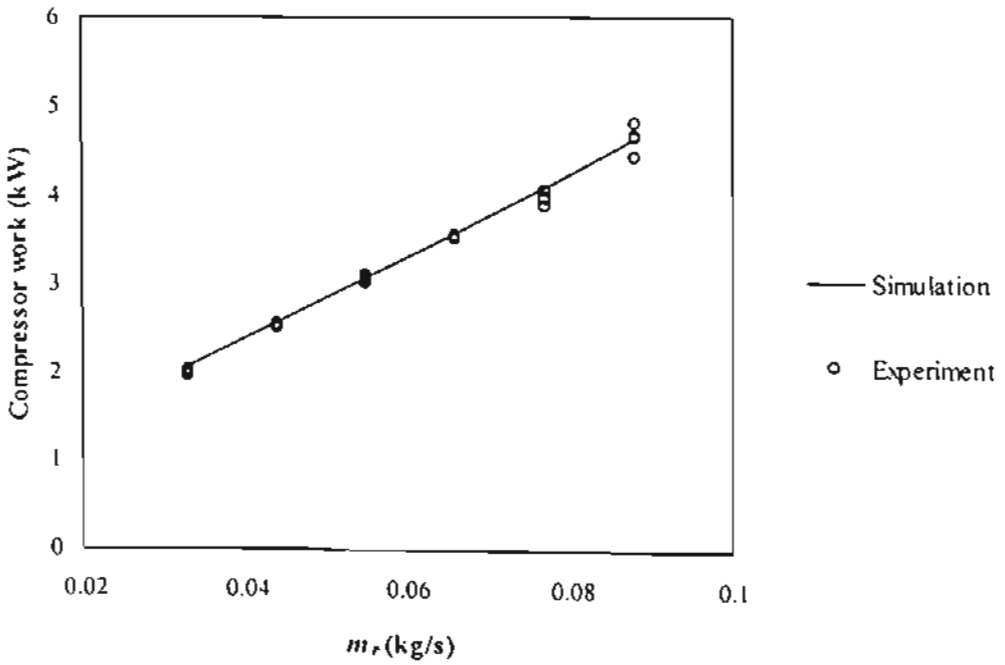

Fig. 4.2. Compressor work of the chilled water system at various refrigerant mass flow rates.

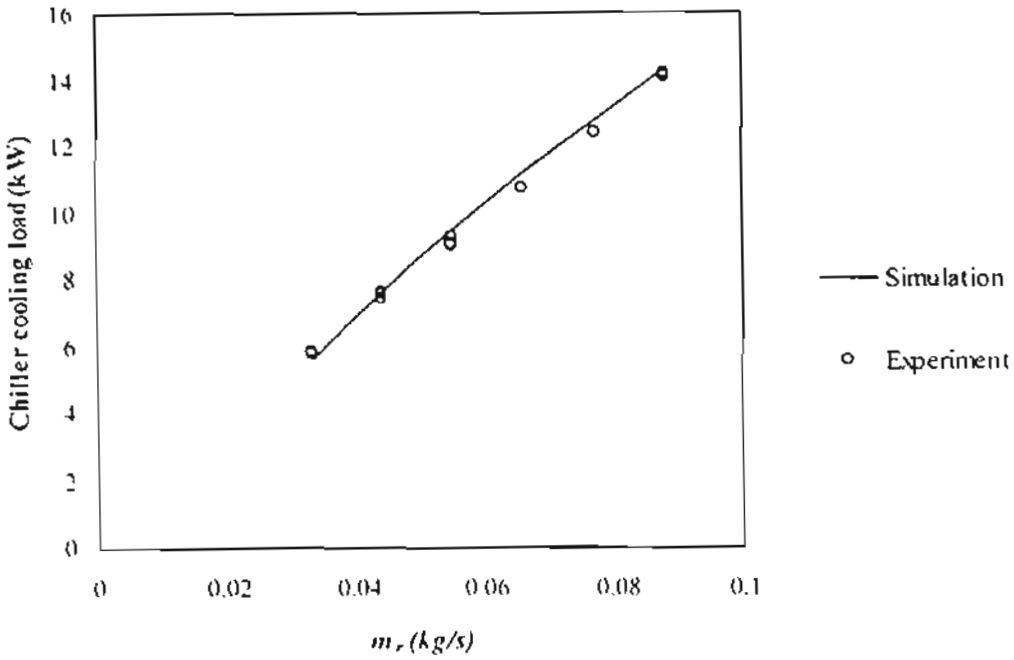

Fig. 4.3. The chiller cooling load at various refrigerant mass flow rates.

From the results, it could be found that the compressor work and the heat transfer rate depend on the refrigerant mass flow rate. As the refrigerant mass flow rate increases, these values are also increased. Moreover, it is noted that the values from the simulation program are closed to the experimental results within 5% error.

4.2.2 Ice storage system

(a) Ice producing process

For the ice storage simulation, the compressor work, the heat transfer rate at the direct contact evaporator and the time used to produce ice are evaluated. At any given value of the refrigerant mass flow rate, the compressor speed and amount of the water in the storage tank, the results from the experiments and the simulation are compared. The compressor work and the heat transfer rate from the experiments are found out by the same method as in the chilled water system. To compare the time used for producing ice, the system is operated for the certain period that firstly calculated from the simulation. After the system is shut off, the water that remains in the storage tank are drained out and measured. The amount of the remained water is compared to the input value of water in the tank to find out the amount of the

produced ice. The results of the experiments and the simulations are shown in Figs. 4.4-4.5 and Table 4.1.

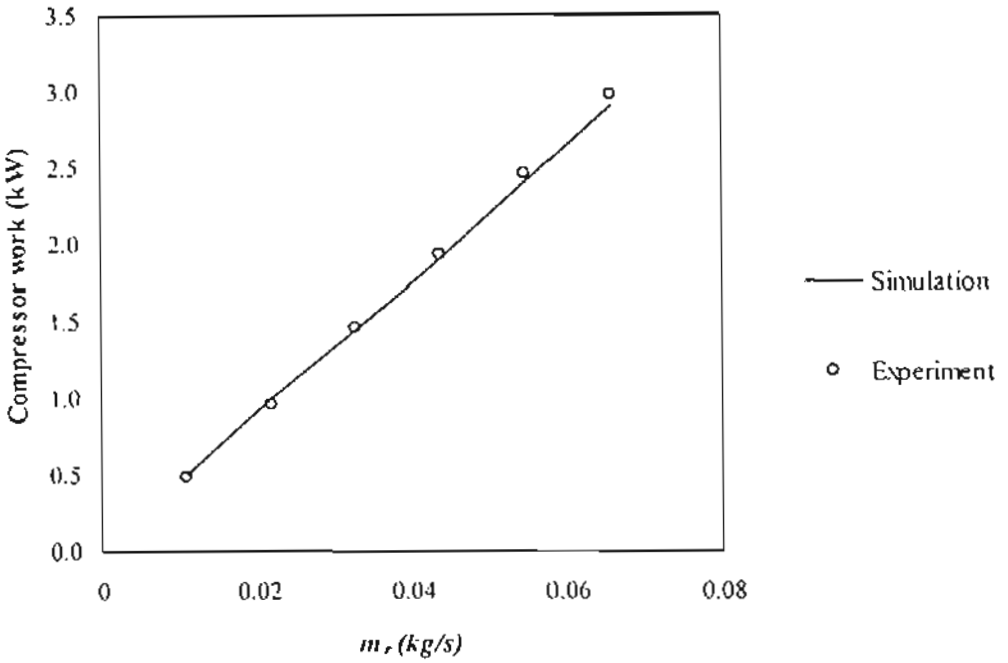

Fig. 4.4. Compressor work of the ice storage system at various refrigerant mass flow rates.

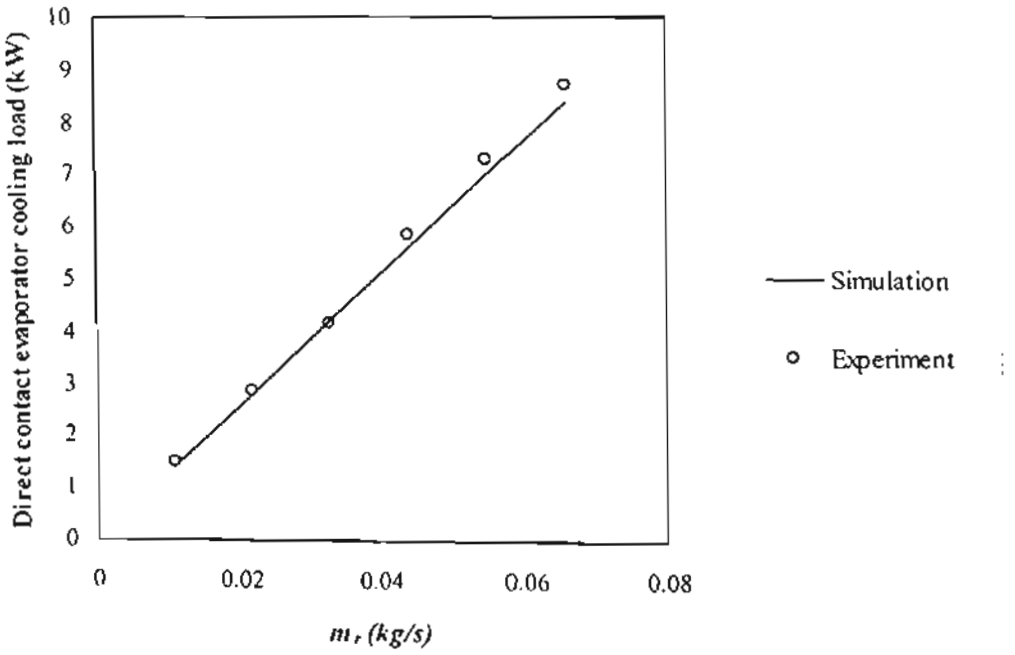

Fig. 4.5. The direct contact evaporator load at various refrigerant mass flow rates.

As shown in Figs. 4.4-4.5, the refrigerant mass flow rate has an effect on the both of the compressor work and the heat transfer rate at the direct contact evaporator. As the mass flow rate increases, the compressor work and the heat transfer rate are also increased. The estimated results agree well with the experimental data within 5% error.

For Table 4.1, with the simulation described before, the time used to produce the required amount of the ice is determined under the assumption that the water in the storage tank is completely turned to be the ice. The amount of the ice calculated from the simulation is also close to that of the experiment.

Table 4.1.The comparison of ice formation between the simulation and the experiment.

Mass of water in storage tank (kg)	m_r (kg/s)	N (rps)	Initial water temp. (°C)	T_{amb} (°C)	Produced ice mass (kg) (sim.)	Time (hr) (sim.)	Produced ice mass (kg) (exp.)	Time (hr) (exp.)
250	0.077	11.8	18.0	29.2	250	3.66	212	3.59
250	0.100	11.8	16.5	30.2	250	3.11	209	3.23
300	0.066	11.8	15.0	28.5	300	5.01	272	4.98
300	0.100	11.8	15.4	26.8	300	3.67	269	3.62

(b) Ice melting process

In this section, the experiment is divided into three parts. First, 200 kg of the ice is produced by the ice storage system and kept in the storage tank. Then, turn off the ITES system and start the second part of the experiment. At this period, the chilled water system is operated at 0.055 kg/s of refrigerant and 0.3833 kg/s of chilled water to support the cooling requirement. The results of the heat transfer rate at chiller could be shown in the first part of Fig. 4.6 (0 – 75 min.). Then, the return-chilled water bypass to the storage tank before turns back to the chiller. The overall heat transfer rate of the chiller including the heat exchange in the storage tank are shown in the second part of Fig. 4.6. Moreover, the values from the experiment are also compared to those of the simulation. It could be found that the experimental results agree well with simulation.

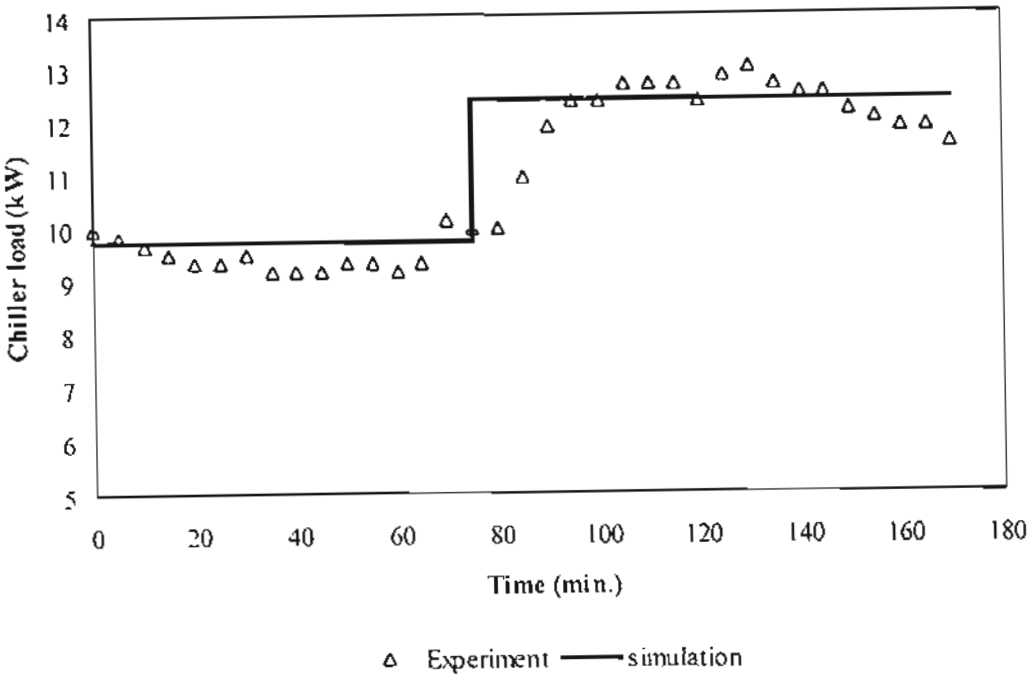

Fig. 4.6 Comparison of the ice melting process.

4.3 System Performance

Since the simulation could be used to estimate the results of the experiment as shown in the previous section, the performance curves of the chilled water system and the ice storage system are created by using the simulation program. The results are illustrated in Figs. 4.7- 4.8.

As the refrigerant mass flow rate is varied for both systems while the compressor speed is varied for only the chilled water system, the coefficient of performance (COP) of the chilled water system depends only on the refrigerant mass flow rates. The highest value of COP for this system shown in Fig. 4.7 is about 3.1 at 0.06 – 0.08 kg/s of refrigerant.

For the ice storage system, COP of the system is higher at higher compressor speed. However, it could be found from the experiments that the condensing temperature of the condenser in the case of adjusting 7.1 rps of compressor speed is approximately 21°C which is lower than the average ambient temperature in summer and rainy season. While the condensing temperature in the case of 9.5 rps is about 29°C which could be caused the heat transfer between the

condenser and the surrounding. Thus, 7.1 rps of the compressor speed is not reasonable. As shown in Fig. 4.8, in the case of 9.5 and 11.8 rps of compressor speed, the refrigerant mass flow rate has slight effect on COP.

Then to operate the combination of chilled water system and ice storage system, the recommended refrigerant mass flow rates are 0.06 – 0.08 kg/s for chilled water system and 0.08-0.09 kg/s which causes the least period of time to produce the amount of the for the ice storage system. The compressor speed for the ITES system should be 9.5 rps due to the high value of COP

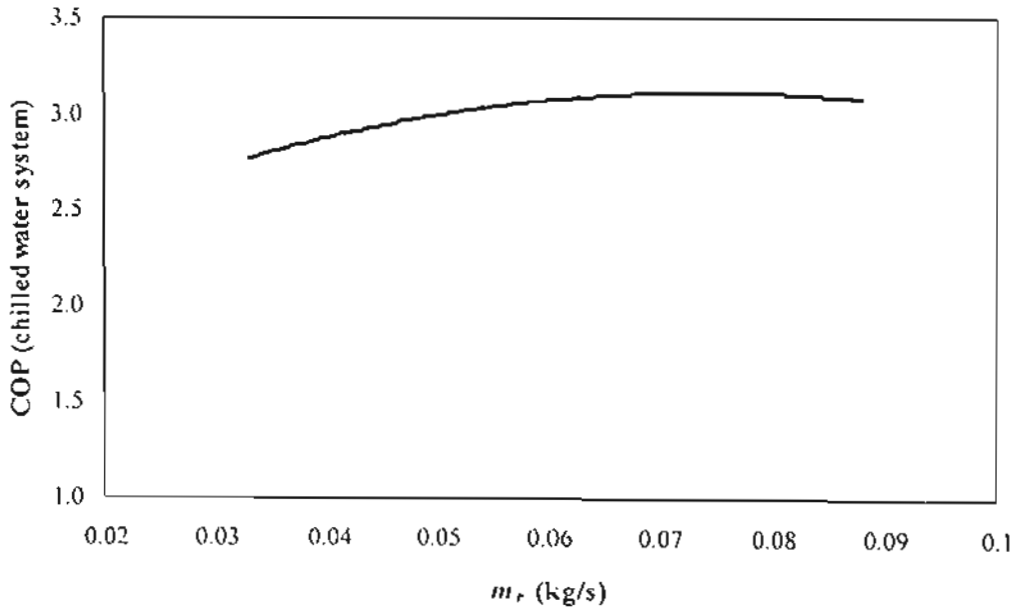

Fig. 4.7. COP of chilled water system.

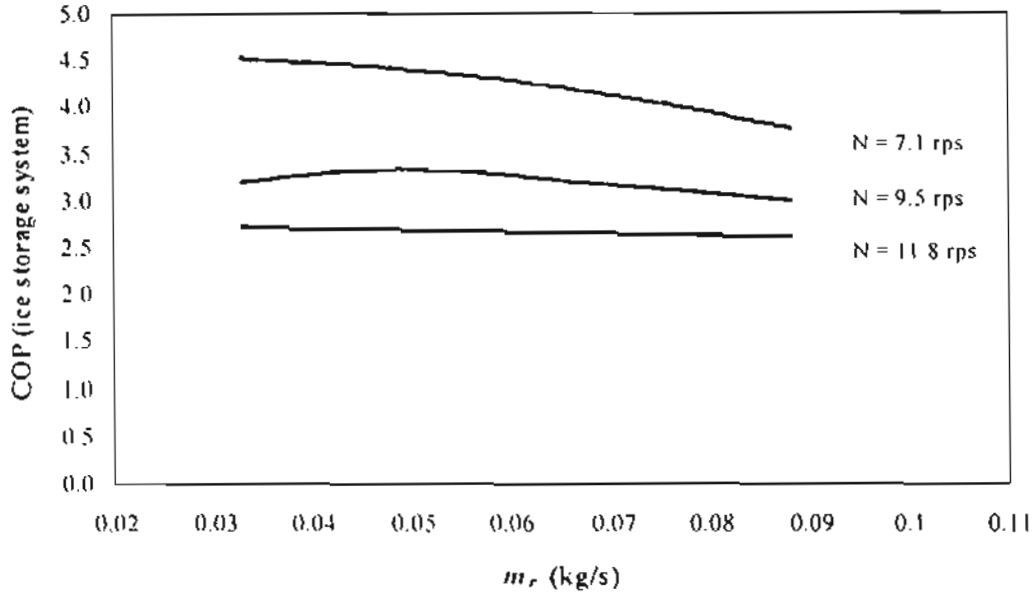

Fig. 4.8. COP of ice storage system.

CHAPTER 5
ELECTRICITY CHARGE SAVING

5.1 Conditions of the Tested Office

The ice thermal energy storage system with direct contact evaporator considered in this research work is operated to support the cooling requirement of the selected office in Chiang Mai University. The office contains 4 laboratories on the first floor, 9 working rooms on the second floor and an auditorium. The characteristics of the electrical energy consumption of the office are as following:

- Electricity consumption during the year 33,954 kW-hr/year
- Maximum energy demand 49.4 kW
- Load factor 0.325
- Power factor 0.69

From the investigation, the electrical energy is consumed in three main parts, air conditioning system, lighting, and other appliances. The portion of the energy consumption in each source is as following Table and Fig.5.1:

Table 5.1. The electrical energy consumed in the office

Part	Energy consumption (kW-hr/year)
Air conditioning system	15,306
Lighting	11,102
Others	7,546
Total	33,954

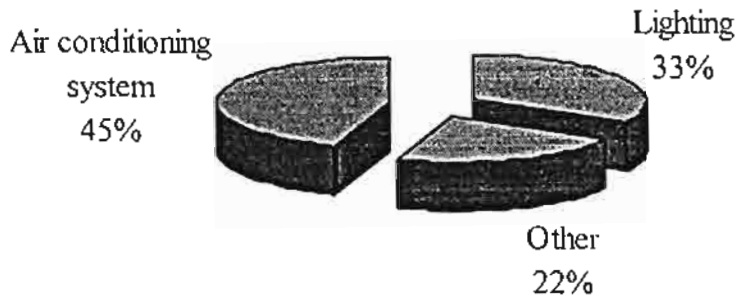

Fig. 5.1. The portion of the electricity consumption in different parts

The experimental unit is provided only for the working rooms which are room R1 to R5 as illustrated in Fig.5.2.The primary condition data stipulated for office cooling load calculation is shown in Table 5.2 and Fig. 5.3.

Table 5.2 The characteristic of the selected office (R1 to R5)

Facing	Description of Construction			
	Office Envelopes	Area (m^2)	Material	Overall Heat Transfer Coefficient (U)(W/m^2-K)
North	- Wall	23.35	80 mm. thick brick, both sides furnish with 10 mm. plaster	2.04
	- Window (1)	25.65	5 mm. thick cool gray glass	2.90
	- Window (2)	22.5	5 mm. thick glass	2.95
West	- Wall	8.35	80 mm. thick brick, both sides furnish with 10 mm. plaster	2.04
	- Window (1)	8.55	5 mm. thick cool gray glass	2.90
South	- Partition	62.5	Hollow concrete block	2.56
	- Door	9	35 mm. thick wood door	2.95
East	- Partition	16.9	Hollow concrete block	2.56
Floor	-	178.75	10 cm. Thick reinforced concrete	1.42
Roof	-	-	5 mm. ceramic 22.5° inclined	0.619
Ceiling	-	178.75	10 mm. gypsum	1.53

Since the selected office locates in Chiang Mai city, the outdoor and indoor conditions for calculating the cooling load on the design day is shown in Table 5.3.

Table 5.3. Design conditions under the design day [17].

Condition	Description
Inside condition	
- Dry bulb temperature	25°C (77°F)
- Relative humidity	50% RH
- Number of people	20 people
- Occupancy period	8.00 a.m. – 5.00 p.m.
Outside condition	
- Dry bulb temperature	35°C (95°F)
- Relative humidity	65% RH

The result of cooling load calculation of the selected office on the design day and the average cooling load in each month based on the temperature data in year 1998 are shown in Table 5.4 and Fig. 5.4.

Table 5.4. The result of the cooling load calculation of the selected office on the design day.

Description	Heat gain (W)	
Solar radiation through transparent surfaces	3284.92	
Heat conduction through exterior walls and roofs	1211.07	
Heat conduction through interior partitions, ceilings and floors	3706.87	
	Sensible	Latent
Heat generated within the space by occupants, lights and appliances	2730.50	1138.31
Energy transfer as a result of ventilation and infiltration of outdoor air	3887.47	1495.79
Total heat gain (W)	6617.97	2634.10
Total heat gain (W)	17454.93	

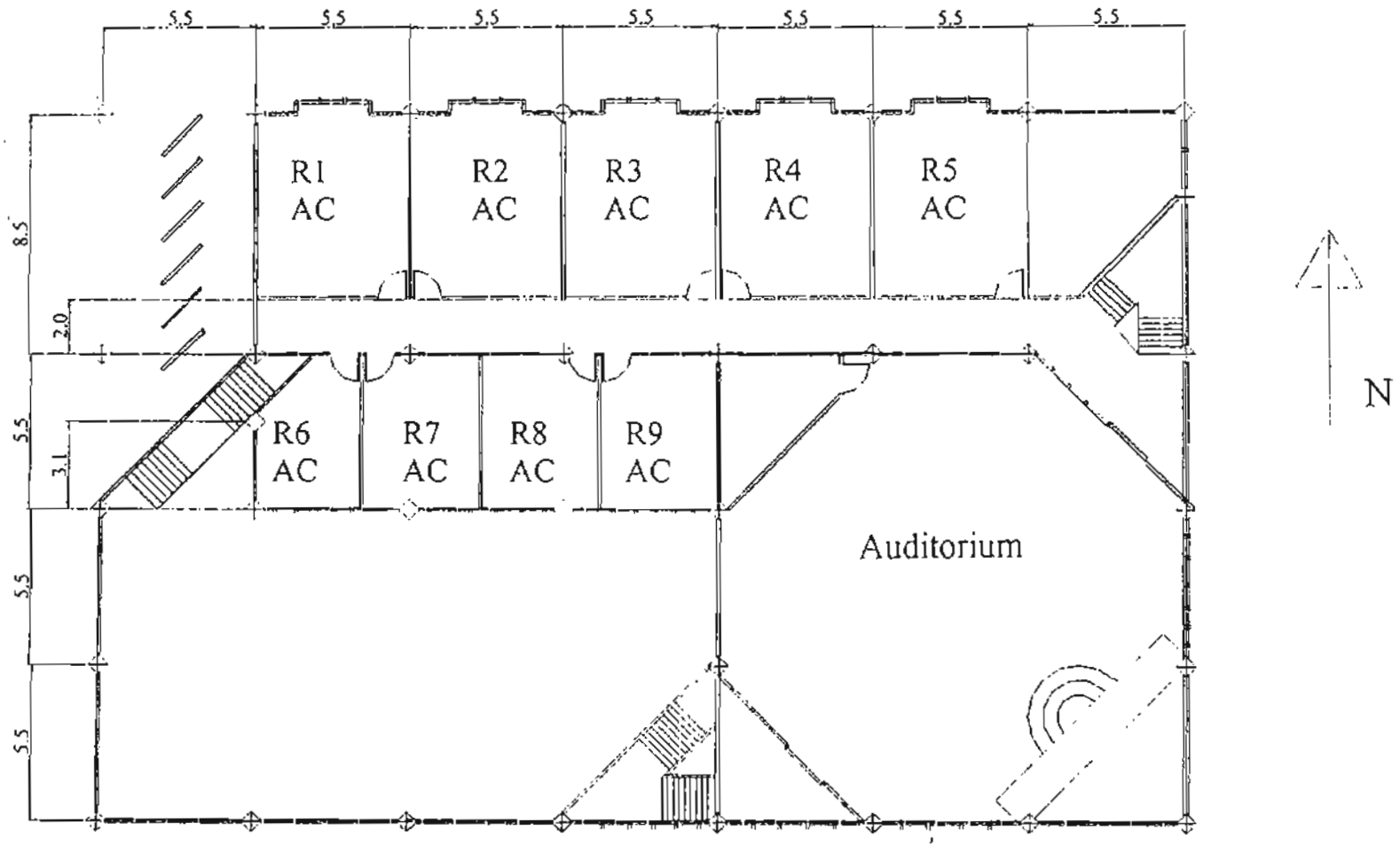

Fig. 5.2. Selected office plan (all dimensions are in meter).

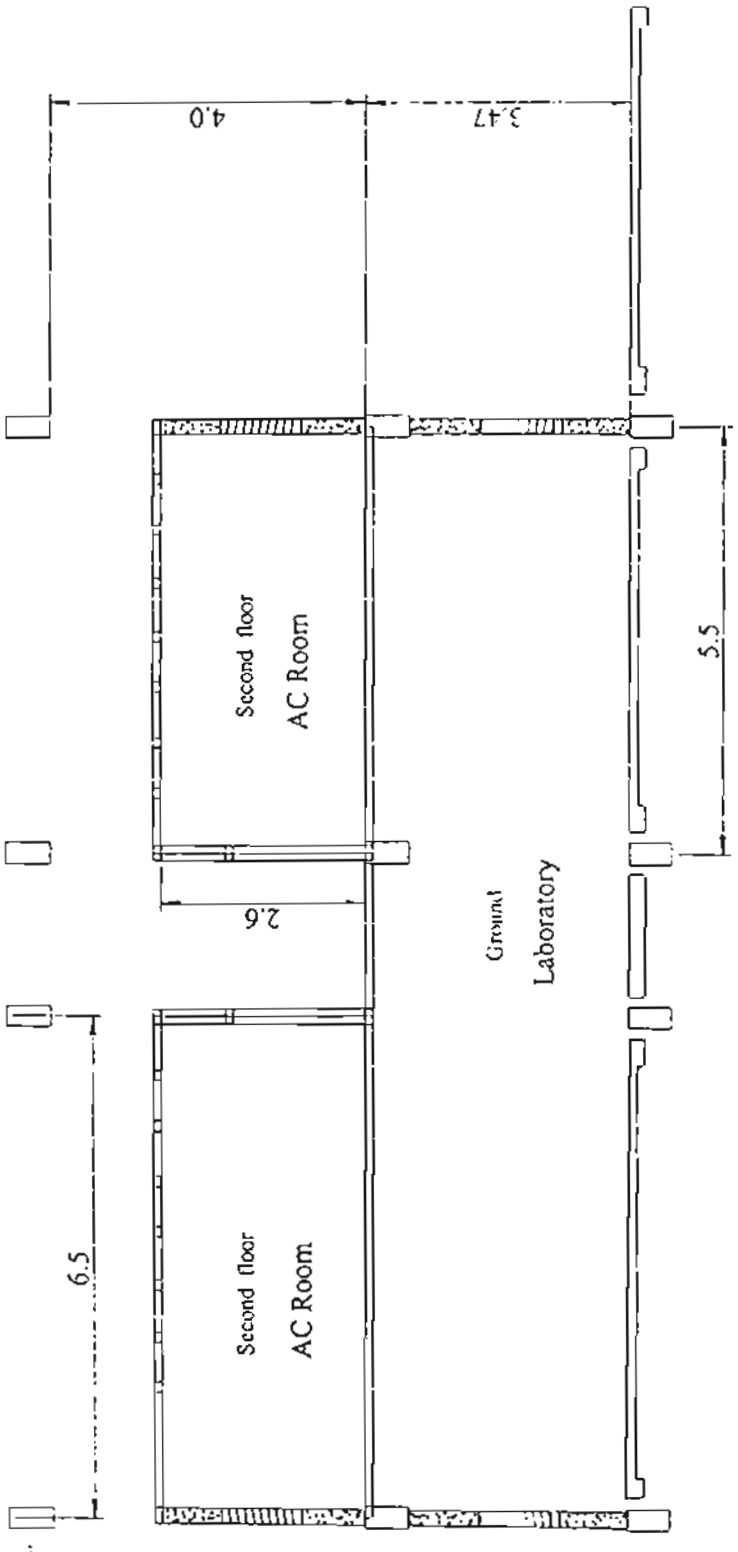

Fig. 5.3. Cross section view of the selected office (all dimensions are in meter).

Moreover, the cooling load profile of the selected office during the year is also carried out as shown in Fig. 5.4. It is calculated from average temperature and average relative humidity during the month based on the data in year 1998 [18].

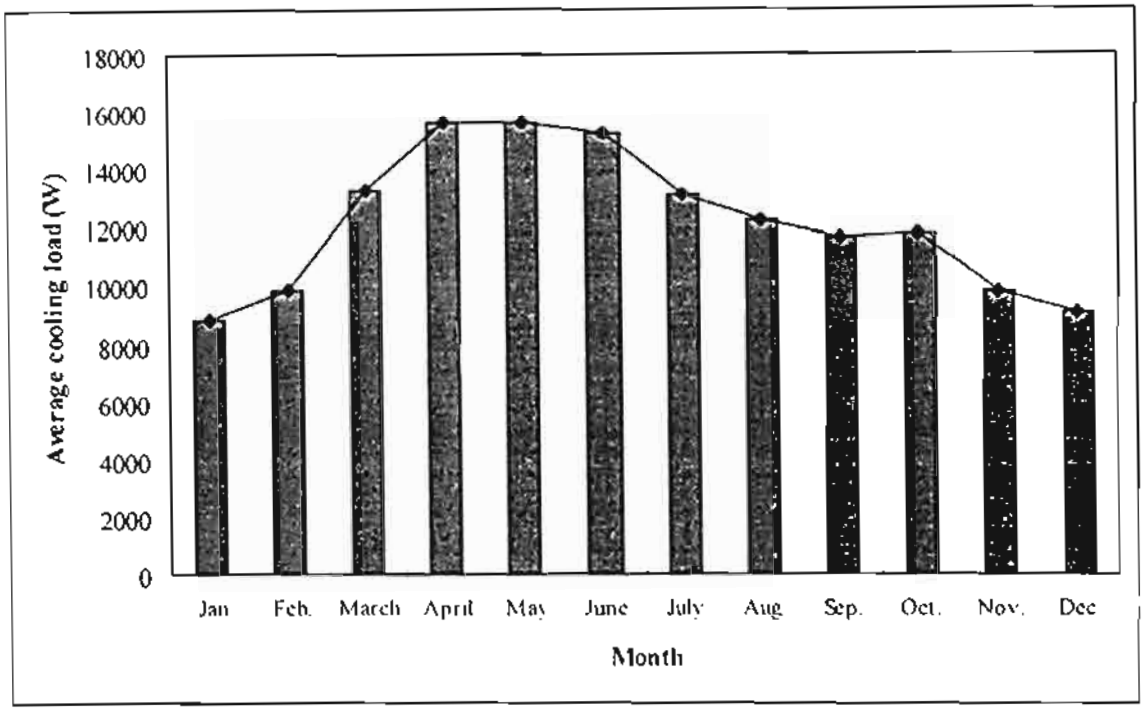

Fig. 5.4 The average cooling load of the selected office during the year.

It could be found that the amount of cooling requirement can be divided into three groups, low, medium and high cooling load. The maximum cooling load is in summer period whereas in April, May and June. While the medium and low cooling loads are occurred in rainy season and winter, respectively. The design day explained in last section is in April. From the temperature data, it is noted that during winter period, although the cooling load is about 9,000 kW-hr/day as shown in Fig. 5.4, the air conditioning system is seldom used due to the low outdoor temperature.

5.2 Appropriate Sizing of the Ice Storage

In this research work, the selected office having 18 kW of maximum design cooling requirement is considered as a case study. Six different air conditioning system combinations have been investigated to determine the appropriate possible combinations which relates to the electricity tariff (TOU rate) as shown in Table 5.5 [1].

Table 5.5. Electricity costs (TOU Rate) for commercial building.

Voltage	Demand Charge (Baht/kW)	Energy Charge (Baht/unit)			Service Charge (Baht/month)
	1*	1*	2*	3*	
>115 kV	102.80	1.5349	0.6671	0.6062	400.00
69 kV	158.88	1.6292	0.6769	0.6153	400.00
22 – 33 kV	200.93	1.7736	0.6861	0.6236	850.00
< 22 kV	214.95	1.8891	0.7283	0.6616	850.00

1* Monday – Saturday 09.00 – 22.00 (On peak)

2* Monday – Saturday 22.00 – 09.00 (Off peak)

3* Sunday 00.00 – 24.00 (Off peak)

The six categories are as the following:

Category 1. Conventional design (no ice storage). The entire cooling requirement is supported by the chiller unit operating during the occupancy period.

Categories 2-5. Partial storage design. The chiller unit is responsible for the less cooling requirement compared to the conventional system. The cooling load is divided into two parts. The first part is supported by the chiller unit during the occupancy time and the other is supported by the ice produced in the ice storage or ITES system operating during the nighttime. The capacity of the chiller unit (TR) that is responsible for the base cooling load in categories 2-5 are 4, 3, 2 and 1 TR, respectively.

Category 6 Full storage design. The entire cooling requirement is supported by the ice storage system. The chiller unit is not provided in this case.

The peak energy demand (kW), the energy consumption (kW-h) and the electricity charge (baht) of each category are considered under the assumptions that

(1) The refrigerant mass flow rate of the chilled water system is varied based on the responsible cooling requirement.

(2) The ice storage system is operated at 0.088 kg/s of refrigerant mass flow rate and 9.5 rps of compressor speed.

(3) The sufficient amount of the ice is produced and completely used in each day.

(4) The value of cooling requirement based on the temperature and humidity data in year 1998.

Table 5.6 shows the peak energy demand occurred during on-peak period of the design day at various categories. The capacity of the chilled water system is decreased in accordance with a number sequence. As the chilled water is responsible for fewer cooling requirement, the ice storage system have to be responsible for more cooling load. The results shows that the peak energy demand during the on-peak period decreases when the cooling load is more shift to the ice storage system. This is due to the fact that the load of the compressor in the chilled water system is shifted to the ice storage system compressor running during the off-peak period. However, for categories 5 and 6, the required period for generating ice is more than 11 hrs which is the limited time for off-peak period as shown in Table 5.5. Then the compressor load of the ice storage overlaps to that of the chilled water system in the on-peak period.

Table 5.6. The peak energy demand occurred during on-peak period at various categories on the design day.

Category	Peak energy demand		
	Chilled water system (kW)	Ice storage system (kW)	Total (kW)
1	9.7	-	9.7
2	7.0	-	7.0
3	5.3	-	5.3
4	3.8	-	3.8
5	2.2	3.7	5.9
6	0	3.7	3.7

Fig. 5.5 shows the electrical energy consumption of the system in each category. As the cooling load responsible by the ice storage system increases, the energy consumption of the chiller decreases and that of the storage increases. However, in categories 1 – 4, the energy consumption of both systems does not occur at the same time. The chilled water system consumes energy during the daytime while the ice storage consumes during the nighttime. Similar to Table 5.6, in categories 5 – 6, the energy consumption of the ice storage system overlaps to that of chilled water system. From all of the results, it makes certain that the ITES technology is not the energy conservation. It is the energy management.

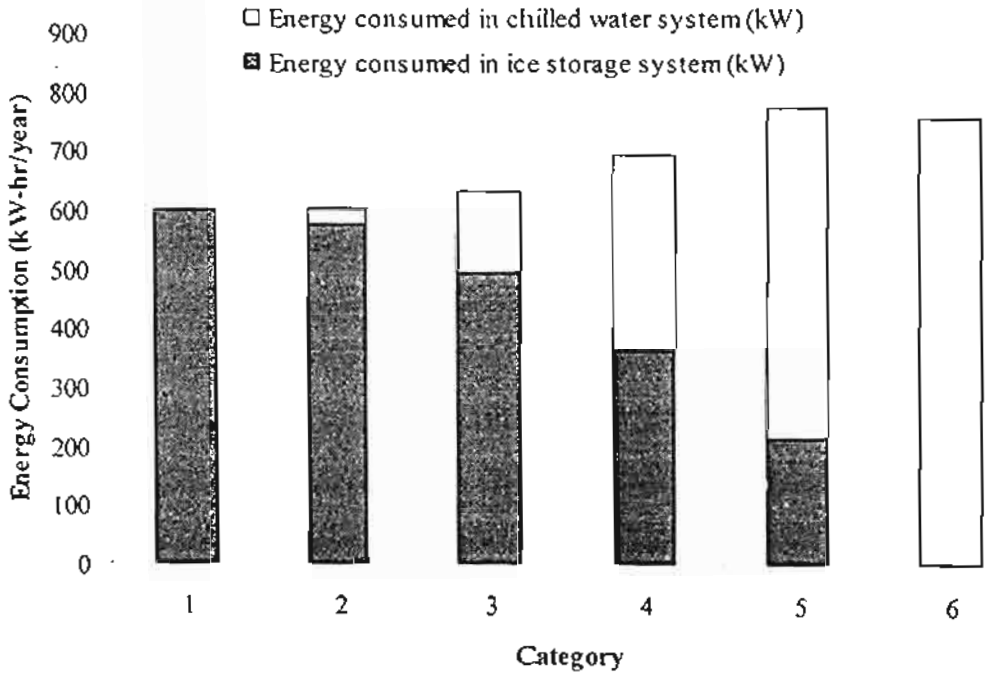

Fig. 5.5. Energy consumed during the year in each category.

To determine the electricity charge, it could be seen that the appropriate design is the 5th category which of the cheapest charge is obtained as shown in Fig. 5.6. At this condition, the energy demand and energy consumption from the daytime could be shifted to the nighttime when the tariff is lowest. The peak energy demand from 9.7 kW in case of the conventional unit (1st category) could be reduced to 5.9 kW (39.2% decreased). The total electricity charge is reduced from 33,720 baht/year for conventional system to 22,940 baht/year resulting in 32% reduction.

Fig. 5.5 shows the electrical energy consumption of the system in each category. As the cooling load responsible by the ice storage system increases, the energy consumption of the chiller decreases and that of the storage increases. However, in categories 1 – 4, the energy consumption of both systems does not occur at the same time. The chilled water system consumes energy during the daytime while the ice storage consumes during the nighttime. Similar to Table 5.6, in categories 5 – 6, the energy consumption of the ice storage system overlaps to that of chilled water system. From all of the results, it makes certain that the ITES technology is not the energy conservation. It is the energy management.

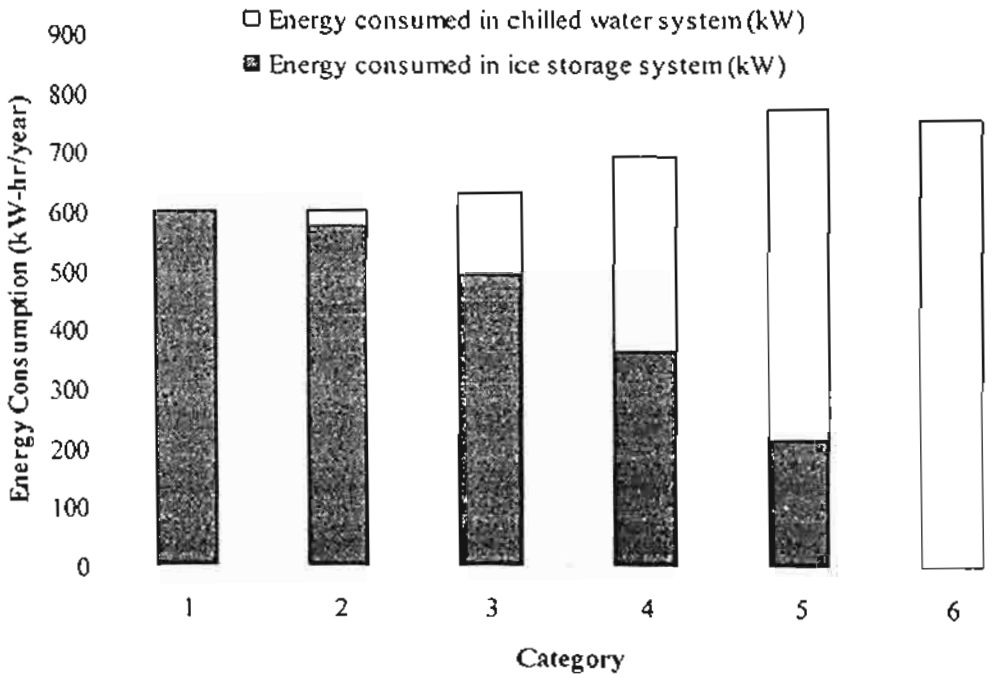

Fig. 5.5. Energy consumed during the year in each category.

To determine the electricity charge, it could be seen that the appropriate design is the 5th category which of the cheapest charge is obtained as shown in Fig. 5.6. At this condition, the energy demand and energy consumption from the daytime could be shifted to the nighttime when the tariff is lowest. The peak energy demand from 9.7 kW in case of the conventional unit (1st category) could be reduced to 5.9 kW (39.2% decreased). The total electricity charge is reduced from 33,720 baht/year for conventional system to 22,940 baht/year resulting in 32% reduction.

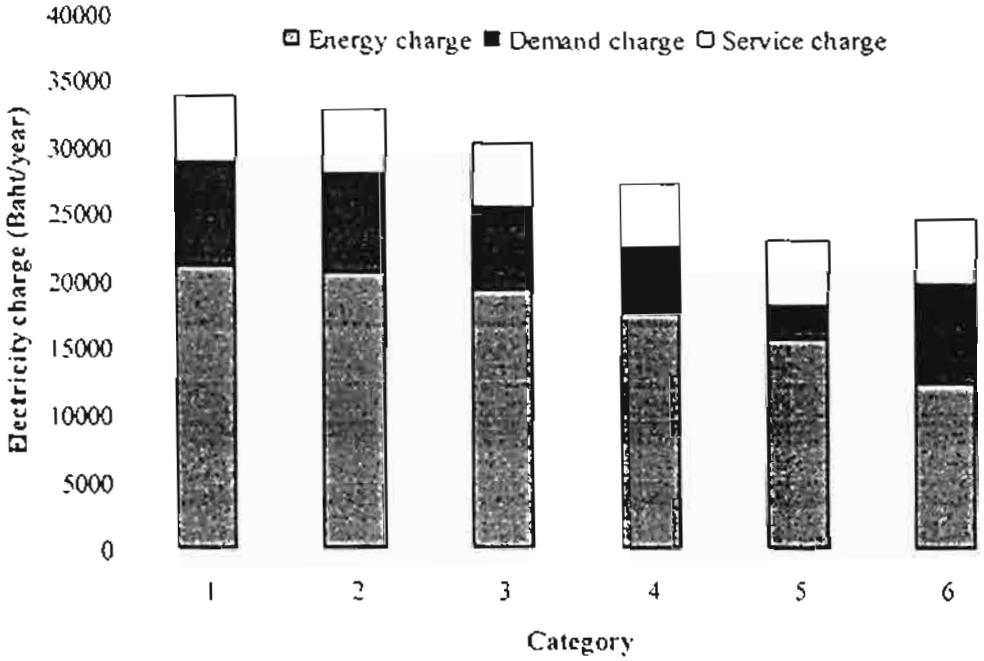

Fig. 5.6. Electricity charge during the year in each category.

Since the 5th category selected in this research work offers the significant economic as shown in Table 5.7 and the installation cost of the ice storage system is as in Table 5.8, it could be found that this system yields a realistic payback.

Table 5.7. Electricity charge of the office during the year due to the 5th category system combination.

Month	Electricity charge (Baht)	
	Conventional System	ITES System
January	2,284	1,585
February	2,229	1,520
March	2,939	1,814
April	3,545	2,513
May	3,536	2,504
June	3,368	2,376
July	3,099	1,931
August	2,702	1,744
September	2,699	1,758

Table 5.7. Electricity charge of the office during the year due to the 5th category system combination (continued).

Month	Electricity charge (Baht)	
	Conventional System	ITES System
October	2,790	1,822
November	2,221	1,513
December	2,311	1,862
Total	33,723	22,942

Table 5.8. The installation cost of the ice storage system.

Component Lists	Cost (Baht)
Compressor	15,000
Condensing	10,000
Direct contact evaporator tank	35,000
Nozzle	3,000
Compressor control motor	5,000
Accessories	5,000
Piping	1,000
Total	74,000

As the ITES system could reduce the electricity charge 10,781 baht/year comparing to the conventional system, the payback period approximately 9 years. It is calculated by the future worth of a uniform series of amounts method. The rate of interest is 8 percent, compounded annually. The rate of inflation is 2.5 percent.

CHAPTER 6
CONCLUSION AND RECOMMENDATION

6.1 Conclusions

6.2.1 The mathematical models of each main component in both of the chilled water system and the ice thermal energy storage with direct contact evaporator are created at various mass flow rates and compressor speeds. The refrigerant mass flow rate is varied from 0.033 kg/s to 0.088 kg/s. The compressor speed is varied from 7.1 rps to 11.8 rps. Then, the system simulation to find out the suitable refrigerant mass flow rate and power input of the chilled water system at any given cooling load is constructed. Moreover, the time used to produce the required amount of the ice and the energy consumption in the ITES system are also carried out. The estimated values from the simulation program are good agreement to the experimental results with 5% errors for chilled water system and for ITES system.

6.2.2 The appropriate refrigerant mass flow rate of the chilled water is 0.06-0.08 kg/s which gives the highest value of the coefficient of performance (COP). COP is approximately 3.1. For the ITES system, the appropriate refrigerant mass flow rate and compressor speed are 0.08-0.09 kg/s and 9.5 rps, respectively. The COP of the ITES system is about 3.1.

6.2.3 For the selected office located in Chiang Mai University which has 18 kW of the cooling load on the design day and 13,045 kW-hr of energy consumption in air conditioning system during the year, the appropriate combination system is the partial storage design system that consists of 3.5 kW of capacity of chilled water system and 14 kW of capacity of ITES system. The chilled water system is operated as the base cycle.

6.2.4 Under the appropriate operating conditions, the peak electricity demand and the electricity charge related to TOU tariff of the office could be decreased 39.2 % and 32% compared to the conventional chiller system, respectively. It is also found that the payback is approximately 9 years.

6.2 Recommendations

6.2.1 Since the chilled water cycle and the ITES cycle are separately operated by the different systems to find the characteristic models and simulation in this research, the system should be re-designed to use the same one for more practical work as the conventional ice-on-coil ITES system. During the office occupancy time, the refrigeration system is operated to produce the chilled water. The refrigerant runs through the chiller to extract heat. Then, during the ice producing process, the same system is operated to produce the ice by bypass the refrigerant from the chiller to the direct contact evaporator. This method should be simple and make optimum use of the chiller to achieve the best system performance.

6.2.2 The high pressure remained in the storage tank after the ice producing process has to be exterminated before utilizing the produced ice. After the required amount of the ice is obtained, the inlet port of the tank is shut off and the compressor of the ice storage system is further operated for about 10 minutes.

6.2.3 From the experiments, the ice formed at outlet of the nozzle blocks the refrigerant flows. It causes high pressure. The nozzle should be redesigned to solve this problem as followings:

(a) The nozzle should be designed as a propeller shaft. In this case, the high turbulence flow of water is obtained. The ice is not formed around the nozzle. Moreover, the ice produced is a slurry ice (as partly melted or watery snow) that will let the refrigerant passes through the ice easily.

(b) There should be a small electric heater rounded at the outlet of the nozzle to melt the ice formed. In this case, the hot wire is operated only a short period. After the ice blocking the refrigerant flow is wiped out, the hot wire is turned off.

REFERENCES

1. Electricity Generating Authority of Thailand (EGAT) (1997), *Thailand power development plan PDP 1997-01*. System Planning Department. Bangkok, Thailand.
2. Akbart, H. and Metro, A. (1990), Technology assessment: Thermal Energy Storage for Cooling of Commercial Building, *Lawrence Berkeley Laboratory Report*, University of California, USA.
3. Carey, C.W, Mitchell, J.W. and Beckman, W.A. (1995), Thermal control of ice storage system, *ASHRAE Journal May 1995*, pp. 32-39.
4. Crane, J. and Dunlop, C. (1994), Ice Storage System for a Department Store, *ASHRAE Journal January 1994*, pp. 49-52.
5. Guluska, E. (1994), Thermal Storage System Reduces Costs of Manufacturing Facility, *ASHRAE Journal March 1994*, pp. 50-52.
6. Subbaiyer, S., Andhole, T.M. and Helmer, W.A. (1991), Computer Simulation of a Vapor-Compression Ice Generator with a Direct Contact Evaporator, *ASHRAE Transactions*, part 1, pp.118-126, paper number 3448.
7. Kiatsiriroat, T., Siriplubpla, P. and Nuntaphan, A. (1998), Performance Analysis of a Refrigeration Cycle Using a Direct Contact Evaporator, *International Journal of Energy Research*, 22, 1179-1190.
8. Nuntaphan, A. (1998), *Performance Analysis of a Refrigerant Cycle Using a Direct Contact Evaporator*. Master Thesis, Mechanical Engineering, Chiang Mai University, Thailand.
9. Kiatsiriroat, T., and Maneechote, T. (1996). Formation and Melting of Ice with Direct Contact Heat Exchange, paper presented in the, *Tri-University International Joint Seminar & Symposium*, Jianxu University of Science & Technology, China.
10. Chatakanonda, T. and Na Bangchang, P. (1998), *A R22 Refrigeration Unit with Direct Contact Evaporator*. Senior Project, Mechanical Engineering, Chiang Mai University, Thailand.
11. Simmonds, P. (1994), A Control Strategy for Chilled Water Production, *ASHRAE Journal. January 1994*, pp. 30-36.

12. Ritthi, S. (1997), *Effectiveness of Ice Storage System in Commercial Building: A Case Study of Thai Rath Press*. Master Thesis, Energy Management Technology, King Mongkut's University of Technology Thonburi, Thailand.
13. Knebel, D. (1995), Predicting and Evaluating the Performance of Ice Harvesting Thermal Energy Storage Systems, *ASHRAE Transactions*, Atlanta, Georgia: ASHRAE, Vol.101, Pt.1.
14. Stoecker, W.F. (1982). *Refrigerant and Air Conditioning*. McGraw-Hill Book Company, New York, USA.
15. Kiatsiriroat, T., Chowcheun, K. and Wibulswas, P. (1994), Simulation of Standard Vapor Compression System, *ASEAN Journal on Science & Technology for Development*, **11(1)**, pp. 167-180.
16. ASHRAE (1994). *ASHRAE Handbook: Refrigeration*. Atlanta: ASHRAE, Inc.
17. Tantakitti, C. (1991). *Cold Storage and Refrigeration Design*, ISBN 974-565-334-9, 4th edition, Department of Mechanical Engineering, Faculty of Engineering, Chiang Mai University, Thailand.
18. Mayhew, Y.R. and Rogers, G.F.C. (1972). *Thermodynamic and Transport Properties of Fluids*, Basil Blackwell, Oxford, U.K.
19. Department of meteorology. (2000), *Temperature data*, Climatology Division, Climatological Data and Information Services.
20. ASHRAE (1994). *ASHRAE Handbook: Refrigeration*. Atlanta: ASHRAE, Inc.
21. Haines, R.W. and Wilson, C.L. (1998). *HVAC System Design Handbook*, 3rd edition, McGraw-Hill Book Company, New York, U.S.A.
22. Stoecker, W.F. (1989). *Design of Thermal Systems*. 3rd edition, McGraw-Hill Book Company, New York, USA.

APPENDIX A

SIMULATION PROGRAM

```
Program Simulation;
Uses  Wincrt;
Var
                        {CHILLED WATER SYSTEM}
  {Compressor} Tcpi, Tcpo, Pcpi, Pcpo, mr, x, y, c1, c2, u, v, k, Tcpi2, Tcpo2,
               Pcpi2, Pcpo2, Tsatcpi, Tsatcpo, hcpi, hcpo, Wcp:real;
  {Condenser}  Tcdi, Tcdo, Pcdi, Pcdo, Qcd, hcdi, hcdo: real;
  {Expansion valve} Texi, Texo, Pexi, Pexo, hexi, hexo: real;
  {Chiller} Pchi, Pcho, Tchi, Tcho, Qch, Cpw, Twi, Two, hchi, hcho, Tsatcho:
            real;
  {General} COP, Cpa, Qload: real;
  i, j : integer;
                        {ICE STORAGE SYSTEM}
  {Compressor} Pcpi1, Pcpo1 ,Tcpi1, Tcpo1, N1, mr1, hcpi1, hcpo1, Wcp1:Real;
  {Condenser} Pcdi1, Pcdo1, Tcdi1, Tcdo1, Tai1, Tao1, UAcd1, ma1, Cpa1,
              hcdi1, hcdo1, Qcd1:Real;
  {Expansion Valve} Texi1, Texo1, Pexi1, Pexo1, hexi1, hexo1:Real;
  {Direct Contact Evaporator} Cpr1, Mw1, Mwi, Mi1, Tw1, Tevi1, Tevo1, hevi1,
              hevo1, Pevi1, Pevo1, Qev1:Real;
  {Others} Qev2, COP1, t1, Tamb1, Pex_ratio1, Pcp_ratio1, Psat1, Tsat1, k1, u1,
              v1, w1, x1, y1, z1:Real;

  {Meaning of Variables (use only in this program)
  COP     =     coefficient of performance
  Cpa     =     specific heat of air (kJ/kg-K)
  Cpr     =     specific heat of refrigerant (kJ/kg-K)
  hcdi    =     inlet enthalpy of condenser (kJ/kg)
  hcdo    =     outlet enthalpy of condenser (kJ/kg)
  hchi    =     inlet enthalpy of chiller (kJ/kg)
  hcho    =     outlet enthalpy of chiller (kJ/kg)
  hcpi    =     inlet enthalpy of compressor (kJ/kg)
  hcpo    =     outlet enthalpy of compressor (kJ/kg)
  hexi    =     inlet enthalpy of expansion valve (kJ/kg)
  hexo    =     outlet enthalpy of expansion valve (kJ/kg)
```

hevi	=	inlet enthalpy of evaporator (kJ/kg)
hevo	=	outlet enthalpy of evaporator (kJ/kg)
k	=	polytropic index
ma	=	mass flow rate of air (kg/s)
mr	=	mass flow rate of refrigerant (kg/s)
Mi	=	mass of ice formution (kg)
Mice	=	required amount of ice (kg)
Mw	=	mass of water in storage tank (kg)
N	=	compressor speed (rps)
Pcdi	=	inlet pressure of condenser (MPa)
Pcdo	=	outlet pressure of condenser (MPa)
Pchi	=	inlet pressure of chiller (MPa)
Pcho	=	outlet pressuer of chiller (MPa)
Pcpi	=	inlet pressure compressor (MPa)
Pcpo	=	outlet pressure of compressor (MPa)
Pcp_ratio	=	pressure ratio of compressor (Pcpi/Pcpo)
Pexi	=	inlet pressure of expansion valve (MPa)
Pexo	=	outlet pressure of expansion valve (MPa)
Pex_ratio	=	pressure ratio of expansion valve (Pexi/Pexo)
Pevi	=	inlet pressure of evaporator (MPa)
Pevo	=	outlet pressure of evaporator (MPa)
Psat	=	saturated pressure (MPa)
Qcd	=	rate of heat transfer of condenser (kW)
Qch	=	rate of heat transfer of chiller
Qev	=	rate of heat transfer of evaporator (kW)
Tai	=	inlet temperature of condenser fan (C)
Tao	=	outlet temperature of condenser fan (C)
Tamb	=	ambient temperature (C)
Tcdi	=	inlet temperature of condenser (C)
Tcdo	=	outlet temperature of condenser (C)
Tchi	=	inlet temperature of chiller (C)
Tcho	=	outlet temperature of chiller (C)
Tcpi	=	inlet temperature of compressor (C)
Tcpo	=	outlet temperature of compressor (C)

```
Tevi    =    inlet temperature of evaporator (C)
Tevo    =    outlet temperature of evaporator (C)
Texi    =    inlet temperature of expansion valve (C)
Texo    =    outlet temperature of expansion valve (C)
Tsat    =    saturated temperature (C)
t       =    time (S)
Tw      =    temperature of water (C)
c       =    variable
u,v,w   =    variable
x,y,z   =    variable
UAcd    =    overall heat transfer coefficient of condenser (kW)
Wcp     =    rate of work input of compressor (kW)}

Begin
    write('Input cooling load responsible by chilled water system (kW)');
    readln(Qload);
    write('Input mass flow rate of refrigerant in chilled water system (kg/s)');
    readln(mr);

                        {CHILLED WATER SYSTEM}
    Repeat
        c1:=-20.114*mr*mr+3.5432*mr+0.1291;
        c2:= 0.7733*c1-0.0194;
        k:= (-2.1397)*sqr(mr)+0.4896*mr+1.1867;
        Tcpi:= 5;
        Tcpo:= 60;
        Pcpi:= 0.3;
        Pcpo:= 1.6;
        For i:=1 to 100 do
  {COMPRESSOR}
        Begin
        Tcpo2:= exp(ln(Tcpi+273.15)-((k-1)/k)*ln(c2))-273.15;
        x:= c2-0.1088;
        y:= x/0.0873;
```

```
Pcpo2:= mr*sqrt(Tcpo)/y:
Tcpi2:= sqr((0.0663-c2)/0.0973*Pcpi/mr);
Pcpi2:= Pcpo*c2;
Tcpi:= Tcpi2;
Tcpo:= Tcpo2;
Pcpi:= abs(Pcpi2);
Pcpo:= abs(Pcpo2);
End;
Tsatcpi:= ((8.96-sqrt(8.96*8.96-(4*1.038*(15.6+ln(Pcpi*10)))))*100/
          (2*1.038))-273.15;
hcpi:= 173.52+13.01*ln(Pcpi*10)+(0.57+0.0826*ln(Pcpi*10))*(Tcpi-
       Tsatcpi);
Tsatcpo:= ((8.96-sqrt(8.96*8.96-(4*1.038*(15.6+ln(Pcpo*10)))))*100/
          (2*1.038))-273.15;
hcpo:= 173.52+13.01*ln(Pcpo*10)+(0.57+0.0826*ln(Pcpo*10))*(Tcpo-
       Tsatcpo);
Wcp:= mr*(hcpo-hcpi);
{CONDENSER}
Tcdi:= Tcpo;
Pcdi:= Pcpo;
Pcdo:= Pcdi;
Tcdo:= ((8.96-sqrt(8.96*8.96-(4*1.038*(15.6+ln(Pcdo*10)))))*100/
       (2*1.038))-273.15;
hcdi:= hcpo;
hcdo:= -239.8+100.6*(Tcdo+273.15)/100;
Qcd:= mr*(hcdi-hcdo);
{EXPANSION VALVE}
Pexi:= Pcdo;
Pexo:= Pexi*c1;
Texi:= Tcdo;
Texo:= ((8.96-sqrt(8.96*8.96-(4*1.038*(15.6+ln(Pexo*10)))))*100/
       (2*1.038))-273.15;
hexi:= hcdo;
hexo:= -239.8+100.6*(Texo+273.15)/100;
```

```
{Chiller}
      Pchi:= Pexo;
      Pcho:= Pcpi;
      Tchi:= Texo;
      Tcho:= Tchi;
      hchi:= hexo;
      hcho:= hcpi;
      Qch:= mr*(hcho-hchi);
      COP:= Qch/Wcp;
      writeln(' mr = ',mr:1:4,' Wcp = ',Wcp:1:2,' Qch = ',Qch:1:2,' Qcd =
            ',Qcd:1:2,' COP = ',COP:1:2);
      If Qch<Qload then
      mr:= mr+0.0001;
      If Qch>Qload then
      mr:= mr-0.0001;
   Until
      abs(Qch-Qload)<=0.01;
   writeln;
   write('Enter any key to start the calculation of the ice storage system');
   readkey;
   writeln;

                        {ICE STORAGE SYSTEM}

   write('Enter cooling load responsible by ice storage system (kJ/day)');
   read(Qev2);
   Mwi:=1.1*Qev2/335;
   writeln;
   write('The require amount of the ice =  ',Mwi:1:2,'kg');
   writeln;
   writeln;
   write(' Enter mass of water in ice storage tank(kg)      ');
   read(Mw1);
   write(' Enter mass flow rate of refrigerant in ice storage system (kg/s)');
```

```
read(mr1);
write(' Enter mass flow rate of air(kg/s)                ');
read(ma1);
write(' Enter compressor speed of the ice storage system (rps)');
read(N1);
write(' Enter initial temperature of water in storage tank (C)  ');
read(Tw1);
write(' Enter ambient temperature (C)                    ');
read(Tamb1);
write(' Enter specific heat of refrigerant (kJ/kg-K)      ');
read(Cpr1);
write(' Enter specific heat of air (kJ/kg-K)             ');
read(Cpa1);
write(' Enter delta time which you want to calculate (s)   ');
read(t1);
writeln('  Sensible Heat Period          ');
writeln('Time  Tw   Tcpi  Tcpo  Tcdi  Tcdo  Pcpi  Pcpo  Wcp  Qve  Qcd COP
        Tevi');
{COMPRESSOR}
Pex_ratio1:=(1.5134*sqr(N1)-32.0125*N1+148.8285)*sqr(mr1)+(-0.1020*sqr(N1)
            +2.0160*N1-5.8329)*mr1+(0.0032*sqr(N1)-0.0824*N1+0.7113);
Pcp_ratio1:=0.954*(Pex_ratio1);
w1:= 0;
Repeat
   Tevo1 := Tw1;
   Tcpi1 := 0;
   Repeat
   Tcpi1 := Tcpi1+0.01;
   x1    := Tevo1+(1/(mr1*0.9))*((-0.4132*sqr(mr1)+0.0409*mr1-0.0012)
        *sqr(Tamb1-(Tevo1+Tcpi1)/2)+(6.0055*sqr(mr1)-0.3648*mr1+0.0448)
        *(Tamb1-(Tevo1+Tcpi1)/2)+((-38.4022)*sqr(mr1)+6.243*mr1-0.2699));
   Until
   abs(Tcpi1-x1)<=0.01;
   k1    := 1.9584*mr1+1.1503;
```

```
Tcpo1 := exp(ln(Tcpi1+273.15)-((k1-1)/k1)*ln(Pcp_ratio1))-273.15;
y1    := -0.00015*sqr(N1)-0.0087*N1+0.3003;
z1    := Pcp_ratio1-0.0022*sqr(N1)-0.0581*N1+0.5824;
Pcpo1 := Mr1*sqrt(Tcpo1)*y1/z1;
Pcpi1 := Pcpo1*Pcp_ratio1;
Tsat1 := 0;
Repeat
Tsat1  := Tsat1+0.01;
x1     := exp(-15.6+8.96*(Tsat1/100)-1.038*sqr(Tsat1/100));
Until
abs((x1/10)-Pcpi1)<=0.01;
hcpi1  := 173.52+13.01*ln(Pcpi1*10)+(0.57+0.0826*ln(Pcpi1*10))
       *(Tcpi1-Tsat1+273.15);
Tsat1  := 0;
Repeat
Tsat1  := Tsat1+0.01;
x1     := exp(-15.6+8.96*(Tsat1/100)-1.038*sqr(Tsat1/100));
Until
abs((x1/10)-Pcpo1)<=0.01;
hcpo1  := 173.52+13.01*ln(Pcpo1*10)+(0.57+0.0826*ln(Pcpo1*10))
          *(Tcpo1-Tsat1+273.15);
Wcp1   := mr1*(hcpo1-hcpi1);
{Condenser}
Pcdi1  := Pcpo1;
Tcdi1  := 0;
Repeat
Tcdi1  := Tcdi1+0.01;
x1     := Tcpo1-(1/(mr1*0.9))*((-0.0001)*sqr((Tcpo1+Tcdi)/2-Tamb)+
          (1.607*sqr(mr1)-0.0298*mr1+0.0146)*((Tcpo1+Tcdi1)/2-Tamb1)+
          (-20.432*sqr(mr1)+1.9399*mr1-0.293));
Until
abs(Tcdi1-x1)<=0.01;
Pcdo1  := Pcdi1-0.034;
Tsat1  := 0;
```

```
    Repeat
    Tsat1  := Tsat1+0.01;
    x1     := exp(-15.6+8.96*(Tsat1/100)-1.038*sqr(Tsat1/100));
    Until
    abs((x1)/10-Pcdi1)<=0.01;
    hcdi1  := 173.52+13.01*ln(Pcdi1*10)+(0.57+0.0826*ln(Pcdi1*10))
              *(Tcdi1-Tsat1+273.15);
    Tcdo1  := Tsat1-273.15;
    hcdo1  := -239.8+100.6*(Tsat1/100);
    Qcd1   := mr1*(hcdi1-hcdo1);
    Tai1   := Tamb1;
    Tao1   := (Qcd1/ma1)+Tai1;
    UAcd1  := (ma1*Cpa1/0.2723)*(((Tao1-Tai1)/(Tcdi1-Tai1))-0.0107);
{Expansion Valve}
    Pexi1  := Pcdo1;
    Pexo1  := Pexi1*Pex_ratio1;
    Tsat1  := 0;
    Repeat
    Tsat1  := Tsat1+0.01;
    x1     := exp(-15.6+8.96*(Tsat1/100)-1.038*sqr(Tsat1/100));
    Until
    abs((x1/10)-Pexo1)<=0.01;
    Texo1  := Tsat1-273.15;
    hexo1  := hcdo1;
{Direct Contact Evaporator}
    Pevi1  := Pexo1;
    Pevo1  := Pevi1;
    Tevi1  := Texo1;
    Tsat1  := 0;
    w1     := w1+1;
    u1     := w1*t1;
    Repeat
    Tsat1  := Tsat1+0.01;
    x1     := exp(-15.6+8.96*(Tsat1/100)-1.038*sqr(Tsat1/100));
```

```
Until
abs((x1)/10-Pevo1)<=0.01;
hevo1  := 173.52+13.01*ln(Pevo1*10)+(0.57+0.0826*ln(Pevo1*10))
          *(Tw1-Tsat1+273.15);
hevi1  := hexo1;
Tw1    := Tw1-(mr1*(hevo1-hevi1)*t1)/(Mw1*4.19+450);
y1     := y1+1;
Qev1   := mr1*(hevo1-hevi1);
COP1   := Qev1/Wcp1;
If Tw1>0.01 Then
writeln(u1:1:0,' ',Tw1:1:1,' ',Tcpi1:1:1,' ',Tcpo1:1:1,' ',
   Tcdi1:1:1,' ',Tcdo1:1:1,' ',Pcpi1:1:2,' ',Pcpo1:1:2,' ',
   Wcp1:1:1,' ',Qev1:1:1,' ',Qcd1:1:1,' ',COP1:1:1,' ',Tevi1:1:1);
If Tw1<=0.01 Then
BEGIN
Tw1    :=0.01;
writeln(u1:1:0,' ',Tw1:1:1,' ',Tcpi1:1:1,' ',Tcpo1:1:1,' ',
   Tcdi1:1:1,' ',Tcdo1:1:1,' ',Pcpi1:1:2,' ',Pcpo1:1:2,' ',
   Wcp1:1:1,' ',Qev1:1:1,' ',Qcd1:1:1,' ',COP1:1:1,' ',Tevi1:1:1);
END;
Until Tw1<=0.01;
writeln;
writeln('Press enter for next calculation');
readkey;
writeln('     Latent Heat Period     ');
hevo1    := 173.52+13.01*ln(Pevo1)+(0.57+0.0826*ln(Pevo1))*(0.01-
            Tsat1+273.15);
v1       := (Mw1*334)/(mr1*(hevo1-hevi1));
z1       := 0;
  Repeat
  Mi1    := Mw1*(z1/v1);
  If Mi1<Mw1 Then
  writeln('Time = ',z1:1:0, 'second  Ice formation = ',Mi1:1:2,'kg');
  If Mi1>=Mw1 Then
```

```
        Begin
        writeln('Time = ',v1:1:0, 'second  Ice formation = ',Mw1:1:2,'kg');
        end;
        z1    := z1+1;
        Until
        Mi1>=Mw1;
        writeln;
        writeln('Press Any Key to Return to Program');
        readkey;
End.
```

APPENDIX B

PAYBACK PERIOD CALCULATION

Payback period calculation [21]

Designing and building a device or system that functions properly is a part of the engineer's task but he basis of most engineering decisions is economic.. The device or system must. in addition. be economic, which means that the investment must show an adequate return. In this study, the payback period of the ice thermal energy storage with direct contact evaporator is considered based on the investment. From Chapter 5, the system in category 5 is selected due to its optimum performance. It consists of the chilled water system and the ice storage system while the conventional system consists of only the chilled water system.

The payback period (years) of the system is normally calculated from

$$Payback\ Period = \frac{C}{(N-R)-(O\&M)} \qquad \text{(B.1)}$$

where C = Capital cost (first cost or investment) (Baht)

N = Conventional system running cost (Baht/year)

R = Selected system running cost (Baht/year)

$O\&M$ = Operating and Maintenance cost (Baht/year)

The capital cost of the selected system is normally the investment evaluated at present. The profit (*N-R-O&M*) is the returning value evaluated per year during the lifetime. As the profit is affected by the interest and inflation, one baht of the profit at the first year does not have the same value as one baht in the year following or later. So, the profit has to be adjusted such that the current value is used in place of the value in years to come to calculate the payback period. If the annual profit is the uniform amount, the present worth of the profit can be calculated from

$$P = A\frac{(1+i)^n - 1}{i(1+i)^n} \qquad \text{(B.2)}$$

and

$$i = \frac{i_f - f}{1+f} \qquad \text{(B.3)}$$

where P = Present worth of the profit in each year (Baht)

A = Annual amount of the profit (Baht)

i = Interest rate including the effect of the inflation (% per year)

i_f = Interest rate (% per year)

f = Inflation rate (% per year)

n = year

In this research, as indicated in Chapter 5, the capital cost of the selected system (C) is 74,000 Baht. The operating and maintenance cost is already included in the running cost of the selected system. Therefore, the term (N-R-$O\&M$) or profit is 11,000 Baht/year and will be available for 10 years of lifetime. The interest rate and the inflation rate is 8% and 2.6%, respectively.

Then the true value of the interest is

$$i = \frac{0.08 - 0.026}{1 + 0.026} = 0.054$$

The profit received at the end of the first year is

$$P = 10781\left[\frac{(1 + 0.054)^1 - 1}{0.054(1 + 0.054)^1}\right] = 10268$$

As the annual profit is received, then, the results of the value calculation of the profit at the end of each year is shown in Table B.1

Table B.1 The present worth of the total profit gained during the lifetime of the system

year	Annual profit (Baht)	Present worth of annual profit (Baht)	Total profit (Baht)
1	10,781	10,267.62	10,267.62
2	10,781	9,778.68	20,046.30
3	10,781	9,313.03	29,359.34
4	10,781	8,869.56	38,228.89
5	10,781	8,447.20	46,676.09
6	10,781	8,044.95	54,721.04
7	10,781	7,661.86	62,382.89
8	10,781	7,297.01	69,679.80
9	10,781	6,949.53	76,629.43
10	10,781	6,618.60	83,248.02

From Table B.1, value of the total profit at the end of the 9^{th} year is more than the capital cost of the system. Hence, the payback period is 9 years.

APPENDIX C

IMPORTANT PICTURES

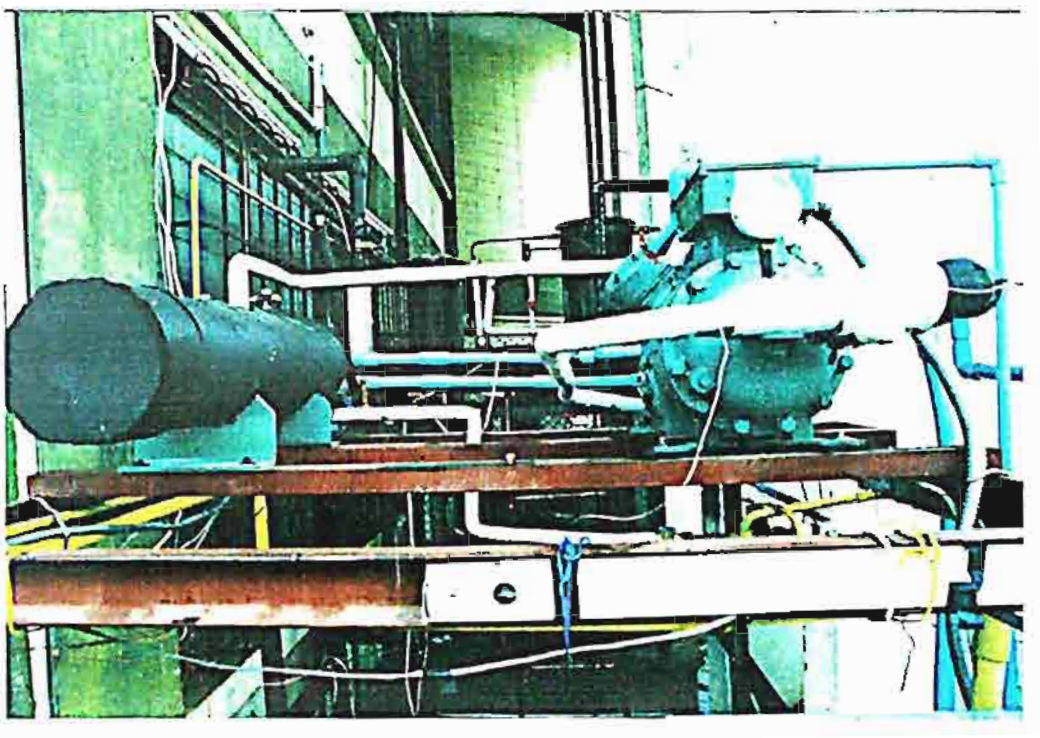

C.1 Chilled water system

C.2 Cooling tower

C.3 Ice storage system (front view)

C.4 Ice storage system (right-side view)

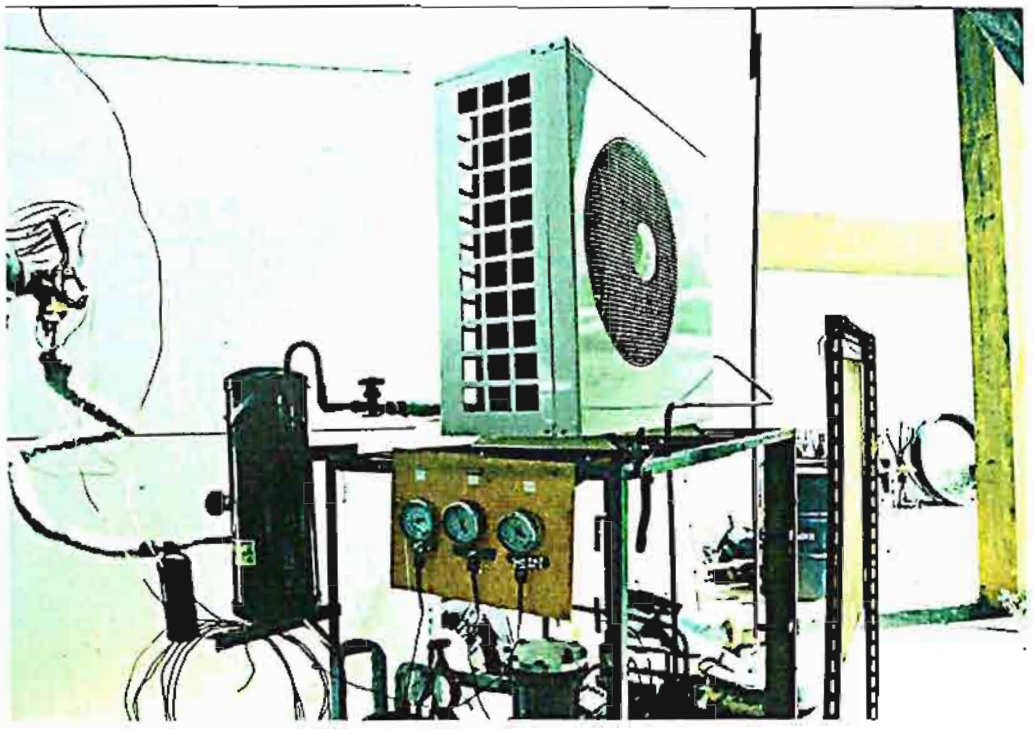

C.5 Condensing unit

C.6 Ice storage tank

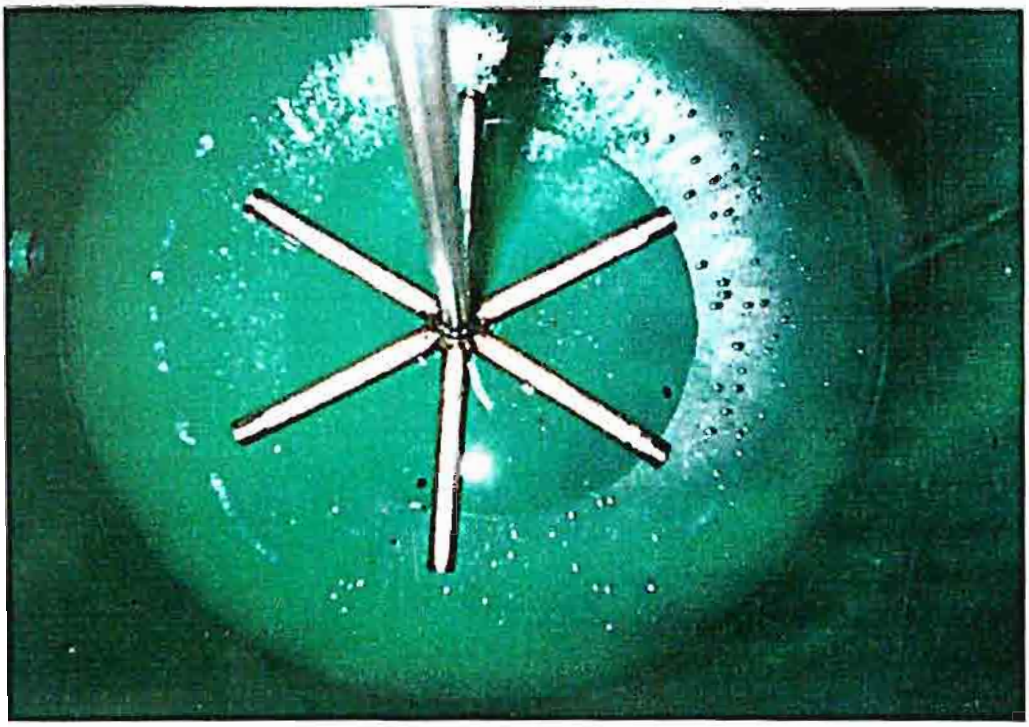

C.7 Nozzle

C.8 Produced ice in the storage tank

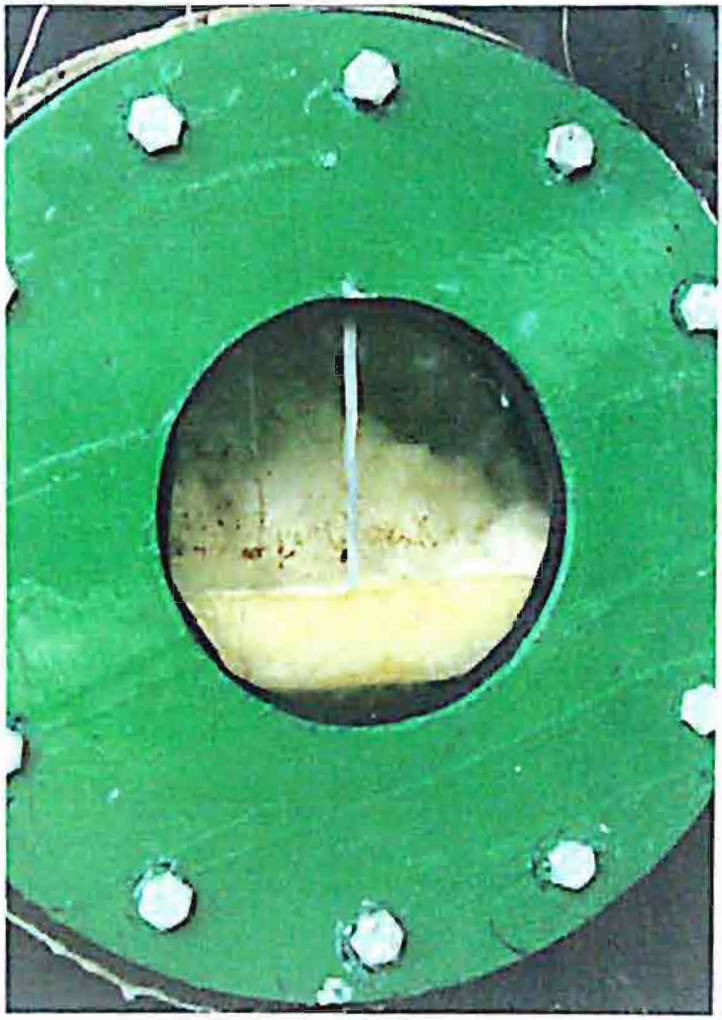

C.9 Produced ice in the storage tank

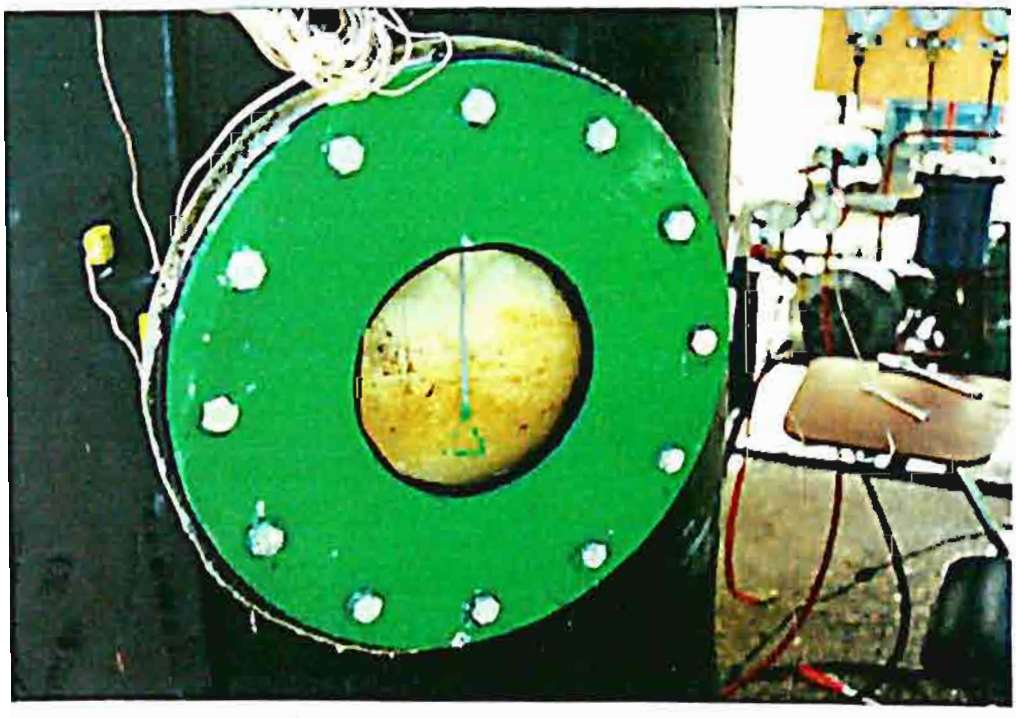

C.10 Produced ice in the storage tank

APPENDIX D

Published Papers

APPENDIX D

Published Papers

1. Energy Analysis of an Ice Thermal Energy Storage Prototype with Direct Contact Evaporator, Energy-The International Journal, Submitted.
2. Heat Transfer Model of a Direct a Direct Contact Evaporator, Applied Energy, Submitted.
3. Feasibility of Using Ice Thermal Energy Storage with Direct Contact Evaporator in an Office Building, Energy Research-The International Journal, Submitted.

Energy Analysis of an Ice Thermal Energy Storage Prototype with Direct Contact Evaporator

N. Vorayos
The Joint Graduate School of Energy and Environment,
King Mongkut's University of Technology Thonburi,
Bangkok 10140, Thailand
A. Nuntaphan, S. Seewattanangkoon and T. Kiatsiriroat
Department of Mechanical Engineering, Chiang Mai University,
Chiang Mai 50200, Thailand

Abstract – In this research, an ice thermal energy storage with direct contact evaporator has been studied and is applied in an office room. The system consists of two processes, air conditioning process and ice storage. The storage has another refrigeration unit and is designed as a partial storage type. From the experimental data, the mathematical models for main components of each process which are compressor, condenser, expansion valve, water chiller and direct contact evaporator are developed and the system simulation is created. From the result, it could be shown that the simulation agrees well with the experiment. From the simulation, it indicates that the appropriate capacity of the ice thermal energy storage system which is 8 kW can shift 48.7 % of peak cooling load from on-peak to off-peak period. Moreover, under this condition, 27% of operating cost are saved comparing to those of the conventional system.

Keywords: Ice thermal energy storage system, direct contact heat transfer, system simulation

Submitted to **Energy – The International Journal,**

Address of Correspondence and proof:
Prof. Dr. Tanongkiat Kiatsiriroat
Department of Mechanical Engineering, Faculty of Engineering,
Chiang Mai University, Chiang Mai 50200, Thailand.
Tel:6653-944144 Fax:6653-944145 E-mail: *tanong@dome.eng.cmu.ac.th*

1. INTRODUCTION

As electricity demand in commercial building is mainly caused by cooling system, ice hermal energy storage (ITES) is a concept that is becoming more attractive to reduce the)perating cost of the building in both of demand and energy charges [1-3]. Demand and energy :harges are based on the peak power consumption during a peak hour and the total energy 'onsumed respectively. The ITES technique shifts the cooling load from peak to off-peak by unning the air

conditioning compressor during the off-peak hour when the energy cost is the lowest to produce :e stored in the storage tank. Water from this tank is circulated for the cooling purpose during ıe on-peak hour. At present, most of the ITES systems used are the ice-on-coil storage system ·f which the ice is formed directly on the coils submerged in the water. There are two main ·roblems, big space for handling the evaporator coil is needed and high thermal resistance is ·btained due to the low thermal conductivity of the ice when it is formed on the coil [4-5].)uring the ice formation process, as the ice thickness is increased, the rate of heat extraction ecreases. Thus, the direct contact heat transfer technique has been much interest in recent years hrough its application to overcome these problems [6-7]. In this paper, an application of an ice hermal energy storage with the direct contact evaporator system for air-conditioning of an office n Chiang Mai, Thailand has been carried out. The mathematical models of the main components n both of air-conditioning and direct-contact ITES system have been developed and the)erformance analysis of the whole system has been investigated.

2. THE AIR-CONDITIONING SYSTEM

The air-conditioning system with the ITES unit used in this work are shown schematically in Fig. 1.

The system consists of two main cycles, chilled water cycle and ice storage cycle. The ITES or ice storage cycle is designed as a partial storage type and the whole system uses R12 refrigerant as the working fluid. During the off-peak period the ice storage cycle is operated to proceed the ice formation process. The ice is stored in the storage tank. During the on-peak hours, chilled water cycle is operated to produce the cooled water to achieve the cooling requirement. The cooled water passes from the chiller to the fan-coil unit to exchange heat and then turns back to the chiller. If the required cooling load is higher than the capacity of the chiller, the chilled water from the fan-coil unit controlled by a two-way valve will pass through the ice storage tank to lower the chilled water temperature before going back to the chiller.

An air conditioning unit is operated to support cooling load of a selected office in Chiang Mai city. The area of the office is 71.5 m^2 of which the maximum peak cooling load gained on the designed day in April is approximately 18 kW.

In this study, modeling equations, which describe the behavior of the main system components have been investigated and the system simulation has been carried out to find out the appropriate size of the ITES.

3. MATHEMATICAL MODEL

In this section, the mathematical models of the main components for the air conditioner including the direct contact ITES could be described as follows:

3.1 Chilled Water Refrigeration Cycle

For chilled-water refrigeration cycle, a standard vapor-compression refrigeration system is simulated under steady-state conditions to produce the chilled water for supporting the cooling load. In this case, the chilled water cycle is operated as a base cycle. The compressor is usually worked at constant full speed. Thus, modeling of each component could be developed at various refrigerant mass flow rates. The details have been described as follows:

Compressor Modeling

Kiatsiriroat et al. [8] generates a mathematical model of a reciprocating compressor, which is modified from Stoecker [9] as

$$\frac{P_{cp,i}}{P_{cp,o}} = f\left(\frac{m_r T_{cp,i}^{0.5}}{P_{cp,i}}, N\right), \tag{1}$$

or

$$\frac{P_{cp,i}}{P_{cp,o}} = f\left(\frac{m_r T_{cp,o}^{0.5}}{P_{cp,o}}, N\right), \tag{2}$$

where N is the compressor speed in rps, m_r is the refrigerant mass flow rate in kg/s, $T_{cp,i}$, $T_{cp,o}$, $P_{cp,i}$ and $P_{cp,o}$ are temperatures and pressures at the inlet and outlet ports of the compressor in K and MPa, respectively.

With the experimental results from Figs. 2 and 3, the relations in Eqs. (1) and (2) can be characterized as

$$\frac{P_{cp,i}}{P_{cp,o}} = 0.0973\left(\frac{m_r T_{cp,i}^{0.5}}{P_{cp,i}}\right) + 0.0663, \tag{3}$$

and

$$\frac{P_{cp,i}}{P_{cp,o}} = -0.0057\left(\frac{m_r T_{cp,o}^{0.5}}{P_{cp,o}}\right)^2 + 0.0936\left(\frac{m_r T_{cp,o}^{0.5}}{P_{cp,o}}\right) + 0.1071. \tag{4}$$

Moreover, the pressure ratio of the compressor could also be calculated from

$$\frac{P_{cp,i}}{P_{cp,o}} = \left(\frac{T_{cp,i}}{T_{cp,o}}\right)^{k/(k-1)} \tag{5}$$

where k is the polytropic index depending on the refrigerant mass flow rate as

$$k = f(m_r). \tag{6}$$

From the experiments, the relations between these two parameters can be expressed as shown in Fig. 4 which is

$$k = 0.2216 m_r + 1.1949. \tag{7}$$

Condenser Modeling

In this work a counter flow heat exchanger having circulating water as a coolant is used to extract heat from the refrigeration system. From the experiment, it could be found that the refrigerant becomes saturated liquid after passing the condenser. The heat extracted can be calculated from

$$Q_{cd} = m_r\left(h_{cd,i} - h_{cd,o}\right). \tag{8}$$

Q_{cd} is the rate of heat extraction, $h_{cd,i}$ and $h_{cd,o}$ are the enthalpies at the inlet and the outlet of the condenser, respectively.

Expansion Valve Modeling

The expansion valve is operated manually to control the refrigerant mass flow and the pressure of the cycle. From the results as shown in Fig. 5, it could be found that the pressure ratio at the valve depends on the refrigerant mass flow rate where

$$\frac{P_{ex,o}}{P_{ex,i}} = f(m_r), \tag{9}$$

and the characteristic equation at the valve can be experimentally expressed as

$$\frac{P_{ex,o}}{P_{ex,i}} = -20.114m_r^2 + 3.5432m_r + 0.1291. \tag{10}$$

Chiller Modeling

The water chiller in this case is a counter flow type and the heat transfer rate could be calculated from

$$Q_{ch} = m_r(h_{ch,o} - h_{ch,i}), \tag{11}$$

or

$$Q_{ch} = m_w C_{cpw}(T_{w,i} - T_{w,o}), \tag{12}$$

and

$$Q_{ch} = (UA)_{ch}\left[\frac{(T_{w,i} - T_{ch,o}) - (T_{w,o} - T_{ch,i})}{\ln\left[\frac{T_{w,i} - T_{ch,o}}{T_{w,o} - T_{ch,i}}\right]}\right]. \tag{13}$$

From the experiments, it could be found that there is a pressure drop across the condenser and the chiller, and it is expressed in terms of the pressure ratios at the expansion valve and compressor as

$$\frac{P_{cp,i}}{P_{cp,o}} = -4.6771\left[\frac{P_{ex,o}}{P_{ex,i}}\right]^2 + 3.1933\left[\frac{P_{ex,o}}{P_{ex,i}}\right] - 0.33. \tag{14}$$

3.2 Ice Storage Refrigeration Cycle

For the ice storage system, another standard vapor compression refrigerant cycle is operated to produce ice. R12 is injected through the expansion valve into the water in the direct contact evaporator/storage tank directly to extract heat. The diagram of the system is shown in Fig. 6.

Compressor Modeling

During the ice producing, the compressor model could be characterized similar to that of the chilled water system. From the results as shown in Figs. 7 and 8, the characteristic equation of the compressor can be expressed as

$$\frac{P_{cp,i}}{P_{cp,o}} = \left[\begin{array}{l}\left(0.0027N^2 - 0.0705N + 0.3297\right)\left[\dfrac{m_r T_{cp,o}^{0.5}}{P_{cp,o}}\right]^2 \\ +\left(-0.0013N^2 + 0.028N + 0.1428\right)\left[\dfrac{m_r T_{cp,o}^{0.5}}{P_{cp,o}}\right] \\ +\left(0.0026N^2 - 0.0685N + 0.6253\right)\end{array}\right], \tag{15}$$

and

$$k = 1.7525m_r + 1.1571. \tag{16}$$

Condenser Modeling

In this case, a cross flow heat exchanger having air circulating as a coolant is used to extract heat from the refrigerant. The temperature ratio could be characterized as

$$\frac{T_{a,o}-T_a}{T_{cd,i}-T_a}=f\left(\frac{(UA)_{cd}}{m_a C_{pa}}\right). \tag{17}$$

From the experiments as shown in Fig. 9, the characteristic equation of the condenser can be expressed as

$$\frac{T_{a,o}-T_a}{T_{cd,i}-T_a}=\frac{0.2723(UA)_{cd}}{m_a C_{pa}}+0.0107. \tag{18}$$

Expansion Valve Modeling

The characteristic equation of the expansion valve similar to Eqn. (9) can be expressed from the results shown in Fig. 10 as

$$\frac{P_{ex,o}}{P_{ex,i}}=\begin{bmatrix}\left(0.4839N^2-12.657N+59.808\right)m_r^2\\+\left(-0.0252N^2+0.5546N+0.9465\right)m_r\\+\left(0.0031N^2-0.0783N+0.6857\right)\end{bmatrix}. \tag{19}$$

As shown in Fig. 6, there are some accessory components in this system such as filter drier, accumulator and receiver. These components cause the pressure drops and heat losses also occur. From the experiments, the pressure drop related to the pressure ratio of the compressor and the expansion valve can be expressed as

$$\frac{P_{cp,i}}{P_{cp,o}}=0.954\left(\frac{P_{ex,o}}{P_{ex,i}}\right). \tag{20}$$

Moreover, it could be found that there is pressure drop across the condenser and it could be expressed as

$$P_{cd,o} = P_{cd,i} - 0.034. \tag{21}$$

Direct Contact Evaporator Modeling

Kiatsiriroat et al [7] generated a mathematical model for a direct contact evaporator by using lump model. The thermal characteristics of the water in the tank analyzed by the energy balance could be expressed as

$$\frac{d}{dt}(M_w h_w) + M_t C_t \frac{dT}{dt} = m_r(h_{ev,i} - h_{ev,o}) + (UA)(T_a - T_w). \tag{22}$$

As shown in the equation, the first three terms relate to the enthalpy change rates of the water, the container and the refrigerant, respectively. The last term relates to the external heat gain from the surrounding ambient. In this study, the direct contact evaporator is well insulated, the heat gain could be neglected. Then, the water temperature of the water inside the tank is separately considered in two processes, which are sensible heat process and ice formation process. The characteristic equations of the direct contact evaporator during the sensible heat process and the ice formation process can be expressed in the following equations, respectively as

$$T_w^* = T_w + \frac{m_r(h_{ev,i} - h_{ev,o})\Delta t}{M_t C_{pt} + M_w C_{pw}} \tag{23}$$

$$M_{ice} = \frac{m_r(h_{ev,o} - h_{ev,i})\Delta t}{L} \tag{24}$$

Due to the long length of the pipes between the evaporator unit, the compressor and the condenser in the direct contact experiment set-up, the heat gain and loss are considered. From the preliminary study, the heat gain between the low temperature refrigerant flowing inside the pipes from the evaporator to the compressor and the surrounding ambient can be characterized as

$$m_r C_{pr}\left(T_{cp,i} - T_{ev,o}\right) = f\left(T_a - \left(\frac{T_{ev,o} + T_{cp,i}}{2}\right), m_r\right) \tag{25}$$

From the experiments, the equation can be expressed as

$$m_r C_{pr}\left(T_{cp,i} - T_{ev,o}\right) = \left[\begin{array}{l} \left(-0.0459 m_r^2 + 0.0005 m_r + 0.0003\right)\left(T_a - \left(\frac{T_{ev,o} + T_{cp,i}}{2}\right)\right)^2 \\ + \left(0.9138 m_r^2 + 0.1596 m_r + 0.0356\right)\left(T_a - \left(\frac{T_{ev,o} + T_{cp,i}}{2}\right)\right) \\ + \left(2.663 m_r^2 + 1.1131 m_r - 0.1304\right) \end{array}\right]. \tag{26}$$

Then, for the high temperature refrigerant flowing through the pipe between the compressor and condenser, the heat loss can be characterized as

$$m_r C_{pr}\left(T_{cp,o} - T_{cd,i}\right) = f\left(\left(\frac{T_{cp,o} + T_{cd,i}}{2}\right) - T_a, m_r\right). \tag{27}$$

In this case, the equation can be expressed from the experiments as

$$m_r C_{pr}\left(T_{cp,o} - T_{cd,i}\right) = \left[\begin{array}{l} \left(1.607 m_r^2 - 0.0298 m_r - 0.0146\right)\left(\left(\frac{T_{cp,o} + T_{cd,i}}{2}\right) - T_a\right) \\ + \left(-20.432 m_r^2 + 1.9399 m_r - 0.293\right) \end{array}\right]. \tag{28}$$

4. SYSTEM SIMULATION

With the mathematical modeling of each main component in the system, the simulation is created to determine the energy consumption of the system at various possible combinations of the conventional chilled water system and the ice thermal energy storage (ITES) system. The computational steps are shown in Fig. 11.

As shown in Fig.11, the simulation consists of two parts, chilled water system and ITES system. The input parameters of the simulation are the total cooling load, Q_{load}; the compressor speed of the ITES system, N_{dc}; the mass flow rate of refrigerant for the ITES system, $m_{r,dc}$; the initial temperature of water in the storage tank, T_{wi}; the ambient temperature, T_{amb} and the properties of the system working fluid.

The cooling load is divided into two parts for chilled water system and ITES system, $Q_{load,ac}$ *and* $Q_{load,dc}$. For the chilled water system, the trial and error has been done to find out the suitable mass flow rate of the refrigerant at the given cooling load. Moreover, the power input of the compressor, the heat transfer rates at the condenser and the chiller are also the output values of the program.

For the ice storage part, the calculation is under the assumption that the leaving temperature of the refrigerant of the ice storage tank is equal to the temperature of the water in the tank because of high turbulence due to the refrigerant injection into the water tank. When the temperature of water is higher than 0.01°C, the calculation is in sensible heat mode. As the water temperature is lower than 0.01°C, the latent heat mode is applied. The outputs of this part are the power consumption at the compressor, the heat transfer rate of the direct contact evaporator and the time consumed for producing ice.

5. RESULTS

5.1 Chilled Water System

In the chilled water system part of the simulation program, after input the initial values of the variables, the compressor work and the heat transfer rate at the chiller are evaluated. The results from the simulation are compared to those of the experiments. The results are illustrated in Figs. 12-13. From the results, it could be found that the compressor work and the heat transfer rate depend on the refrigerant mass flow rate. As the refrigerant mass flow rate increases, these values are also increased. Moreover, it is noted that the values from the simulation program are closed to the experimental results.

5.2 Ice Storage System

For the ice storage simulation, the compressor work, the heat transfer rate at the direct contact evaporator and the time used to produce ice are evaluated. The results are shown in Figs. 14-15 and Table 1. They agree well with those of the experiments.

As shown in Figs. 14-15, the refrigerant mass flow rate has an effect on the both of the compressor work and the heat transfer rate at the direct contact evaporator. As the mass flow rate increases, the compressor work and the heat transfer rate are also increased.

The calculation above lead to the determination of the ice mass produced in the ice storage system and the results are shown in Table 1 in which good agreement is seen between the results from the simulation and the experiments.

5.3 Appropriate Sizing of the Ice Storage

In this research work, an office having 18 kW of cooling requirement is considered as a case study. Eight different air conditioning system combinations have been investigated to determine the appropriate possible combinations which relates to the electricity tariff (TOU rate) as shown in Table 2 [10].

The eight categories are as the following:

Category 1. Conventional design (no ice storage). The entire cooling requirement is supported by the chiller unit operating during the occupancy period.

Categories 2-8. Partial storage design. The chiller unit is responsible for the less cooling requirement compared to the conventional system. The cooling load is divided into two parts. The first part is supported by the chiller unit during the occupancy time and the other is supported by the ice produced in the ice storage or ITES system operating during the nighttime. The ratio of the cooling load supported by the chiller unit (kW) to the cooling load supported by the ITES system (kW) for categories 2-8 are 16:2, 14:4, 12:6, 10:8, 8:10, 6:12 and 4:14, respectively.

From the system simulation, the peak energy demand (kW) of each category is shown in Table 3 while the energy consumption (kW-h/day) and the operating cost of each categories are illustrated in Figs. 16-17.

From Table 3, it could be found that the peak energy demand during the on-peak period decreases when the capacity of the ITES system increases. This is due to the fact that the load of the compressor in the chilled water system is shifted to the ITES compressor running during the off-peak period. However, for categories 7 and 8 in which the capacities of the ITES are 12 and 14 kW, respectively, the required period for generating ice is more than 11 hrs. Then the

compressor load of the ice storage overlaps to that of the chilled water system in the on-peak period.

Fig. 16 shows the electrical energy consumption of the system in each category. Similar to Table 3, as the size of the storage increases, the energy consumption of the chiller decreases and that of the storage increases. For categories 2 –5, the total energy consumption does not exceed the conventional system (1st category). For categories 6 – 8, it could be found that the designs are not appropriat since the energy consumption is higher than that of the conventional unit.

To determine the operating cost, it could be seen that the appropriate design is the 5th category whereas the cheapest cost is obtained as shown in Fig. 17. At this condition, the energy demand and energy consumption from the daytime could be shifted to the nighttime when the tariff is lowest. The peak energy demand from 9.7 kW in case of the conventional unit could be reduced to 5 kW (48.7% decreased). The operating cost is reduced from 4,200 baht/month for conventional system to 3,100 baht/month resulting in 27% reduction.

It could be found that this system yields a realistic payback. In this research work, the installation cost of the ice storage system is approximately 70,000 baht and the operating cost is reduced for 1,100 baht/month. If the ITES is chosen to operate during March to October which has high opportunity to use the ice storage system, then, the payback period could be approximately 8 years.

6 CONCLUSION

The mathematical of each main component in the ice thermal energy storage with direct contact evaporator is created and the system simulation to find out the suitable refrigerant mass flow rate at any given cooling load, the time used to produce the required amount of the ice and energy consumption has been carried out with good agreement to the experimental results. It is also indicated that for the office having 18 kW of cooling requirement considered as a case study, the appropriate size of the ITES system is 8 kW. Under this operating condition, the peak electricity demand and the operating cost could be decreased 48.7 % and 27%, respectively comparing to the conventional chiller system. The payback is about 8 years.

Acknowledgement - The authors gratefully acknowledge the support provided by Thailand Research Fund and The Joint Graduate School of Energy and Environment for carrying out this study.

REFERENCES

1. S.A. Tassou and Y.K. Leung, Energy Conservation in Commercial Air Conditioning through Ice Storage and Cold Air Distribution Design, *Heat Recovery Systems & CHP*, Vol.12, pp.419-425, 1992.
2. Simmonds P., A Control Strategy for Chilled Water Production, *ASHRAE Journal*, pp. 30-36, January 1994.
3. Limmeechokchai, B. and Chungpaibulpatana, S., Application of Cool Storage Air Conditioning in Commercial Building Sector, Paper accepted for publication in *Applied Energy*, September 2000.
4. Crane, J. and Dunlop, C., Ice Storage System for a Department Store, *ASHRAE Journal*, pp. 49-52, January 1994.
5. Guluska, E., Thermal Storage System Reduces Costs of Manufacturing Facility, *ASHRAE Journal*, pp. 50-52, March 1994.
6. Subbaiyer, S., Andhole, T.M. and Helmer, W.A., Computer Simulation of a Vapor-Compression Ice Generator with a Direct Contact Evaporator, *ASHRAE Transactions*, part 1, pp. 118-126, paper number 3448, 1991.
7. Kiatsiriroat, T., Siriplubpla, P. and Nuntaphan, A., Performance Analysis of a Refrigeration Cycle Using a Direct Contact Evaporator, *International Journal of Energy Research*, **22**, 1179-1190, 1998.
8. Kiatsiriroat, T., Chowcheun, K. and Wibulswas, P., Simulation of a Standard Vapor-Compression Refrigeration System, *ASEAN Journal on Science & Technology for Development*, Vol 11, no.1, pp. 167-180, 1994.
9. Stoecker, W.F., *Design of Thermal Systems*, McGraw-Hill, USA, 1989.

10. Electricity Generating Authority of Thailand (EGAT), 1997. *Thailand power development plan PDP 1997-01.* System Planning Department. Bangkok, Thailand.

NOMENCLATURE

C_P	specific heat capacity (kJ/kgK)
DC	demand charge (Baht/kW)
EC	energy charge (Baht/unit)
h	specific enthalpy (kJ/kg)
k	polytropic index
L	latent heat (kJ/kgK)
m	mass flow rate (kg/s)
M	mass (kg)
N	compressor speed (rps)
OC	overall charge (Baht))
P	pressure (MPa)
Q	heat transfer rate (kW)
T	Temperature (°C)
Δt	period of time (s)
UA	overall heat transfer coefficient (kW/m^2K)

Subscripts

a	air
cd	condenser

ch chiller

cp compressor

ev evaporator

ex expansion valve

i inlet

o outlet

r refrigerant

w water

CAPTIONS OF FIGURES AND TABLES

Fig. 1. Schematic diagram of the experimental set-up.

Fig. 2. The relation between pressure ratio of the compressor and a function of $m_r T_{cp,i}^{0.5}/P_{cp,i}$.

Fig. 3. The relation between pressure ratio of the compressor and a function of $m_r T_{cp,o}^{0.5}/P_{cp,o}$.

Fig. 4. The relation between mass flow rate of the refrigerant and the polytropic index of the compressor in chilled water system.

Fig. 5. The relation between the pressure ratio in the chilled water system and the refrigerant mass flow rate.

Fig. 6. Schematic diagram of the experimental set-up for the ice storage system.

Fig. 7. The relation between pressure ratio of the compressor in the ice storage system and a function of $m_r T_{cp,o}^{0.5}/P_{cp,o}$ and N.

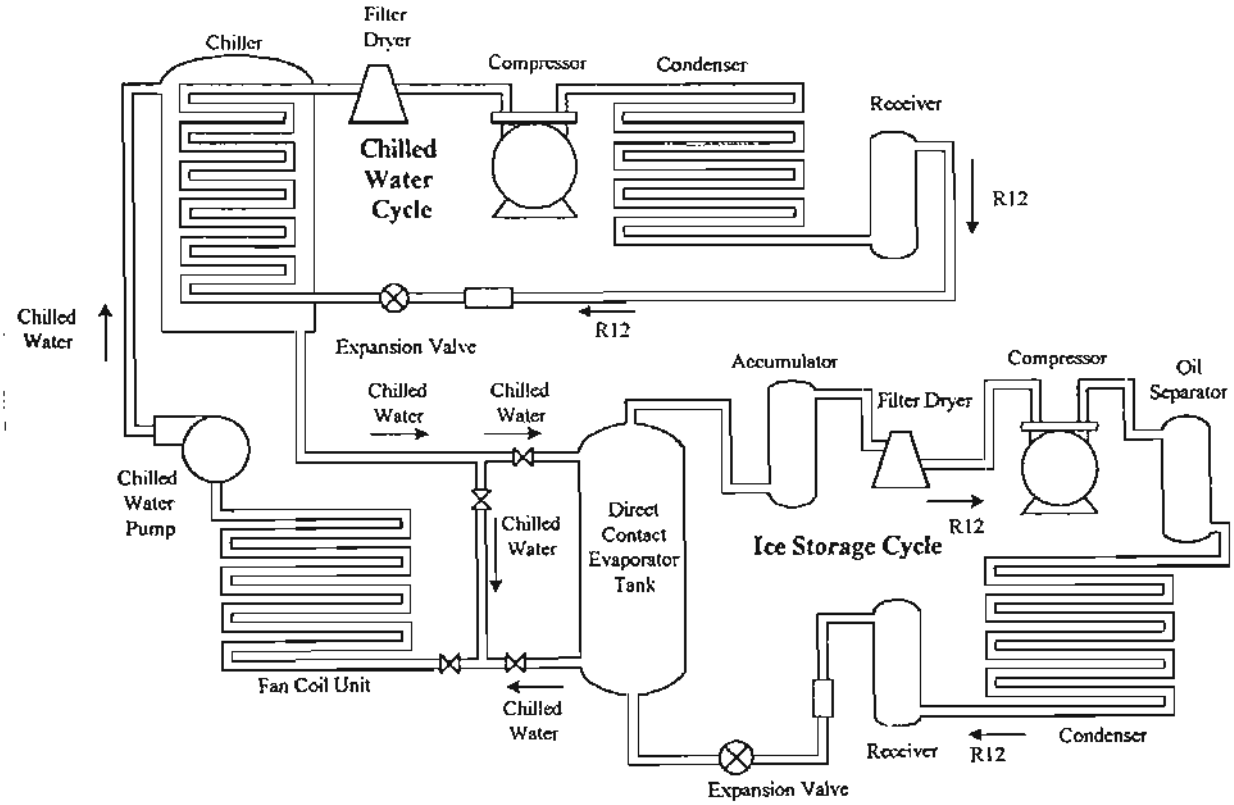

Fig.1. Schematic diagram of the experimental set-up.

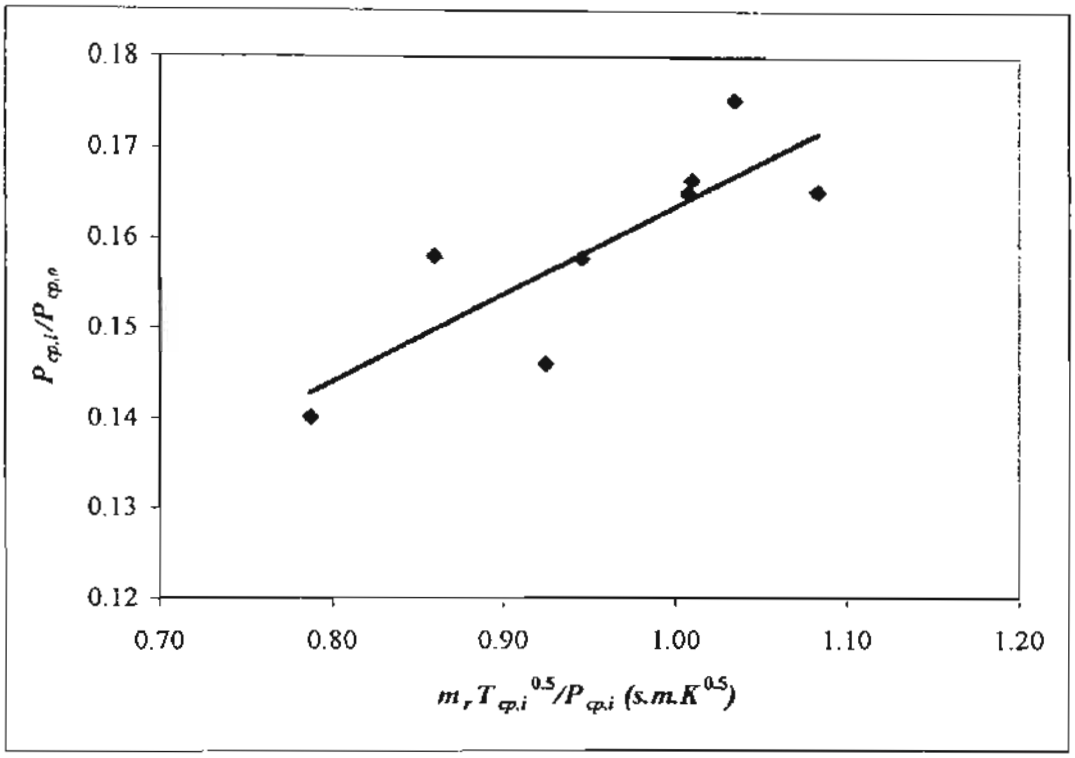

Fig.2. The relation between pressure ratio of the compressor and a function of $m_r T_{cp,i}^{0.5}/P_{cp,i}$.

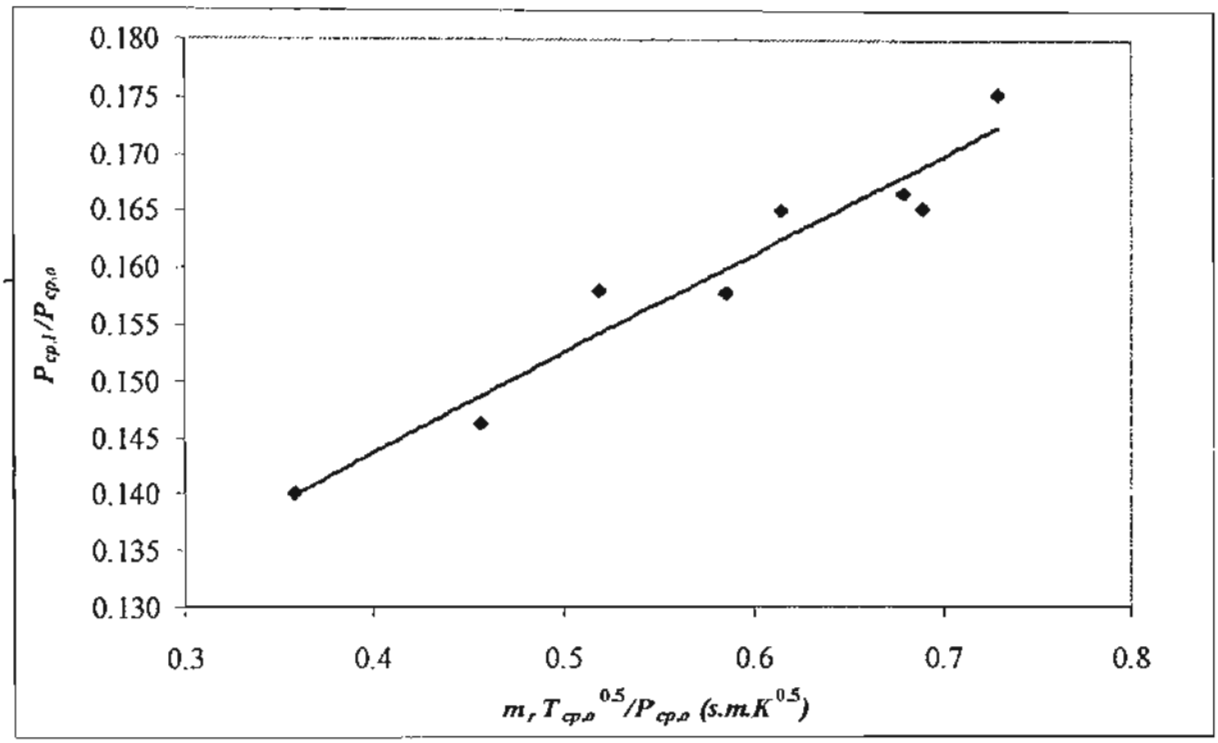

Fig.3. The relation between pressure ratio of the compressor and a function of $m_r T_{cp,o}^{0.5}/P_{cp,o}$

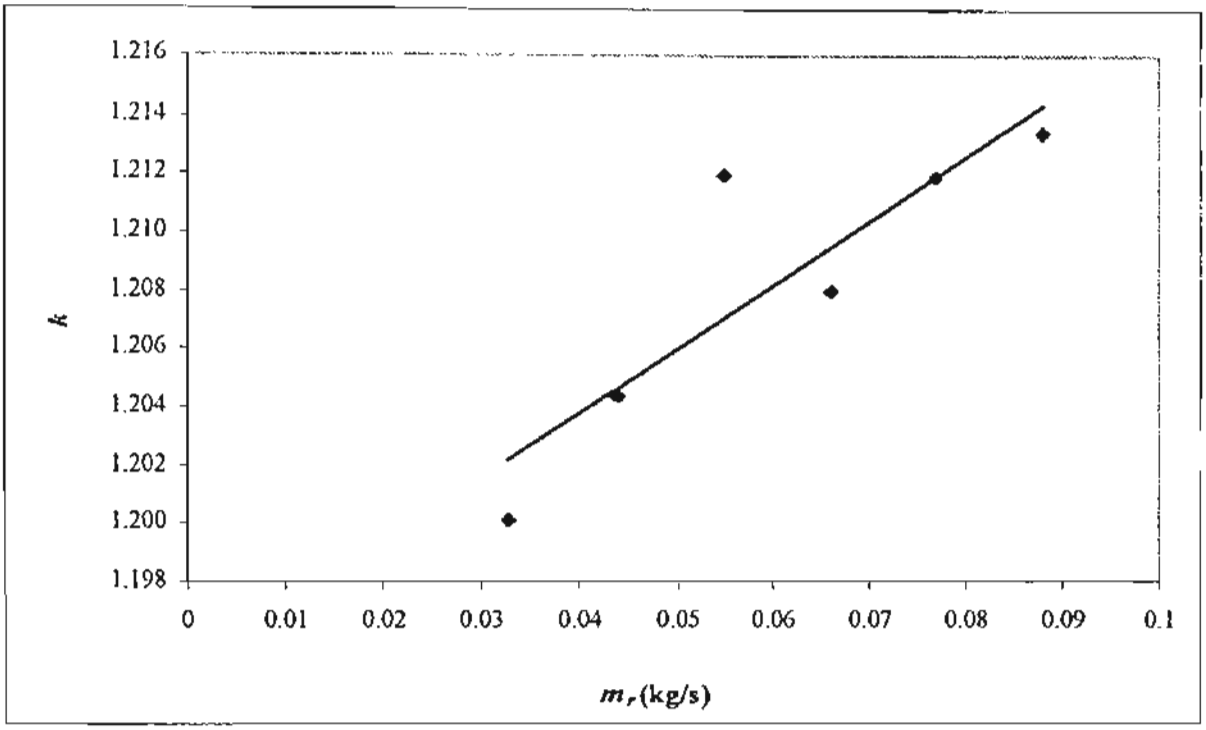

Fig.4. The relation between mass flow rate of the refrigerant and the polytropic index of the compressor in chilled water system.

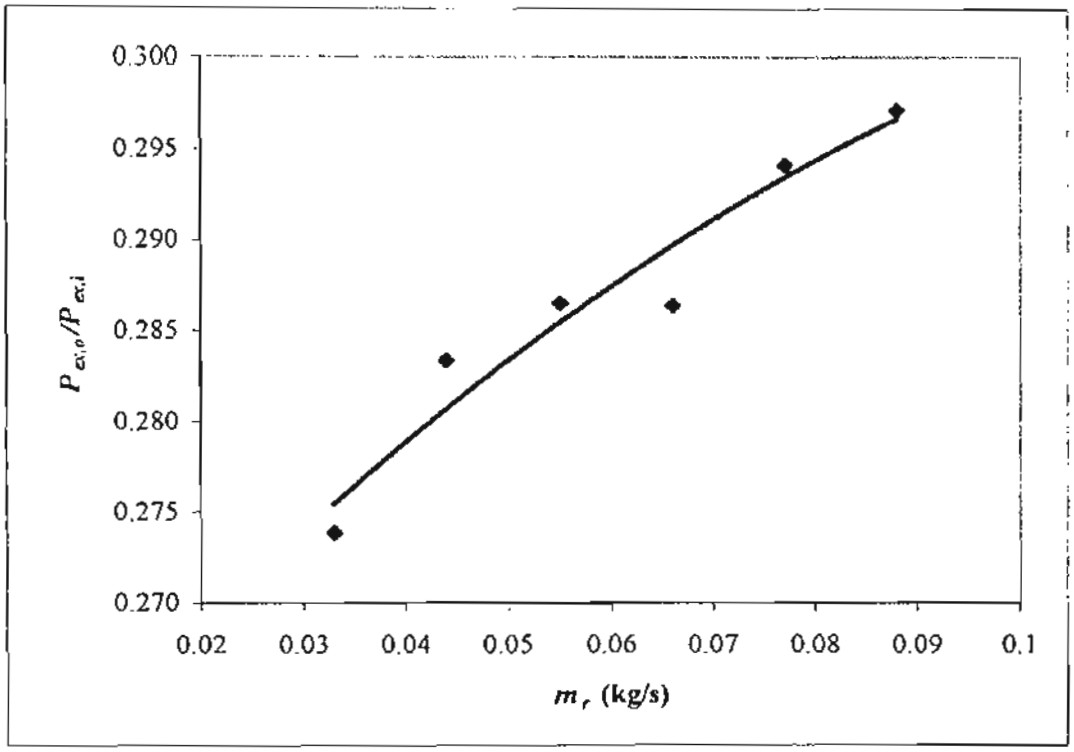

Fig.5. The relation between the pressure ratio in the chilled water system and the refrigerant mass flow rate.

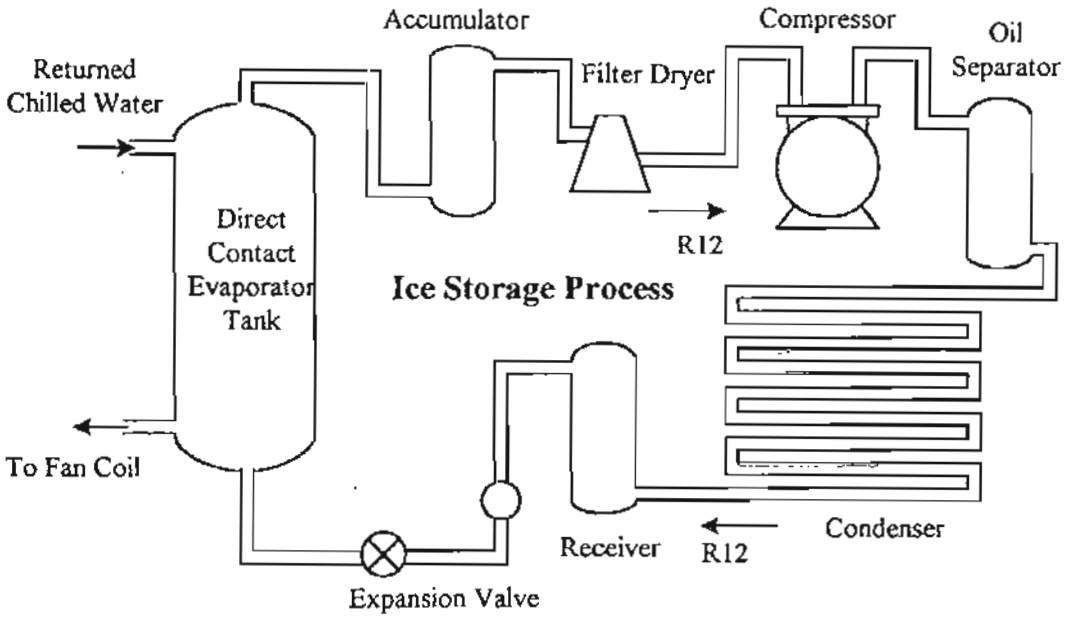

Fig.6. Schematic diagram of the experimental set-up for the ice storage system.

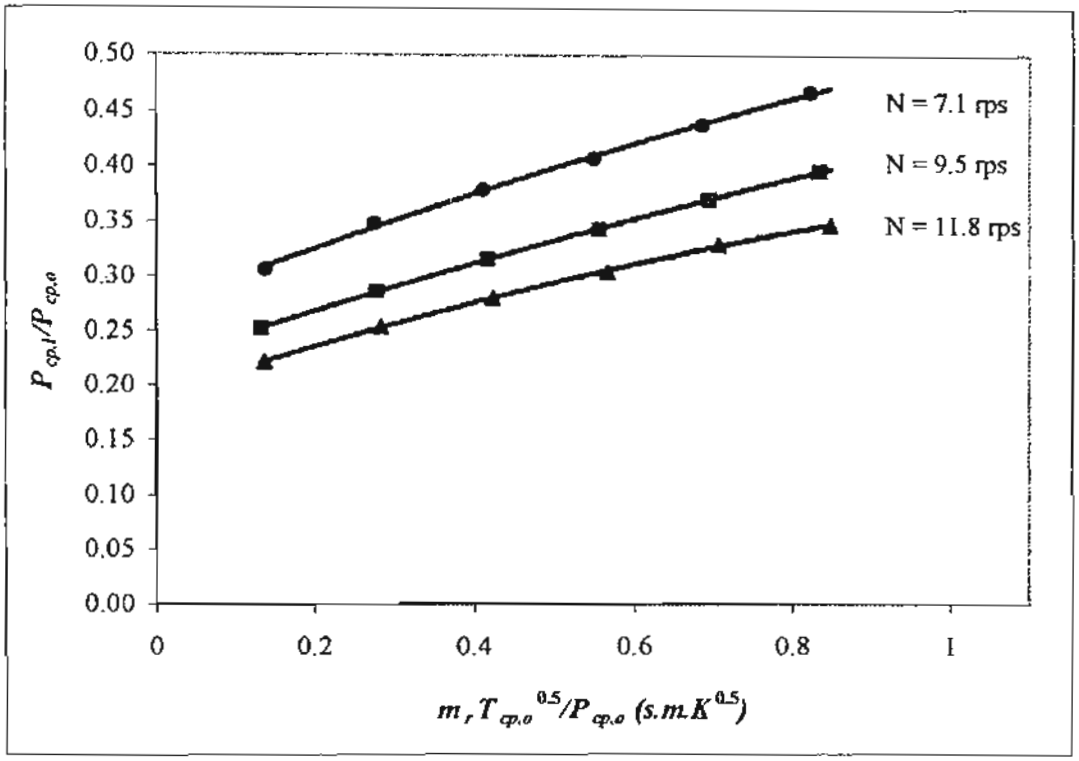

Fig.7. The relation between pressure ratio of the compressor in the ice storage system and a function of $m_r T_{cp,o}^{0.5}/P_{cp,o}$ and N.

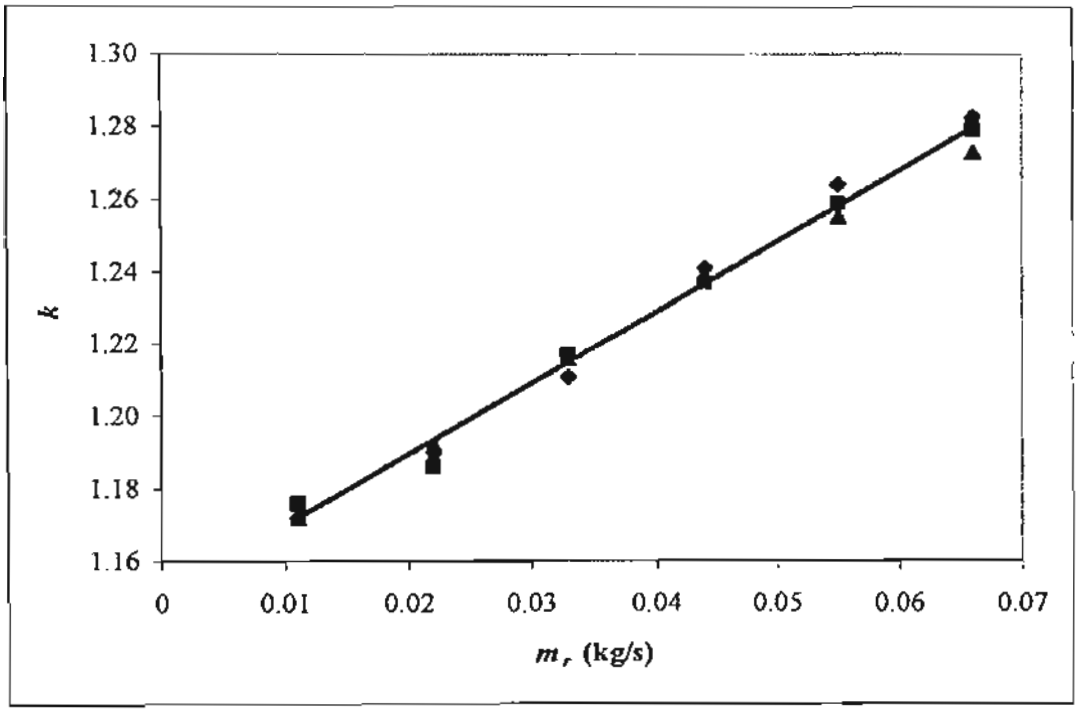

Fig.8. The relation between mass flow rate of refrigerant and the polytropic index of the compressor in ice storage system.

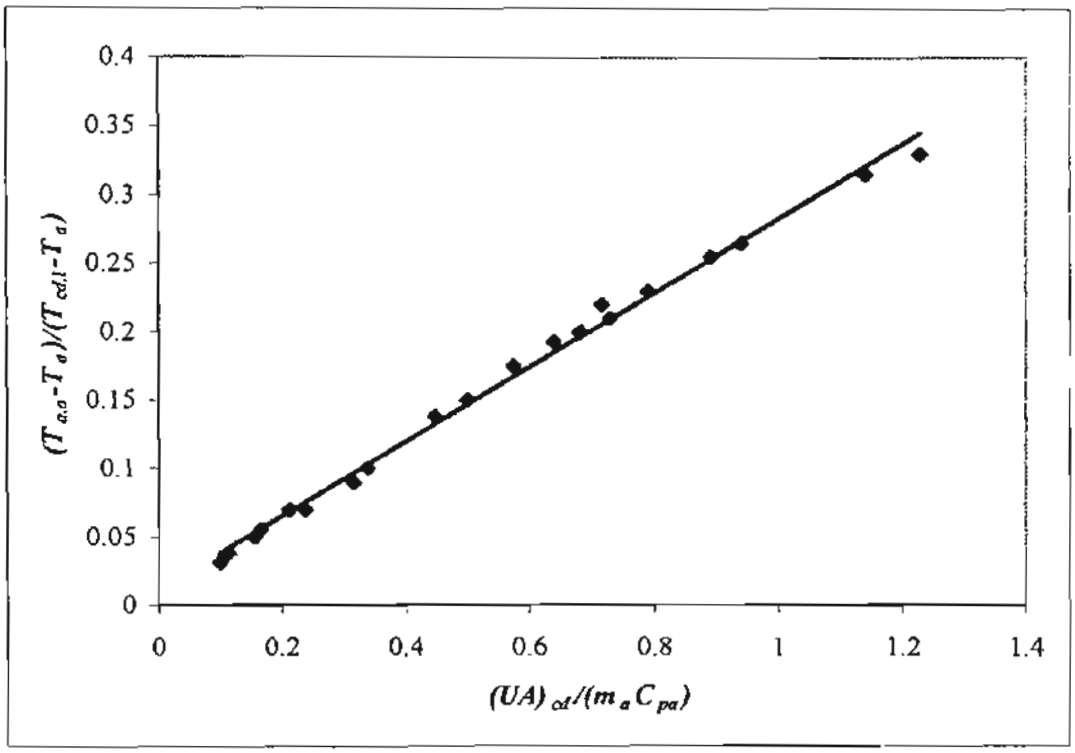

Fig.9. The effect of mass flow rate of air and total heat transfer coefficient to outlet temperature of air.

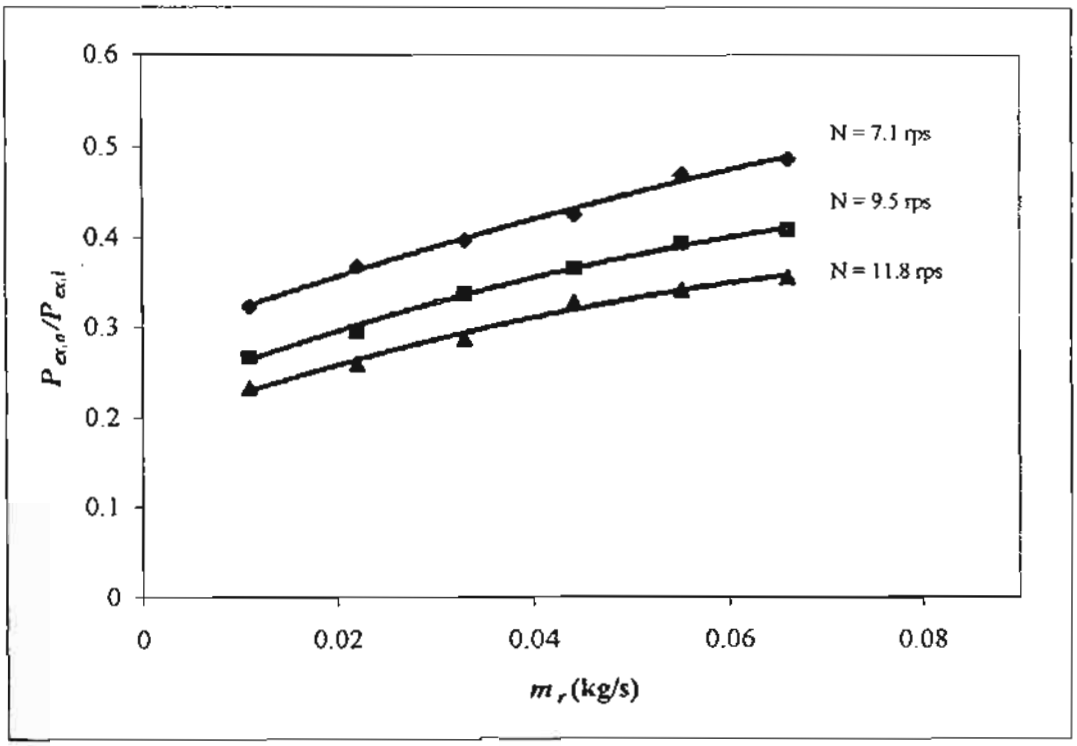

Fig.10. The relation between pressure ratio of the expansion valve in the ice storage system and mass flow rate of refrigerant at various compressor speeds.

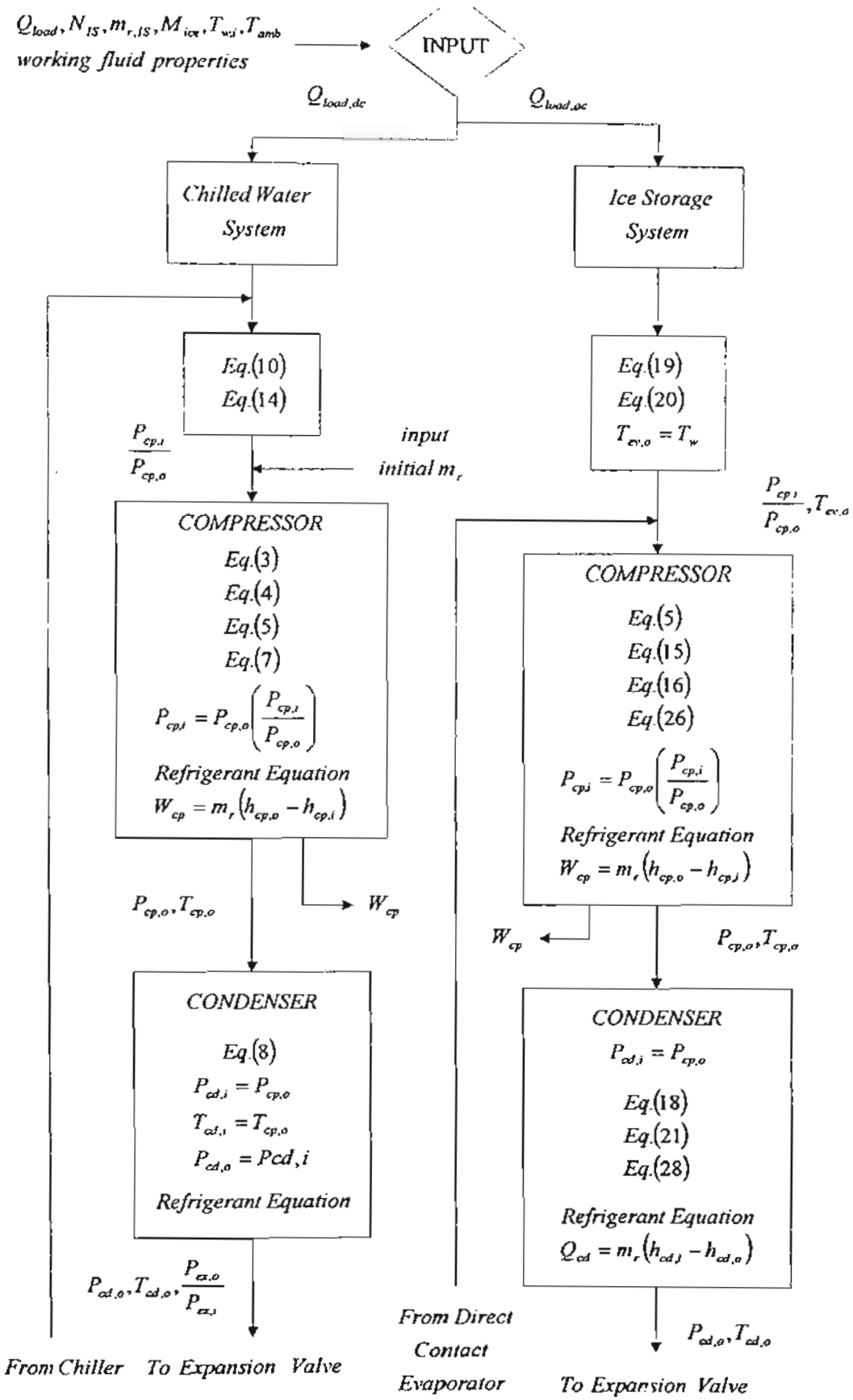

Fig. 11. Information flow diagram of the system simulation.

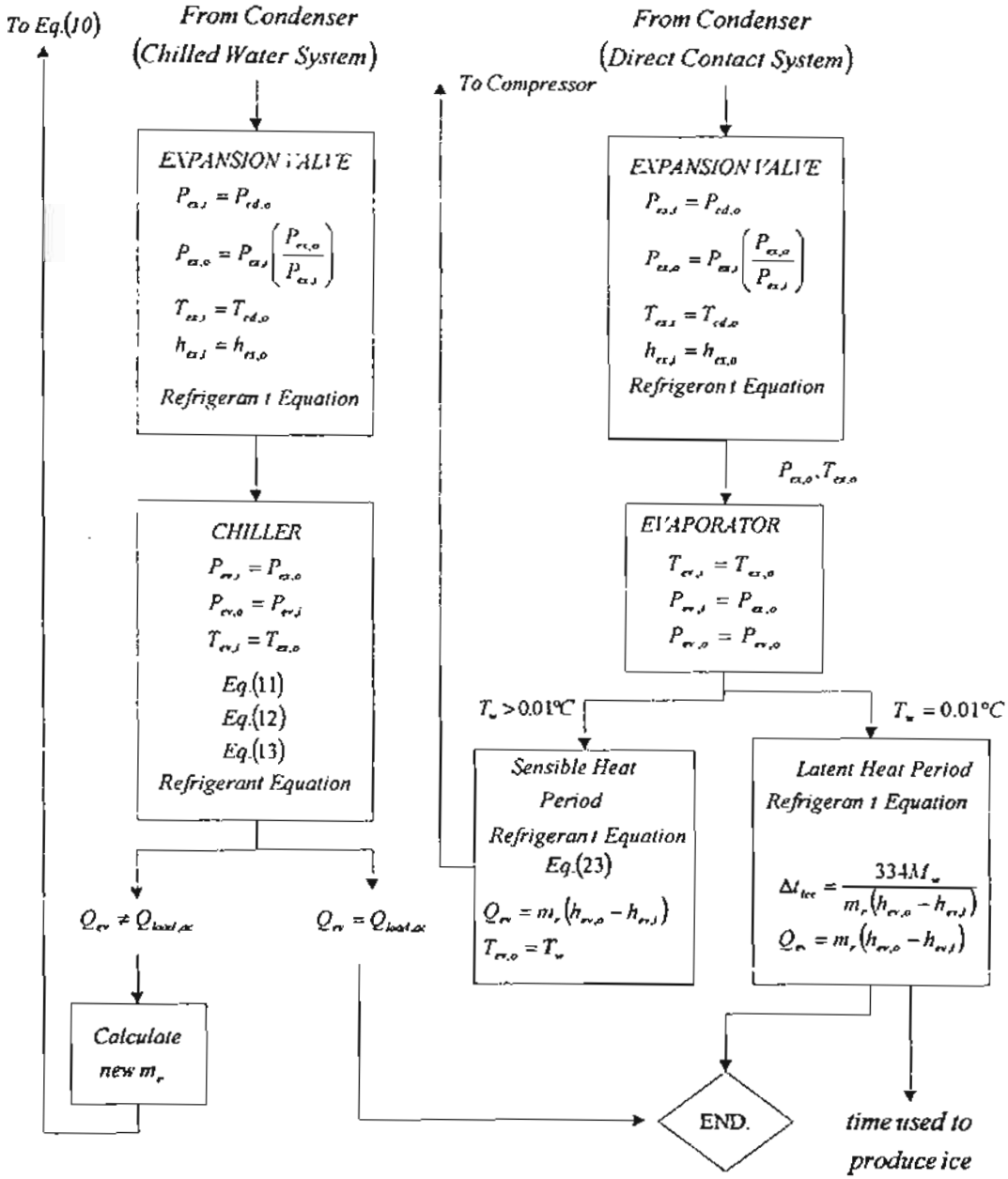

Fig. 11. Information flow diagram of the system simulation (continued).

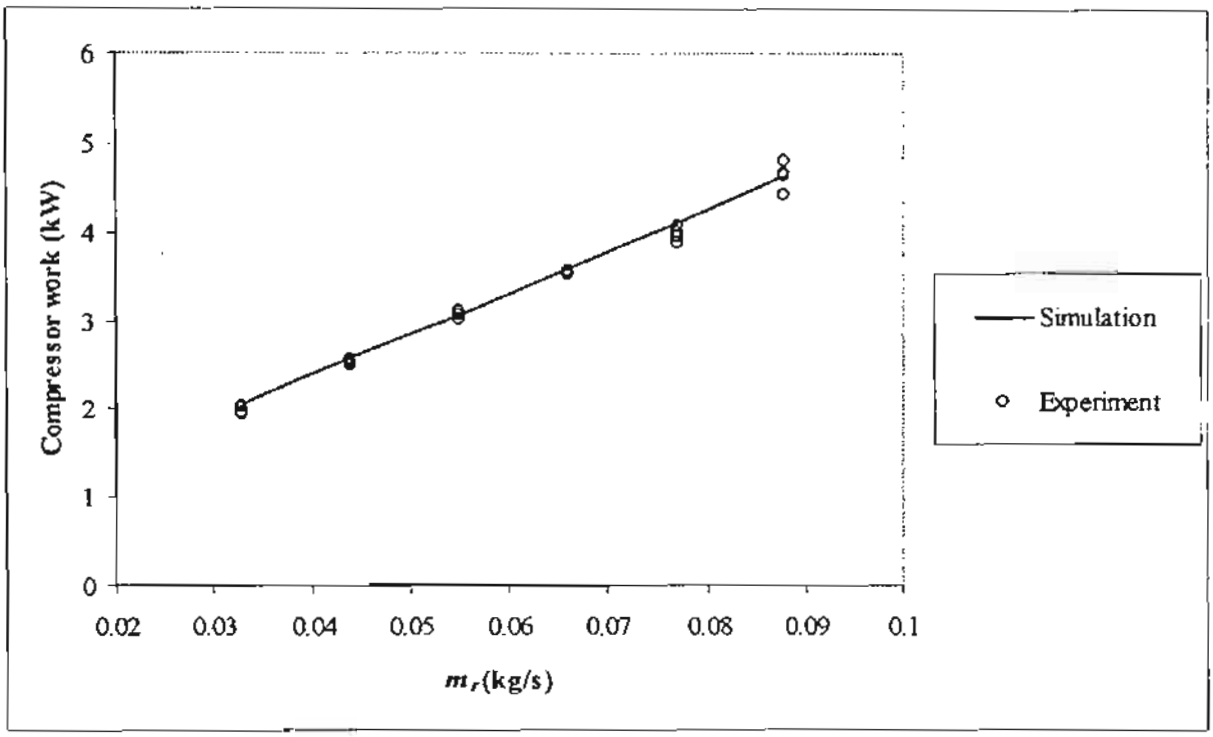

Fig. 12. Compressor work of the chilled water system at various refrigerant mass flow rates.

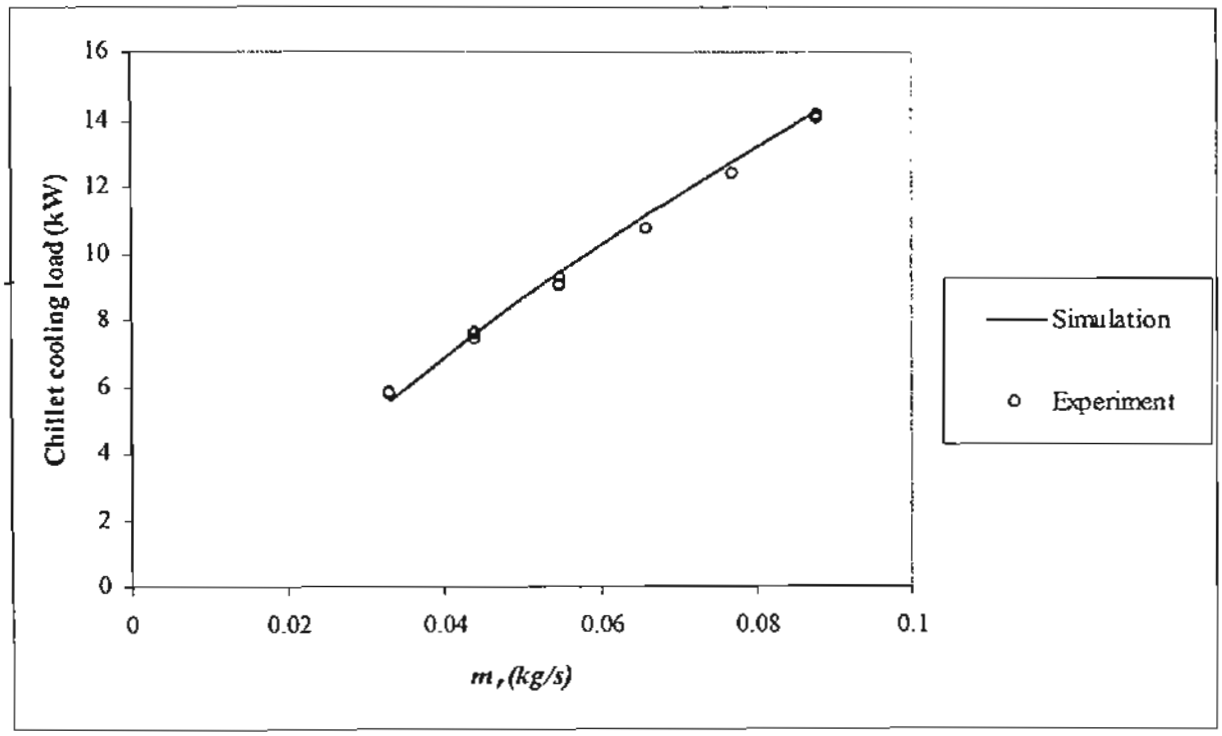

Fig. 13. The chiller cooling load at various refrigerant mass flow rates.

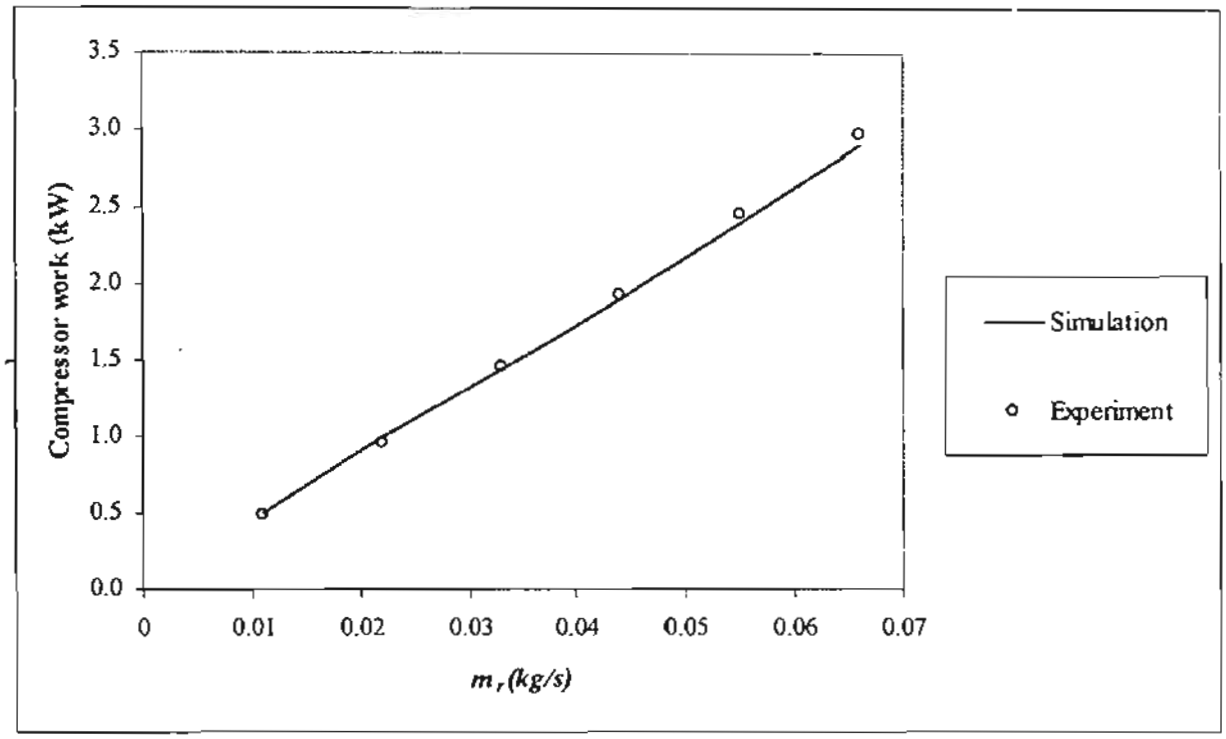

Fig. 14. Compressor work of the ice storage system at various refrigerant mass flow rates.

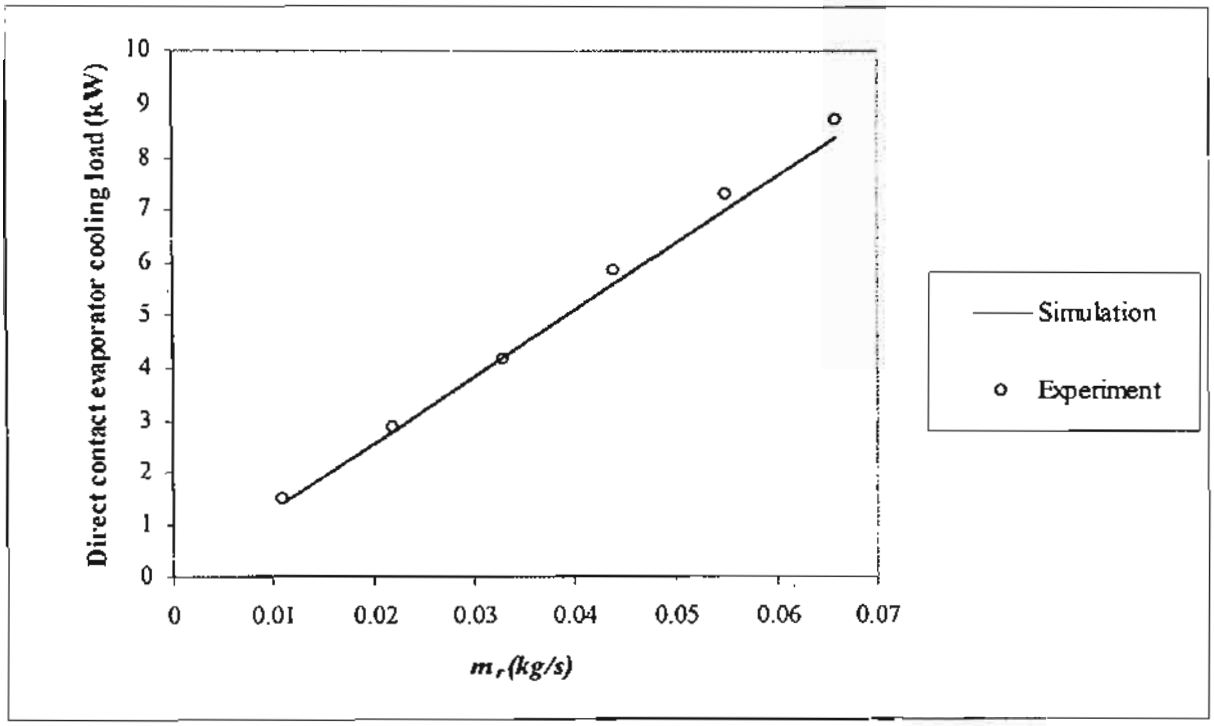

Fig. 15. The direct contact evaporator cooling load at various refrigerant mass flow rates.

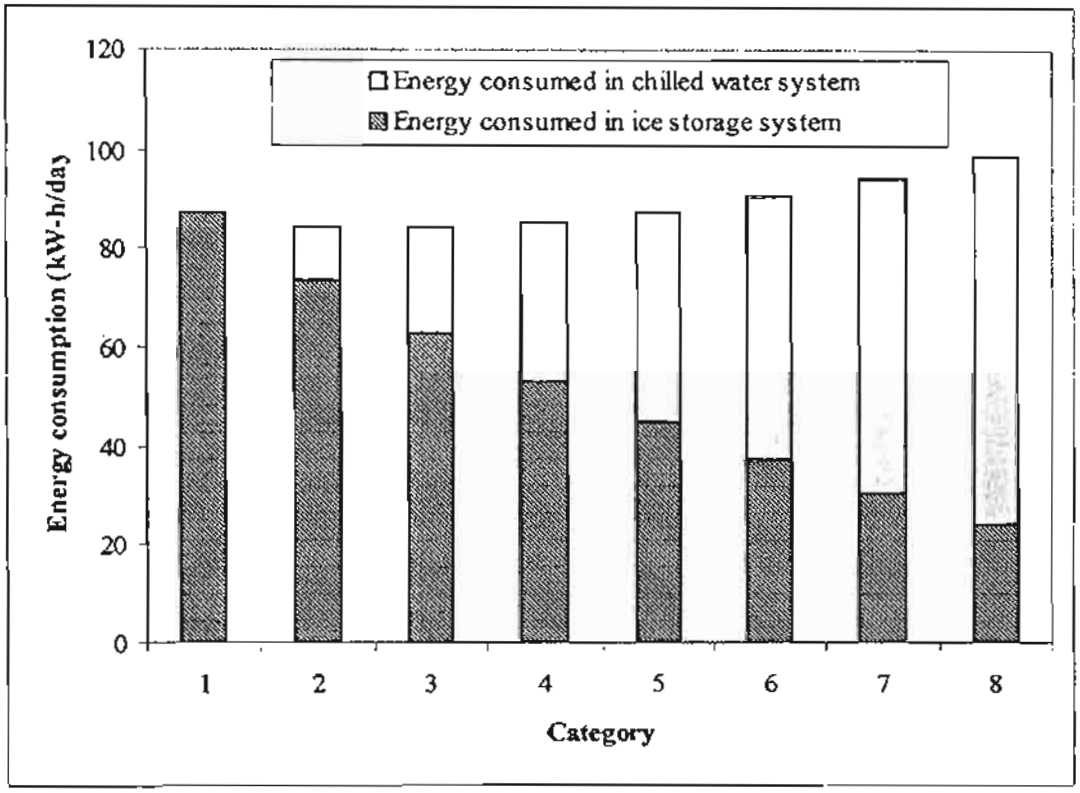

Fig.16. Energy consumed in each category.

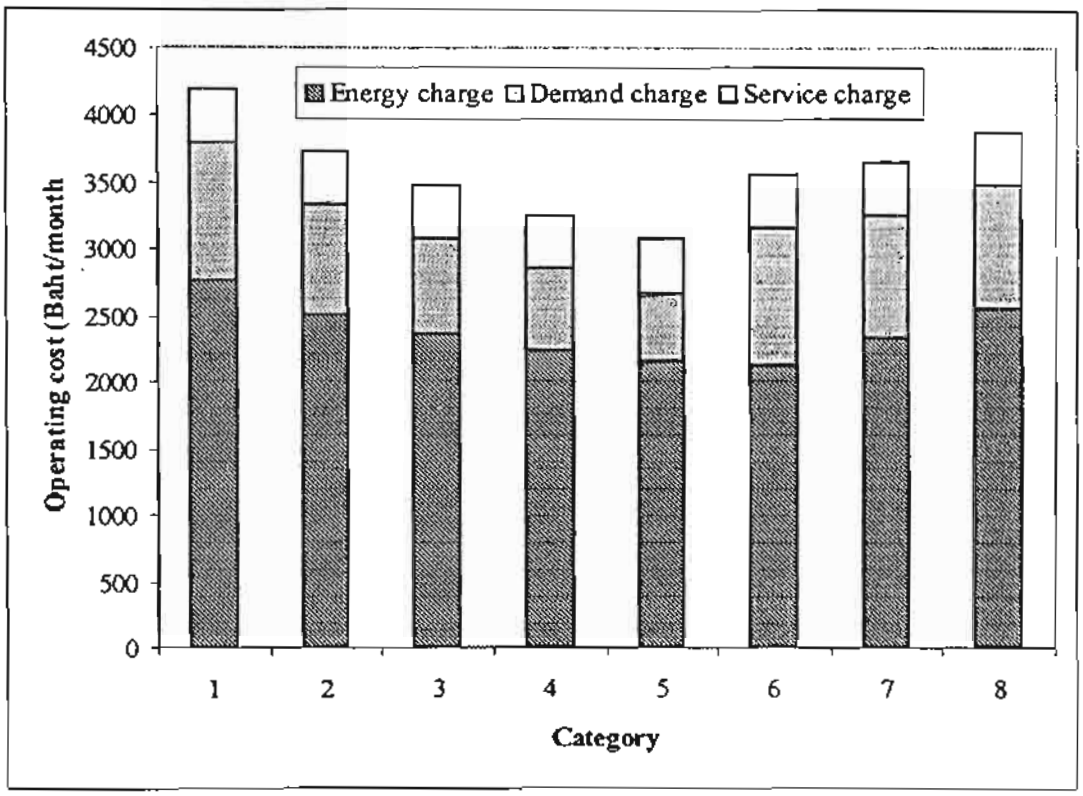

Fig. 17. Operating cost in each category

Table 1. The comparison of ice formation between the simulation and the experiment.

Mass of water in storage tank (kg)	m_r (kg/s)	N (rps)	Initial water temp. (°C)	Tamb (°C)	Produced ice mass (kg) (sim.)	Time (hr) (sim.)	Produced ice mass (kg) (exp.)	Time (hr) (exp.)
250	0.077	11.8	18.0	29.2	250	3.66	212	3.59
250	0.100	11.8	16.5	30.2	250	3.11	209	3.23
300	0.066	11.8	15.0	28.5	300	5.01	272	4.98
300	0.100	11.8	15.4	26.8	300	3.67	269	3.62

Table 2. Electricity cost (TOU Rate) for commercial building [10]

Voltage	Demand Charge (Baht/kW)	Energy Carge (Baht/unit)			Service charge (Baht/month)
	1*	1*	2*	3*	
>115 kV	102.80	1.5349	0.6671	0.6062	400.00
69 kV	158.88	1.6292	0.6769	0.6153	400.00
22 –23 kV	200.93	1.7736	0.6861	0.6236	850.00
<22 kV	214.95	1.8891	0.7283	0.6616	850.00

1* Monday – Saturday 09.00 – 22.00 (On-peak)

2* Monday – Saturday 22.00 – 09.00 (Off-peak)

3* Sunday 00.00 – 24.00 (Off-peak)

Table 3. The peak energy demand occurred during on-peak period at various categories.

Category	Ice storage system capacity (kW)	Peak energy demand		
		Chilled water system (kW)	Ice storage system (kW)	Total (kW)
1	0	9.7	-	9.7
2	2	8.2	-	8.2
3	4	7.0	-	7.0
4	6	5.9	-	5.9
5	8	5.0	-	5.0
6	10	4.1	-	4.1
7	12	3.4	5.5	8.9
8	14	2.6	5.5	8.1

Heat Transfer Model of a Direct Contact Evaporator

T. Kiatsiriroat, S. Vithayasai and N. Vorayos
Department of Mechanical Engineering
Chiang Mai University, Chiang Mai 50200, Thailand

A. Nuntaphan
South East Asia Center for Training in Energy for Development
Electricity Generating Authority of Thailand
Mae Moh, Lampang 52220, Thailand

N. Vorayos
Joint Graduate School of Energy and Environment
King Mongkut's University of Technology Thonburi
Bangkok 10140, Thailand

ABSTRACT

This research work studies heat transfer characteristic of a direct contact evaporator. A cold two-phase refrigerant (R12 or R22) is injected into water kept in a storage tank to exchange heat with the water directly. The water temperature is reduced to the freezing point and ice could be formed. The lump model is used to predict the water temperature and it is found that this model can predict the water temperature quite well. A correlation which relates the dimensionless parameters such as Stanton number, Stephan number, Prandtl number and pressure ratio is also developed.

Keywords: *Direct contact heat exchange, Ice thermal energy storage, Heat transfer correlation.*

Submitted to **Applied Energy, June, 2001**

Address of Correspondence and Proof:
Prof. Dr. Tanongkiat Kiatsiriroat
Department of Mechanical Engineering, Faculty of Engineering,
Chiang Mai University, Chiang Mai 50200, Thailand.
Tel:6653-944144 Fax:6653-944145
E-mail: *tanong@dome.eng.cmu.ac.th*

INTRODUCTION

For several years, the electrical energy consumption has increased and becomes a serious problem in developing countries. In Thailand, the electricity demand increases approximately 12% every year [1]. The demand-side management policy is set as a method to overcome this problem by charging the consumers with a high premium rate for the energy consumed during the peak period and a low rate during the off-peak period. Uniform load factor and reduction of peak demand then are anticipated.

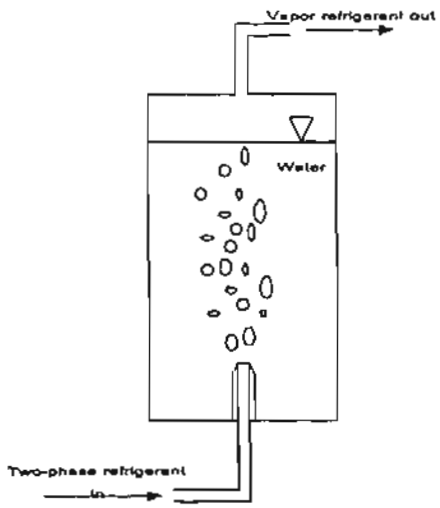

Figure 1 Direct contact evaporator.

In case of commercial building, 60% of the electrical energy consumption comes from the air-conditioning system [2]. This system is normally operated during the daytime or on-peak period which consequently increases the electrical peak demand and thereby is charged with a high electrical charge rate. To alleviate this problem, ice thermal energy storage has been conducted. During the nighttime or off-peak period, ice could be formed in a storage tank and

during the daytime a circulation of cool water from a storage tank is used for air-conditioning purpose. As the result, the uniform load and reduction of the peak demand are achieved.

The most common design of ice thermal energy storage is ice-on-coil system. The refrigerant is circulated inside the submerge coil in a water tank on which ice formation takes place. However, because of low thermal conductivity of ice, the ice layer forming on the coil severely inhibits the transfer of heat. To improve the performance of the ice storage, the direct contact evaporator is conducted. Figure 1 shows the principle of the direct contact evaporator. The cold two-phase refrigerant is injected into the water in the storage tank to extract heat from water directly. The water temperature is decreased and ice is formed when the freezing point is reached. The refrigerant vapor leaves the storage tank through the upper channel.

Some studies on the injection of immiscible fluid into phase change materials for exchangining heat directly have been carried out. The applications are thermal storages for heating and a few for cooling purposes. Blair et al. [3] studied the heat transfer characteristic of R113 droplet injected into a water column. It was found that the column height affected the degree superheat of the refrigerant and the mass flow rate of refrigerant played an important role on the volumetric heat transfer coefficient which approximately equaled 122 kW/m^3K. Sideman and Gat [4] also found that the volumetric heat transfer coefficient of pentane injecting into water was about180 kW/m^3K which was in the same order as Blair et al. In contrast, Goodwin et al. [5] reported that the volumetric heat transfer coefficient of pentane injecting into water was only about 3-8 kW/m^3K. However no further explanation was elaborated.

Subbaiyer et al. [6] showed a simulated result of a refrigeration unit with a direct contact evaporator. The unit required only 50-60% of electrical energy consumption per ton of refrigerant compared with a cooling coil ice generator. Kiatsiriroat et al. [7] studied the

phenomenon of ice forming around a jet stream of refrigerant injected from the bottom of a water column. Different types of refrigerant, R12, R22 and R134a were used. It was found that the stream of R22 showed better heat transfer, and ice could be formed quicker than those with the other refrigerants. A numerical model to predict the water temperature and the thickness of ice forming was developed, and the results agreed quite well with those of experiment.

In this present study, the heat transfer model of a direct contact evaporator has been investigated. R12 and R22 are selected as the refrigerants and water is chosen as the phase change material. The effects of the volume of water, the inlet temperature and the mass flow rate of refrigerant are investigated and their relation in terms of dimensionless groups is also developed.

THE EXPERIMENTAL SETUP

Figure 2 shows the experimental setup which consists of a direct contact evaporator, a dryer unit, a compressor - condensing unit, a receiver tank and an expansion valve. The direct contact evaporator is a stainless steel storage tank with 30 cm diameter and 110 cm height. The refrigerant from a receiver is injected through the expansion valve to reduce the pressure and temperature. This valve not only controls the mass flow rate of the refrigerant but also controls the temperature and the pressure of refrigerant injected into the storage tank. The cold two-phase refrigerant injected extracts heat from the water directly. As a result, the water temperature is decreased and ice could be formed when the temperature reaches the freezing point. The refrigerant after getting heat becomes vapor and leaves the storage tank to the compressor-condenser unit. The dryer unit is used to eliminate the moisture which might come along with the

refrigerant vapor. The vapor condenses in the condensing unit and the liquid refrigerant returns back to the receiver.

In this study, the refrigerant mass flow rate, the inlet and the outlet temperatures and pressures at the expansion valve, and the water temperature of the storage tank are recorded. Table 1 shows the testing conditions of the experiment.

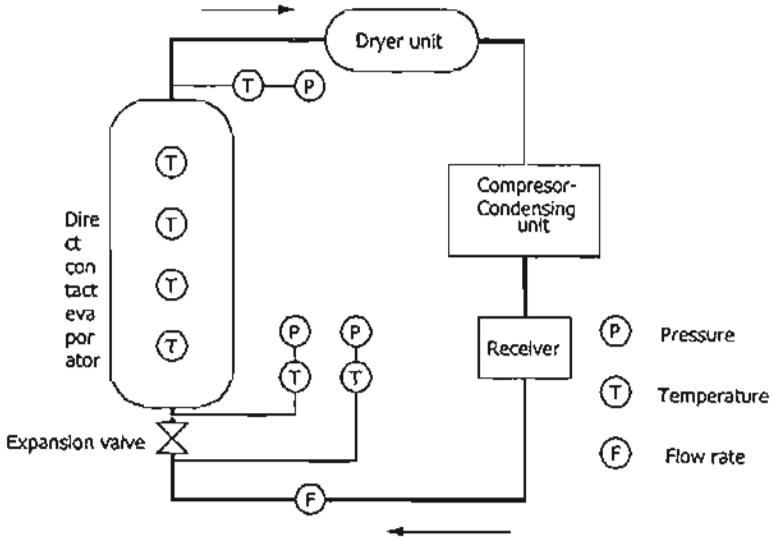

Figure 2 Schematic diagram of the experimental apparatus.

Table 1 The testing conditions of this research work.

Item	Conditions
Mass of water in a storage tank	20-40 kg
Mass flow rate of refrigerant	0.02-0.08 kg/s
Inlet temperature of refrigerant	-8 – -15 °C

MATHEMATICAL MODEL

In our previous studies [2, 8, 9], it was found that high turbulence was found in the water column during the refrigerant injection then the temperature of water was found to be uniform. Moreover, the temperature of the refrigerant that leaving out from the water was close to that of water in the storage tank. Therefore the lumped model could be conducted to analyze the thermal characteristic of the water in the storage tank.

The energy balance at the direct contact evaporator could be written as

$$\frac{d}{dt}(m_w h_w) + m_t Cp_t \frac{dT_w}{dt} = \dot{m}_r (h_{ri} - h_{ro}) + (UA)(T_a - T_w). \qquad [1]$$

The left-hand terms are the rate of enthalpy changes of the water and the container respectively. The first right-hand term is the rate of enthalpy change of the refrigerant and the final term is the external heat gain from the surrounding ambient. When the unit is well insulated, the heat gain could be neglected.

During the sensible heat process and the tank temperature is assumed to be the same as that of the water inside, equation [1] could be rewritten in numerical form as

$$T_w^{t+\Delta t} = T_w^t + \frac{\dot{m}_r (h_{ri} - h_{ro}) \Delta t}{m_t Cp_t + m_w Cp_w} \quad . \qquad [2]$$

During the ice formation, the temperature of water is constant around the freezing point. Consequently, equation [1] could be written as

$$m_w \frac{dh_w}{dt} = \dot{m}_r (h_{ri} - h_{ro}) \Delta t \qquad [3]$$

or

$$h_w^{t+\Delta t} - h_w^t = \frac{\dot{m}_r \Delta t}{m_w}\left(h_{ri} - h_{ro}\right) \quad . \qquad [4]$$

$$m_{ice}^t = \frac{m_w\left(h_l - h_w^t\right)}{\lambda} \qquad [5]$$

With the initial condition and the properties of the refrigerant entering, the temperature decrease during the sensible heat process and the amount of ice formation during the latent heat process could be evaluated.

RESULTS AND DISCUSSION

Thermal Analysis of the Direct Contact Evaporator

Figures 3 and 4 show the water temperature in the storage tank compared with that evaluated from the lump model. Since adiabatic storage tank is assumed the temperature from the model drops slightly quicker than that of the experiment. Figure 3 also shows the effect of the refrigerant mass flow rate on the water temperature in the storage tank. When the mass flow rate increases higher heat transfer rate is obtained which results in quicker drop of the water temperature.

Figure 4 shows the effect of the water volume on the rate of temperature drop. It is found that higher amount of the water results in higher the total heat capacity and the temperature drops with a lower rate.

Figure 5 shows the comparison between the amounts of ice formed in the experiment with those from the model. The model gives higher amount of ice than the experimental results approximately 20-30% because of quicker temperature drop.

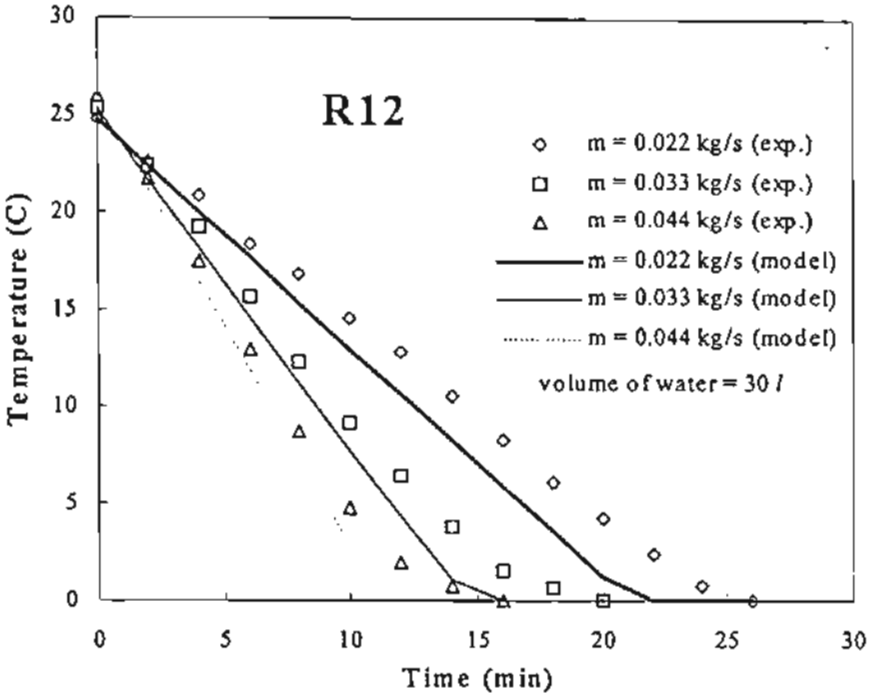

Figure 3 Comparison of water temperatures in the storage tank between the experiment and the lump model at various refrigerant mass flow rates; volume of water = 30 l.

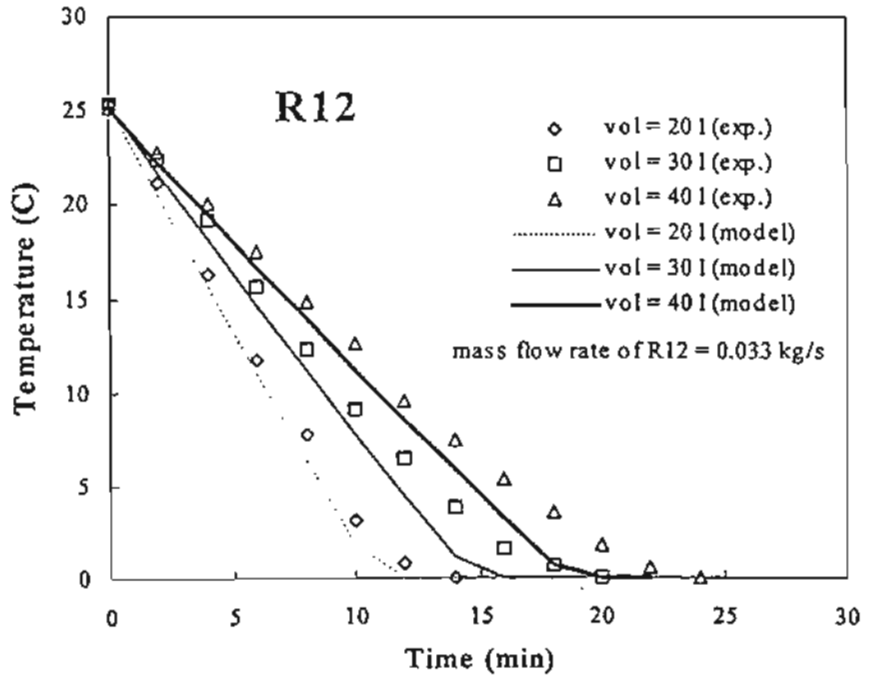

Figure 4 Comparison of water temperatures in the storage tank between the experiment with the lump model at various amounts of water; mass flowrate of refrigerant = 0.033 kg/s.

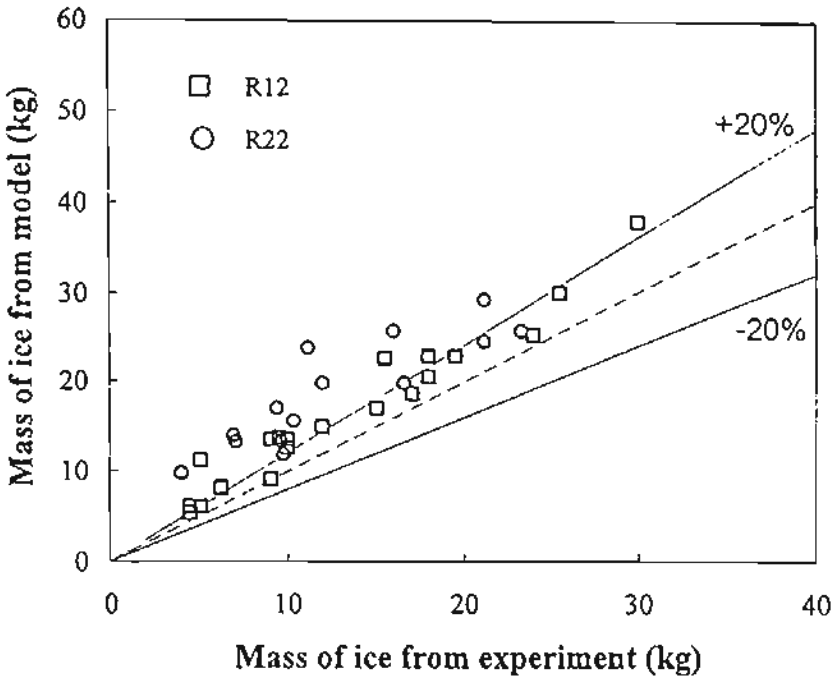

Figure 5 Comparison of amount of ice in the storage tank from the experiment with the model.

Figure 6 shows the volumetric heat transfer coefficient (U_v) of the heat exchange in the storage tank which can be calculated from

$$U_v = \frac{\dot{m}_r (h_{ro} - h_{ri})}{V(T_w - T_{ri})}, \qquad [6]$$

where V is the volume of water in a storage tank.

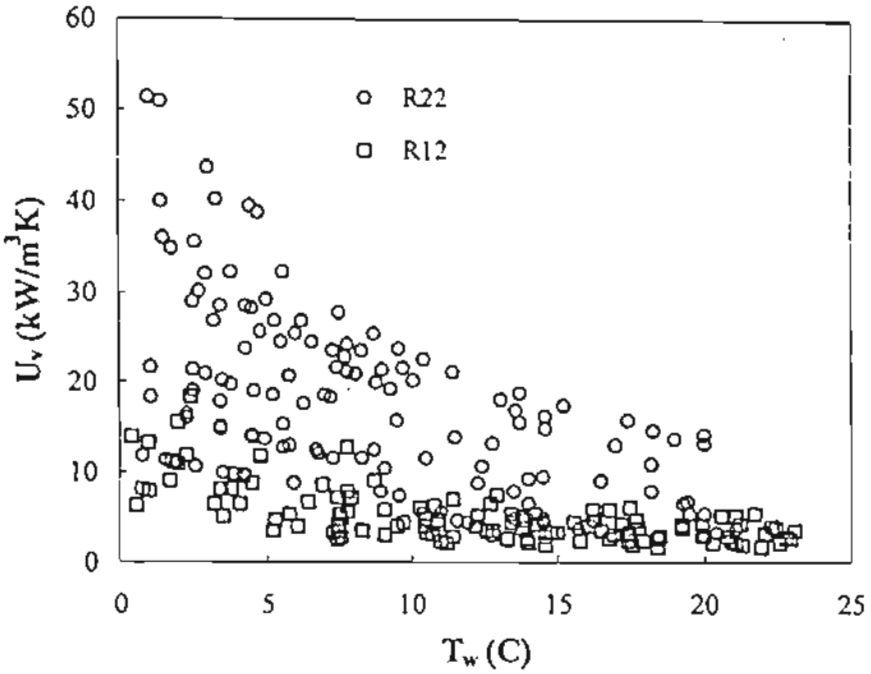

Figure 6 Volumetric heat transfer coefficient of the direct contact evaporator at various conditions.

From Figure 6 it is found that the volumetric heat transfer coefficient increases when the temperature of water decreases. As the temperature of water nearly freezing point, the volumetric heat transfer coefficient increases drastically. It is found that the range of the volumetric heat transfer coefficient is around 2-16 kW/m^3 in case of R12 and around 2-52 kW/m^3 in case of R22. These values are low compared to the results of Blair et al. [3] (122 kW/m^{3}K; R113-water), Sideman and Gat [4] (180 kW/m^{3}K; pentane-water) and slightly high compared to that of Goodwin et al. [5] (3-8 kW/m^{3}K; pentane-water). The differences possibly arise from many reasons. Firstly is the method of testing, Blaire et al.[3], Sideman and Gat [4] and Goodwin et al. [5], inject the refigerant into the continuous flow of water (Figure 7) while the present experiment uses the stagnant water (no flow). In the previous studies, the water temperature is

nearly constant while the water temperature in our experiment continually decreases. Moreover, in the previous works, there are no data on the temperature difference of the dispersed and continuous phases. From Equation 6, if this temperature difference is smaller, higher volumetric heat transfer coefficient is obtained.

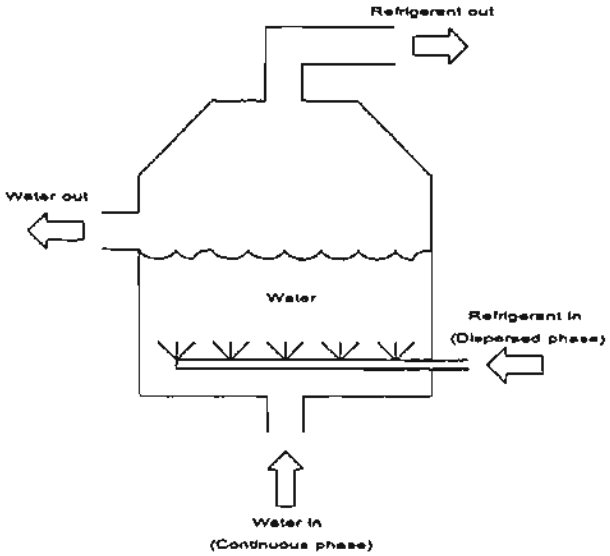

Figure 7 The direct contact heat exchange technique with dispersed and continuous phase.

The second reason is the effect of the size of the storage tank. Table 2 shows the comparison of the testing conditions from our study with the other researchers. The storage tank diameters (or the tank capacities) of Blair et al. [3] and Sideman and Gat [4] are smaller compared to the present study and that of Goodwin et al. [5]. From Equation 6, the value of water in a storage tank plays an important role to the volumetric heat transfer coefficient. Lower amount of water in the tank will get higher volumetric heat transfer coefficient. This is the reason why the volumetric heat transfer coefficient of our study and Goodwin et al. [5] are lower than those of Blair et al. [3] and Sideman and Gat [4].

Table 2 Comparison of working conditions of direct contact heat transfer systems.

	Present study	Sideman and Gat	Blair et al.	Goodwin et al.
U_v (kW/m^{3}K)	2-16, 2-52	180	122	3-8
Dispersed phase	R12, R22	pentane	R113	pentane
Mass flow rate of dispersed phase (kg/s)	0.02-0.08	0.022	0.023	1.90
Mass flow rate of continuous phase (kg/min)	-	0.042	0.101	17.1
Diameter of storage tank (m)	0.30	0.07	0.095	0.61

Heat Transfer Correlation of the Direct Contact Evaporator

The parameters affecting the heat transfer of the direct contact evaporator could be grouped into the dimensionless parameters which could be listed in terms of Stanton number, Stephan number and Prandtl number, where

$$St = \frac{U_v V}{(\dot{m} Cp)_r}, \qquad [7]$$

$$Ste = \frac{Cp_w (T_w - T_n)}{\lambda_w}, \qquad [8]$$

$$Pr = \left(\frac{Cp\mu}{k}\right)_r. \qquad [9]$$

St is Stanton number, *Ste* is Stephan number and *Pr* is Prandtl number. The dimensionless group could be expressed as

$$St = f\left(Ste\ Pr^{0.25}\left(\frac{p}{Pa}\right)^{-1}\right). \qquad [10]$$

Note that P/Pa is the pressure ratio of the pressure in the storage tank and that of the surrounding ambient.

Figure 8 shows the relation of the dimensionless parameters when using R12 and R22. St increases when $StePr^{0.25}(P/Pa)^{-1}$ is decreased. Lower Ste means the temperature difference (T_w-T_{ri}) is reduced which results in higher values of U_v and St. The values of U_v and St are very high when the water temperature is close to the freezing point. Lower the value of P results in lower the refrigerant temperature then there is a bigger difference between the water and the refrigerant temperatures thus higher heat transfer is obtained.

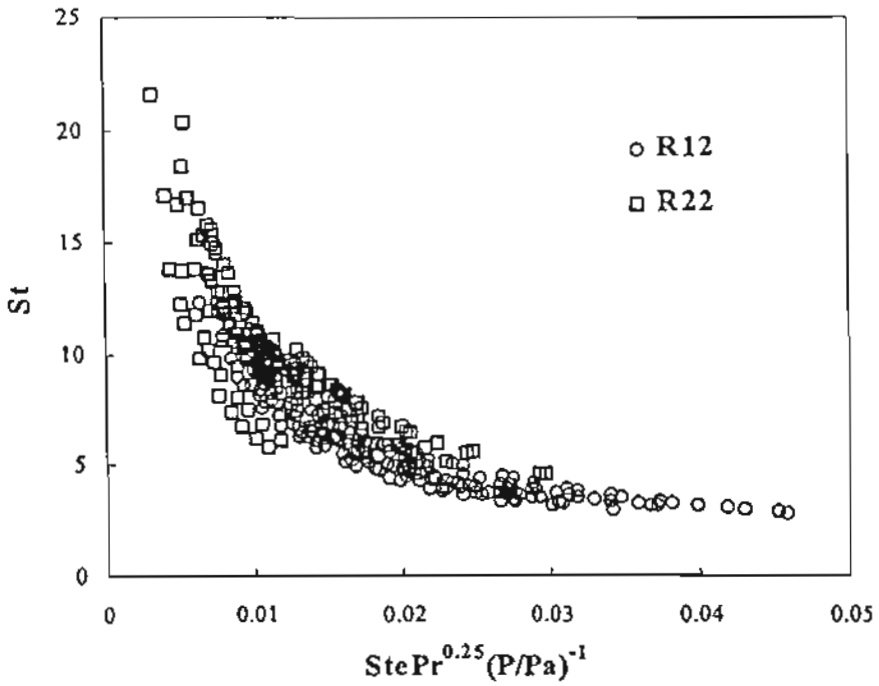

Figure 8 The relation of the dimensionless parameters.

By fitting all the experimental data the dimensionless group could be expressed as

$$St = 0.1967\left(Ste\ Pr^{0.25}\left(\frac{P}{Pa}\right)^{-1}\right)^{-0.8445} \quad . \qquad [11]$$

Figure 9 also shows the comparison of the Stanton number calculated from Equation (11) and the experimental data. It is found that the model can predict the experimental data within ± 30% error.

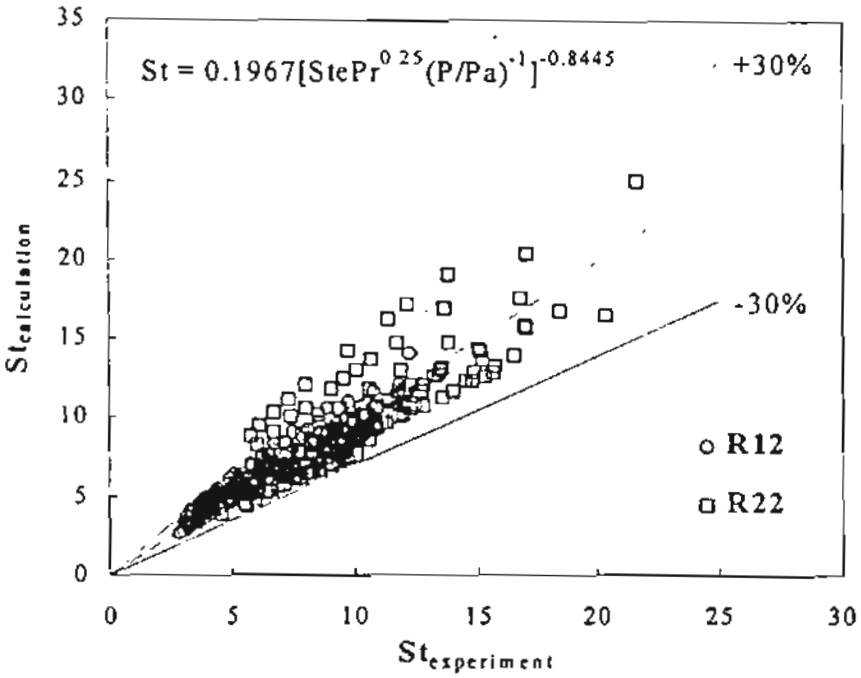

Figure 9 Comparison of *St* calculated from Equation 11 with the experimental data.

CONCLUSION

The direct contact heat transfer technique with injection of refrigerant gives high heat transfer rate. The lump model can be modified to predict the temperature of the water during the sensible heat period and the amount of ice during latent heat period. The relation of the dimensionless parameters is expressed and it can be used to predict the experimental value quite well.

Acknowledgement

The authors gratefully acknowledge the financial support provided by Thailand Research Fund (TRF) for carrying out this study. Sincere thank is also extended to Mr. Tanai Chatakanonda and Mr. Piya Na Bangchang for their valuable data.

REFERENCES

1. Electricity Generating Authority of Thailand (EGAT), Thailand power development plan PDP 1997-01, System Planing Department, Bangkok, Thailand, 1997 (in Thai).
2. Vorayos N., Development of a prototype of an ice thermal energy storage with direct contact evaporator, M.Phil. Thesis, The Joint Graduate School of Energy and Environment, King Mongkut's University of Technology Thonburi, Bangkok, Thailand, 2001.
3. Blair C.K., Boehm R. and Jacobs H., Heat transfer characteristics of a direct contact volume type boiler, ASME, 1976; 76-HT-26.
4. Sideman S. and Gat Y., Direct-contact heat transfer with change of phase: Spray column studies of a three phase heat exchanger, AIChE Journal, 1966;12(3):296-303.
5. Goodwin P., Cobin M. and Boehm R., Evaluation of the flooding limits and column, ASME National Heat Transfer Conference, Denver, 1985; 85-HT-49.
6. Subbaiyer S., Andhole T.M. and Helmer W.A., Computer simulation of a vapor-compression ice generator with direct contact evaporator, ASHRAE Transactions, 1991; Part 1(3448): 118-126.
7. Kiatsiriroat T., Na Thalang K. and Dabbhasuta S., Ice formation around a jet stream of refrigerant, Energy Conversion & Management, 2000; 41: 213-221.

8. Nuntaphan A., Performance analysis of a refrigeration cycle using a direct contact evaporator, M.Eng. Thesis, Department of Mechanical Engineering, Chiang Mai University, Chiang Mai, Thailand, 1998.

9. Chatakanonda T. and Na Bangchang P., A R22 refrigeration unit with direct contact evaporator, Senior Project, Department of Mechanical Engineering, Chiang Mai University, Chiang Mai, Thailand, 1999.

Nomenclature

A	area (m^2)
Cp	specific heat (kJ/kgK)
h	enthalpy (kJ/kg)
k	thermal conductivity (kW/mK)
m	mass (kg)
$\dot{m}$	mass flowrate (kg/s)
P	pressure (Pa)
Pa	ambient pressure (Pa)
Pr	Prandtl number
T	temperature (°C)
t	time (s)
U_v	volumetric heat transfer coefficient (kW/m^3K)
St	Stanton number
Ste	Stephan number
V	volume (m^3)

Greek symbols

λ latent heat of formation (kJ/kg)

μ dynamic viscosity (Pa.s)

Subscripts

i inlet

l liquid

o exit

r refrigerant

t storage tank

w water

Feasibility of Using Ice Thermal Energy Storage with Direct Contact Evaporator in an Office Building

T. Kiatsiriroat
Department of Mechanical Engineering
Chiang Mai University, Chiang Mai 50200, Thailand
N. Vorayos
Joint Graduate School of Energy and Environment
King Mongkut's University of Technology Thonburi
Bangkok 10140, Thailand
A. Nuntaphan
South East Asia Center for Training in Energy for Development
Electricity Generating Authority of Thailand
Mae Moh, Lampang 52220, Thailand

Abstract - In this research, an ice thermal energy storage with direct contact evaporator has been studied by applying to an office located in Chiang Mai University, Chiang Mai, Thailand. The system consists of two cycles, basic chilled water and ice storage. The mathematical models for main components composing of compressor, condenser, expansion valve, water chiller and direct contact evaporator are developed and the system simulation is created. Evidently from the results, the simulation agrees well with the experiments with 5% error. Different options of the energy storage types, full storage, partial storage and demand-limited storage, have been considered. The simulation also indicates that the demand-limited storage design system is the most appropriate storage option for the selected office. Under this operating condition, the system can shift 39.3% of peak electricity demand from on-peak period to off-peak period. Therefore, 33.8% of electricity charge is saved comparing to those of the conventional system.

Keywords: Ice thermal energy storage, direct contact heat transfer technique, system simulation, economic feasibility

Submitted to **Energy Research – The International Journal**

Address of Correspondence and Proof:
Prof. Dr. Tanongkiat Kiatsiriroat
Department of Mechanical Engineering, Faculty of Engineering,
Chiang Mai University, Chiang Mai 50200, Thailand.
Tel: 6653-944144 Fax: 6653-944145 E-mail: *tanong@dome.eng.cmu.ac.th*

1. INTRODUCTION

In tropical countries, electricity requirement is mainly caused by air conditioning system due to high ambient temperature. In Thailand, the peak electricity demand increases 12% annually and occurs during the day and in the evening [1]. Instead of constructing new power plants to meet the increment, the Electricity Generating Authority of Thailand introduces electricity tariff which charges the consumers with high premium rate for the energy consumed during the on-peak period and low rate during the off-peak period to achieve uniform load factor. Ice thermal energy storage (ITES) is an energy management technique that is becoming an attractive alternative for buildings to avoid the high electricity demand charge for space cooling. The principle of this technique is that the coolness is produced at night in form of ice stored in a well-insulated storage. The coolness could be used to supply the cooling requirement during the daytime. At present, the most common ITES systems used is the ice-on-coil storage system of which ice is formed on the surface of the cooling coil submerged in the water. There are two main problems, big space for handling the evaporator coil is needed and high thermal resistance is obtained due to the low thermal conductivity of the ice forming on the coil [2,3]. To overcome these problems, the application of direct contact heat transfer technique has been interested [4-6]. In this paper, the mathematical models of the main components and the system simulation of the ITES unit with direct contact evaporator using R12 as working fluid have been developed. The paper also investigates in the application of the system for an office in Chiang Mai, Thailand. The concentrated storage options are full storage, partial storage and demand-limited storage.

2. COOLING LOAD AND ITES CATEGORIES

The ITES system with direct contact evaporator considered in this research work is operated to support the cooling requirement of the selected office in Chiang Mai University. The cooling area of the office is 178.75 m^2 of which the cooling load profile based on the data in year1998 is shown in Fig. 1.

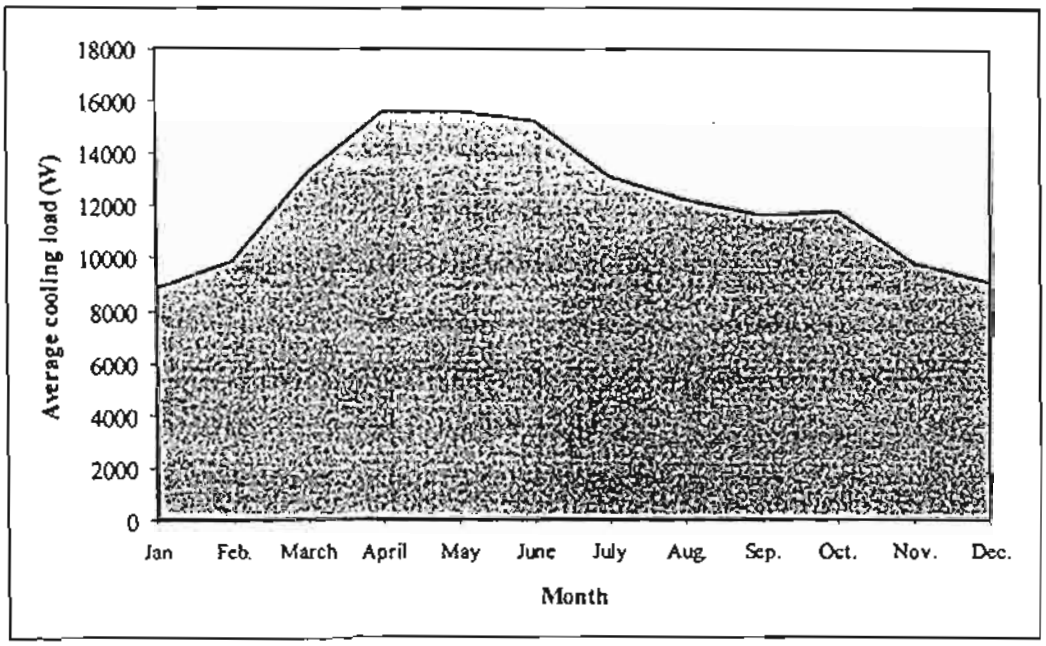

Fig. 1. The cooling load profile of the selected office during the year 1998.

The electricity consumption of the office during the year is 27163 kW-hr/year. In this case, the air conditioning system consumes 45% of total energy. Due to the load profile shown in Fig. 2, the maximum energy demand is 24.7 kW. It includes 9.7 kW of the electricity demand for cooling system and 15 kW for other purposes. The electricity tariff used to calculate the electricity charge of the office or TOU rate is given in Table 1[1].

Table 1. Electricity cost (TOU Rate)

Demand Charge (Baht/kW)	Energy Charge (Baht/kW-hr)			Service Charge (Baht/month)
1*	1*	2*	3*	
102.80	1.5349	0.6671	0.6062	400

1*	Monday – Saturday	09.00 – 22.00 (On-peak)
2*	Monday – Saturday	22.00 – 09.00 (Off-peak)
3*	Sunday	00.00 – 24.00 (Off-peak)

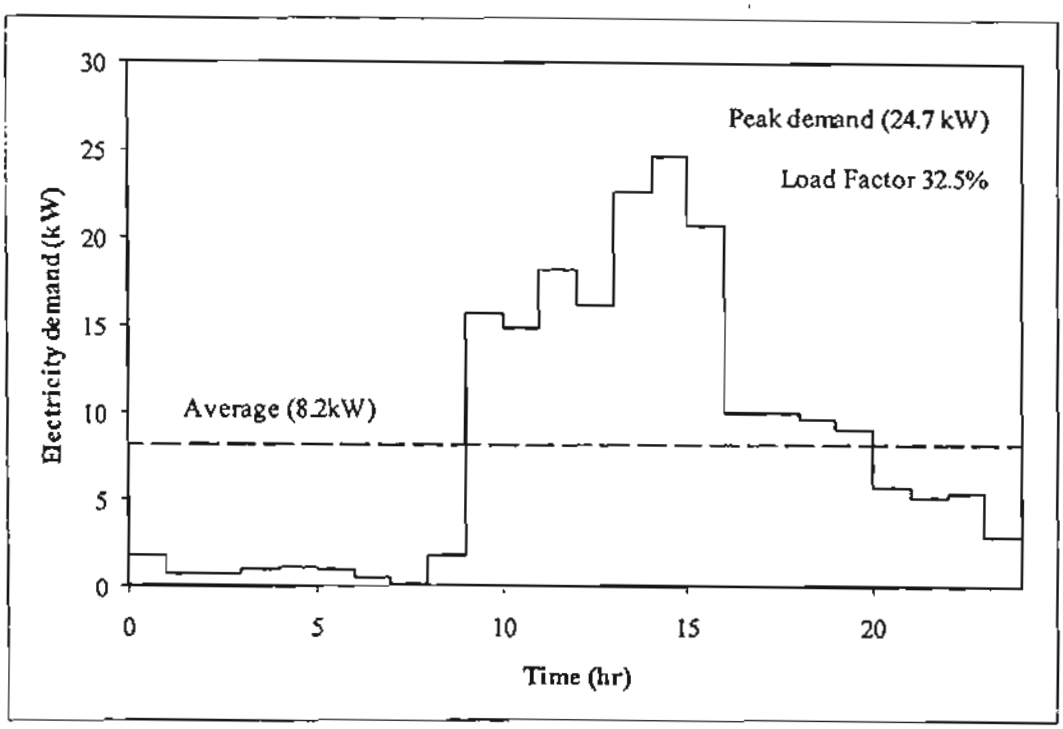

Fig. 2. The profile of electricity demand of the office during the design day.

To find out the appropriate storage option, different ITES designs have been investigated which are as follows:

Category 1. Conventional design (no ice storage). The entire cooling load requirement of the office is supported by a chilled water system operating during the occupancy period.

Categories 2-5. Partial storage design. The cooling load is divided into two parts. The first part called the base load which is supported by the chiller unit during the occupancy time and the excess is supported by the ice in storage tank produced by an ITES system operating during the nighttime. The portion of the base load for the categories 2-5 are 75%, 60%, 40% and 20%, respectively.

Categories 6. Demand-limited storage design. The peak electricity demand of the office is limited at 15 kW. In this category, the chilled water system runs during the occupancy period except the hours that the total electricity demand of the office reaches the limited value.

Category 7. Full storage design. The entire cooling load requirement is supported by the ice storage system. The chiller unit is not provided in this case.

3. THE ICE THERMAL ENERGY STORAGE CYCLES

The space cooling of the office is normally supported by a conventional chiller unit of about 5 TR (18 kW). To modify the unit with the ITES system, another 2 TR (7 kW) refrigeration unit is used for the ice storage unit. The schematic diagram of the air conditioning system with the ITES unit is shown in Fig. 3.

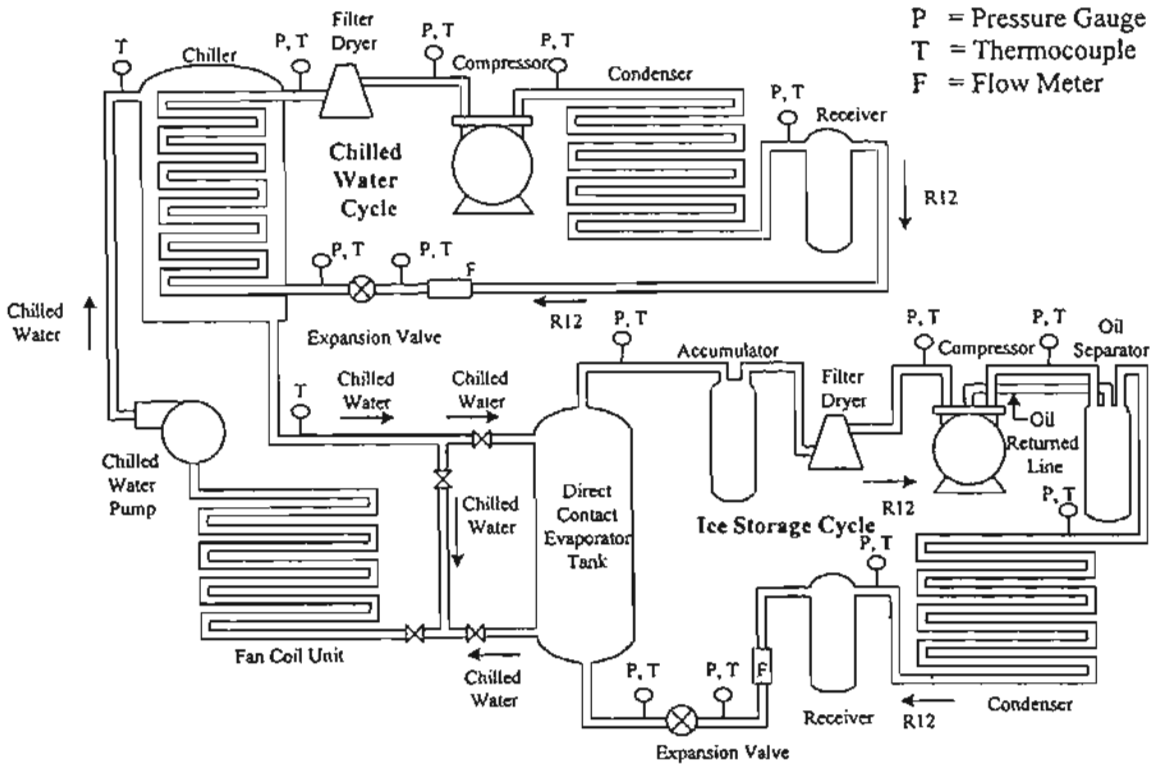

Fig. 3. Schematic diagram of the ice thermal energy storage.

The system consists of two main cycles, the ITES cycle and the chilled water cycle. During the ice formation process, the ITES cycle normally runs during the off-peak period. R12 refrigerant is injected through the expansion valve then the pressure and the temperature of R12 decrease. The low temperature R12 exchanges heat with water in the storage tank directly and it leaves the tank as vapor and turns back to the condensing unit. During the on-peak period, for partial and demand-limited storages, the base-cooling load is supported by the chilled water cycle and the excess is supported by the coolness stored in the storage tank. In case of full storage, all cooling load requirement is supported by the stored coolness.

The mathematical model of each system is separately investigated as follows:

3.1 Ice Thermal Energy Storage (ITES) System

A standard 2 TR (7 kW) open-type reciprocating compressor is used in the ice storage cycle with a direct contact evaporator. To formulate the mathematical models of the system, the refrigerant (R12) mass flow rate is varied from 0.02 – 0.09 kg/s and the compressor speed is controlled at 7.1, 9.5 and 11.8 rps. The characteristic models of main components in the system are created from the experimental data as followings:

Compressor Model

Kiatsiriroat et al. [7] generates a mathematical model of a reciprocating compressor, which is modified from Stoecker [8] as

$$\frac{P_{cp,i}}{P_{cp,o}} = f\left[\frac{m_r T_{cp,o}^{0.5}}{P_{cp,o}}, N\right], \tag{1}$$

where N is the compressor speed in rps, m_r is the refrigerant mass flow rate in kg/s, $T_{cp,o}$, $P_{cp,i}$ and $P_{cp,o}$ are outlet temperature and pressures at the inlet and outlet of the compressor in K and MPa, repectively.

The correlation can be deduced from the experimental results as

$$\frac{P_{cp,i}}{P_{cp,o}} = \left[\begin{array}{l}\left(-0.0015N^2 - 0.0087N + 0.3003\right)\left[\dfrac{m_r T_{cp,o}^{0.5}}{P_{cp,o}}\right] \\ +\left(0.0022N^2 - 0.0581N + 0.5824\right)\end{array}\right] \tag{2}$$

The pressure ratio of the compressor can be additionally calculated from

$$\frac{P_{cp,i}}{P_{cp,o}} = \left(\frac{T_{cp,i}}{T_{cp,o}}\right)^{k/(k-1)} \tag{3}$$

where k is the polytropic index depending on the refrigerant mass flow rate. The relation between the flow rate and the index can be expressed as

$$k = 1.9584\, m_r + 1.1503\,. \tag{4}$$

Condenser Model

The mathematical modeling of air-cool condenser could be modified from

$$\frac{(T_{a,o} - T_a)}{(T_{cd,i} - T_a)} = f\left[\frac{(UA)_{cd}}{m_a C_{pa}}\right] \tag{5}$$

where T_a is ambient temperature in °C, $T_{a,o}$ is the outlet air temperature in °C, $T_{cd,i}$ is inlet refrigerant temperature in °C, $(UA)_{cd}$ is overall heat transfer coefficient of condenser in kW/K, m_a is air mass flow rate in kg/s and C_{pa} is specific heat of air in kJ/kg.K.

Deduced from the experiment, the characteristic equation of the condenser can be expressed as

$$\frac{T_{a,o} - T_a}{T_{cd,i} - T_a} = \frac{0.2723(UA)_{cd}}{m_a C_{pa}} + 0.0107\,. \tag{6}$$

Expansion Valve Model

The expansion valve is operated manually to control the refrigerant mass flow rate and the pressure of the system. The relation between the pressure ratio at the valve and the refrigerant mass flow rate can be modified from

$$\frac{P_{exo}}{P_{exi}} = f(m_r, N). \tag{7}$$

where the characteristic equation can be experimentally expressed as

$$\frac{P_{ex,o}}{P_{ex,i}} = \begin{bmatrix} (1.5134N^2 - 32.0125N + 148.8285)m_r^2 \\ +(-0.1020N^2 + 2.0160N - 5.8329)m_r \\ +(0.0032N^2 - 0.0824N + 0.7113) \end{bmatrix}. \tag{8}$$

Direct Contact Evaporator Model

The mathematical model for the direct contact evaporator is formulated by a lump model [6]. Using the energy balance, the thermal characteristics of the water in the tank can be expressed as

$$\frac{d}{dt}(M_w h_w) + M_t C_t \frac{dT}{dt} = m_r(h_{ev,i} - h_{ev,o}) + (UA)(T_a - T_w). \tag{9}$$

As shown in the equation, the first three terms relate to the enthalpy change rates of the water, the container and the refrigerant, respectively. The last term relates to the external heat gain from the surrounding ambient. In this study, the direct contact evaporator is well insulated, the external heat gain then can be neglected. The water temperature of the water inside the tank changes in two steps according to two related processes, which are sensible heat process and ice formation process. The characteristic equations of the direct contact evaporator during the sensible heat process and the ice formation process can be expressed in the following equations, respectively as

$$T_w^{t+\Delta t} = T_w^t + \frac{m_r(h_{ev,i} - h_{ev,o})\Delta t}{M_t C_{pt} + M_w C_{pw}}, \tag{10}$$

and

$$M_{ice} = \frac{m_r(h_{ev,o} - h_{ev,i})\Delta t}{L}. \tag{11}$$

Due to the long length of the pipes between the evaporator unit, the compressor and the condenser, the heat gain and loss can not be ruled out. From the preliminary study, the heat gain

between the low temperature refrigerant flowing inside the pipes from the evaporator to the compressor and the surrounding ambient can be characterized as

$$m_r C_{pr}\left(T_{cp,i} - T_{ev,o}\right) = f\left(T_a - \left(\frac{T_{ev,o} + T_{cp,i}}{2}\right), m_r\right) \tag{12}$$

The equation can be expressed from the experimental results as

$$m_r C_{pr}\left(T_{cp,i} - T_{ev,o}\right) = \begin{bmatrix} \left(-0.4132m_r^2 + 0.0409m_r - 0.0012\right)\left(T_a - \left(\frac{T_{ev,o} + T_{cp,i}}{2}\right)\right)^2 \\ + \left(6.0055m_r^2 - 0.3648m_r + 0.0448\right)\left(T_a - \left(\frac{T_{ev,o} + T_{cp,i}}{2}\right)\right) \\ + \left((-38.4022)m_r^2 + 6.243m_r - 0.2699\right) \end{bmatrix}. \tag{13}$$

As the high temperature refrigerant flows through the pipe between the compressor and condenser, the heat loss occurs and can be characterized as

$$m_r C_{pr}\left(T_{cp,o} - T_{cd,i}\right) = f\left(\left(\frac{T_{cp,o} + T_{cd,i}}{2}\right) - T_a, m_r\right). \tag{14}$$

The heat loss characteristic is experimentally observed. The empirical relation between this loss and aforementioned relevant parameters is deduced as

$$m_r C_{pr}\left(T_{cp,o} - T_{cd,i}\right) = \begin{bmatrix} \left(-0.0001\right)\left(\left(\frac{T_{cp,o} + T_{cd,i}}{2}\right) - T_a\right)^2 \\ \left(1.607m_r^2 - 0.0298m_r - 0.0146\right)\left(\left(\frac{T_{cp,o} + T_{cd,i}}{2}\right) - T_a\right) \\ + \left(-20.432m_r^2 + 1.9399m_r - 0.293\right) \end{bmatrix}. \tag{15}$$

Observed from the results, there is a pressure drop across the condenser which can be expressed as

$$P_{cd,o} = P_{cd,i} - 0.034 \tag{16}$$

where $P_{cd,i}$ and $P_{cd,o}$ are the pressure at the inlet and outlet of condenser in MPa.

3.2 Chilled Water System.

A standard 5 TR (18 kW) vapor-compressor refrigeration system is simulated under steady-state conditions to produce the chilled water to support the cooling load requirement. The compressor is usually worked at constant full speed. The modeling of each main component is developed as the followings:

Compressor Model

The mathematical model of the compressor can be generated [7] as

$$\frac{P_{cp,i}}{P_{cp,o}} = f\left[\frac{m_r T_{cp,o}^{0.5}}{P_{cp,o}}, N\right], \tag{1}$$

and

$$\frac{P_{cp,i}}{P_{cp,o}} = f\left[\frac{m_r T_{cp,i}^{0.5}}{P_{cp,i}}, N\right]. \tag{17}$$

From eqs. 1 and 17, the characteristic equations of the compressor in the chilled water system can be experimentally deduced as

$$\frac{P_{cp,i}}{P_{cp,o}} = 0.0973\left(\frac{m_r T_{cp,i}^{0.5}}{P_{cp,i}}\right) + 0.0663, \tag{18}$$

and

$$\frac{P_{cp,i}}{P_{cp,o}} = 0.0873\left(\frac{m_r T_{cp,o}^{0.5}}{P_{cp,o}}\right) + 0.1088. \tag{19}$$

The relation between the refrigerant mass flow rate and the polytropic index of the compressor can be expressed as

$$k = -2.1397 m_r^2 + 0.4896 m_r + 1.1867. \tag{20}$$

Condenser Model

A shell and tube heat exchanger having circulating water as a coolant is used as a condenser to extract heat from the refrigeration system. The extracted heat is calculated from

$$Q_{cd} = m_r\left(h_{cd,i} - h_{cd,o}\right). \tag{21}$$

Q_{cd} is the rate of heat extraction in kW, m_r is refrigerant mass flow rate in kg/s and $h_{cd,i}$ and $h_{cd,o}$ are the enthalpies at the inlet and the outlet of the condenser (kJ/kg).

Expansion Valve Model

The mathematical modeling of the manual-controlled expansion valve can be modified from eq. 7 and expressed as

$$\frac{P_{ex,o}}{P_{ex,i}} = -20.114m_r^2 + 3.5432m_r + 0.1291. \tag{22}$$

Chiller Model

The water chiller used in this case is a shell-and-tube flow type of which the relevant heat transfer rate is calculated from

$$Q_{ch} = m_r\left(h_{ch,o} - h_{ch,i}\right), \tag{23}$$

or

$$Q_{ch} = m_w C_{cpw}\left(T_{w,i} - T_{w,o}\right), \tag{24}$$

and

$$Q_{ch} = (UA)_{ch}\left[\frac{\left(T_{w,i} - T_{ch,o}\right) - \left(T_{w,o} - T_{ch,i}\right)}{\ln\left[\frac{T_{w,i} - T_{ch,o}}{T_{w,o} - T_{ch,i}}\right]}\right], \tag{25}$$

where $(UA)_{ch}$ is overall heat transfer coefficient of chiller in kW/K.

It is observed that there is a pressure drop across the condenser and the chiller which can be expressed in terms of the pressure ratio as

$$\frac{P_{cp,i}}{P_{cp,o}} = 0.7733\left[\frac{P_{ex,o}}{P_{ex,i}}\right] - 0.0194. \quad (26)$$

3.3 System Simulation

With the mathematical modeling of each component in the system, the simulation is created to determine the energy consumption of the system at various possible combinations of the conventional chilled water system and the ice thermal energy storage (ITES) system. The computational steps are shown in Fig.4.

As shown in Fig.4, the simulation consists of two parts, chilled water system and ITES system. The input parameters of the simulation are the total cooling load, Q_{load}; the compressor speed of the ice storage system, N_{dc}; the mass flow rate of the refrigerant for the ice storage system, $m_{r,dc}$; the initial temperature of water in the storage tank, T_{wi}; the ambient temperature, T_{amb} and the properties of the working fluid.

The cooling load is divided to be $Q_{load,ac}$ for the chilled water system and $Q_{load,dc}$ for the ice storage system. For the chilled water system, the trial and error technique has been carried out to find the suitable mass flow rate of the refrigerant at a given cooling load and the power input of the compressor is also the output result. The equations used to calculate the properties of R12 refrigerant are [9]:

For the saturated conditions,

$$\ln(P_{sat} \times 10) = -15.6 + 8.96\left(\frac{T_{sat} + 273.15}{100}\right) - 1.038\left(\frac{T_{sat} + 273.15}{100}\right)^2 \quad (27)$$

$$h_f = -239.8 + 100.6\left(\frac{T_{sat} + 273.15}{100}\right) \quad (28)$$

$$h_g = 187.28 + 0.4722(T_{sat}) \quad (29)$$

The suffixes "*f*" and "g" refer to saturated liquid and saturated gas conditions, respectively and the suffix "*sat*" refers to saturated condition.

For superheat conditions,

$$h = 173.52 + 13.01(\ln(P \times 10)) + (0.57 + 0.0826 \ln(P \times 10))(T - T_{sat}) \qquad (30)$$

P and T are pressure and temperature in MPa and K, respectively and h is the specific enthalpy in kJ/kg.

For the ice storage part, the calculation method of each component is similar to that of the chilled water system. Note that, the refrigerant temperature leaving the ice storage tank is close to the water temperature in the tank because of high turbulence due to the refrigerant injection. When the temperature of water is higher than the freezing point, the calculation is in sensible heat mode. As the water temperature is the same as the freezing point, the latent heat mode is applied. The outputs of this part are the power consumption at the compressor, the heat transfer rate of the direct contact evaporator and the time consumed for producing ice.

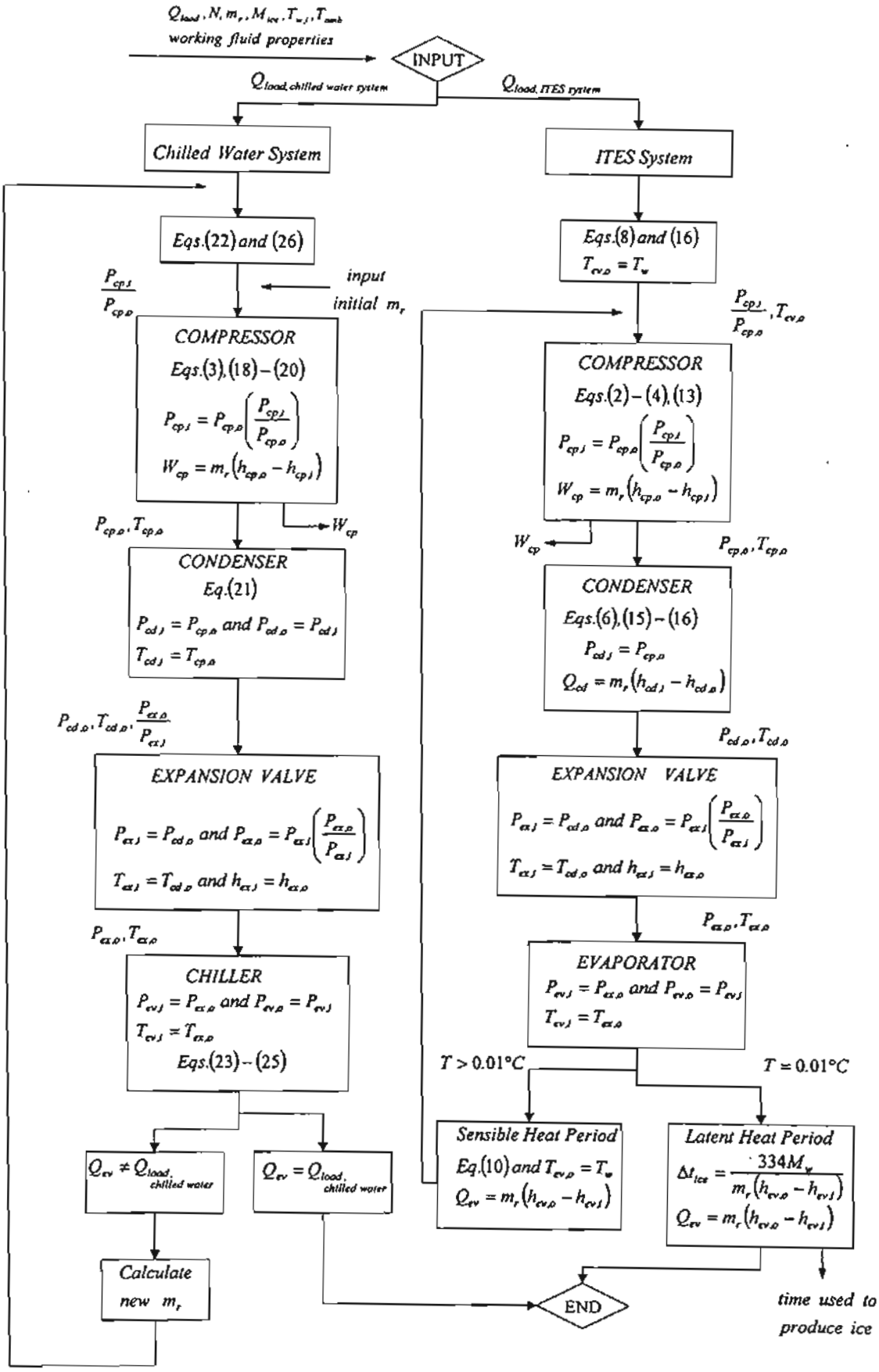

Fig. 4. Information flow diagram of the system simulation.

3.4 Simulation Results

Chilled Water System

With a given cooling load, and ambient temperature, the compressor work of the chilled-water system could be evaluated. The results from the simulation are compared to those of the experiments as illustrated in Fig. 5.

It is noted that the values from the simulation program are close to the experimental results within 5% error.

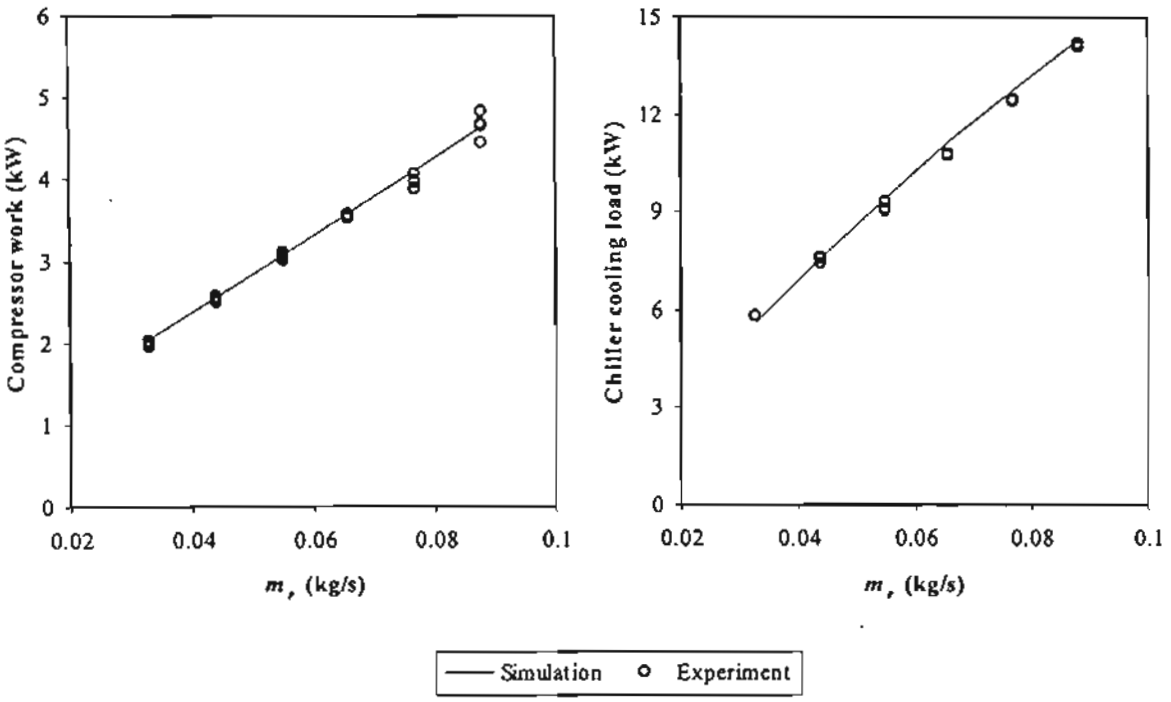

Fig. 5. Compression work and cooling load of the chilled-water system.

ITES System

(a) Ice formation process

For the ice storage simulation, the compressor work, the heat transfer rate at the direct contact evaporator the time used to produce ice and the amount of ice are evaluated. Fig. 6 shows the results of the compression work and the cooling capacity in the direct contact evaporator. The simulated results are in good agreement with those of the experiments within 5 % error.

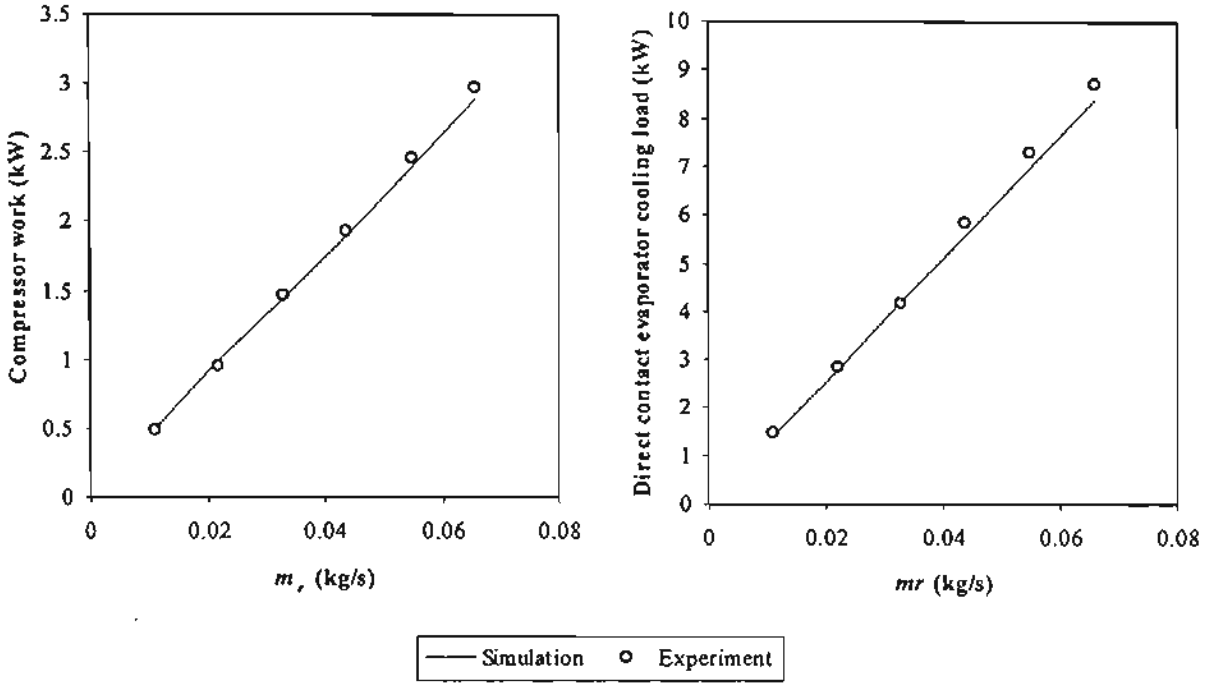

Fig. 6. Compression work and evaporator cooling load of the ITES system.

Table 2 shows the time used to generate ice and the amount of ice formed in the evaporator-storage tank. The results agree quite well with those of the experiments.

Table 2.The amount of ice formed and time used.

Mass of water in storage tank (kg)	m_r (kg/s)	N (rps)	Initial water temp. (°C)	T_{amb} (°C)	Produced ice (kg) (sim.)	Time (hr) (sim.)	Produced ice (kg) (exp.)	Time (hr) (exp.)
250	0.077	11.8	18.0	29.2	250	3.66	212	3.59
250	0.100	11.8	16.5	30.2	250	3.11	209	3.23
300	0.066	11.8	15.0	28.5	300	5.01	272	4.98
300	0.100	11.8	15.4	26.8	300	3.67	269	3.62

(b) Use of ice storage for cooling

To verify the system performance when the coolness stored in the form of ice is used for space cooling, 200 kg of ice is generated and kept in the storage tank. The ITES unit is now working with the main chilled water cycle. The base load is supported by the chilled-water cycle and the excess is supported by the ITES. Fig. 7 shows the simulated results and those from the experiments. Both agree quite well.

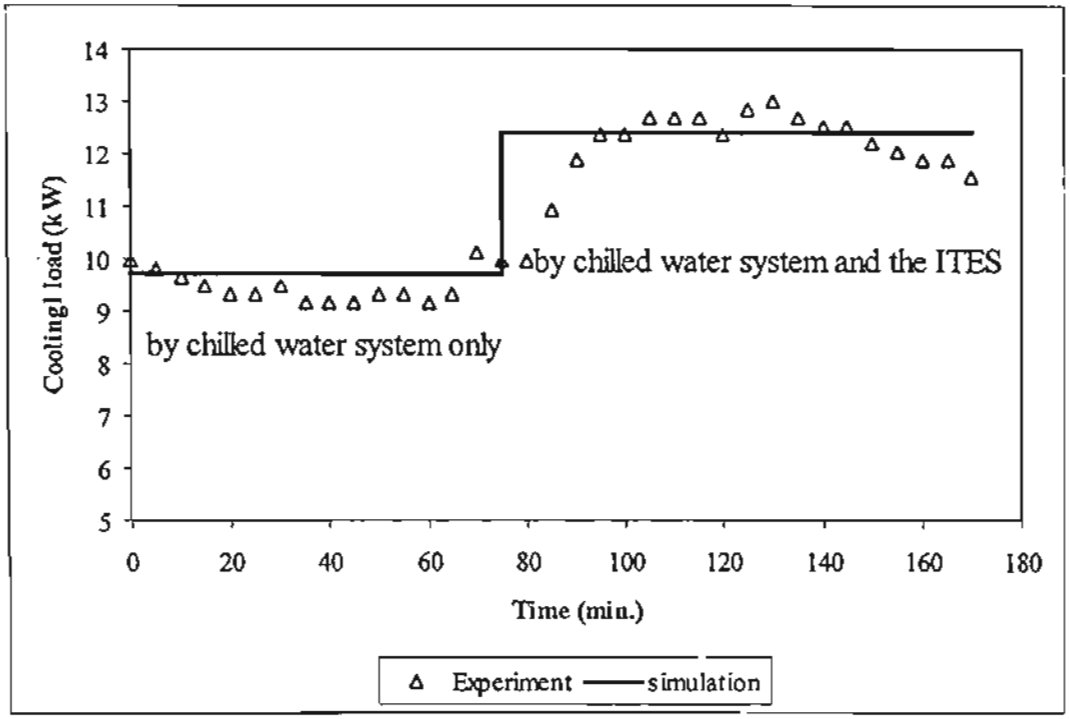

Fig. 7. Use of ice storage for cooling.

4.5 System Performance

In this section, the system performance is simulated to find out the appropriate working conditions. The results are illustrated in Figs. 8 and 9. As the refrigerant mass flow rate is varied for both cycles, the coefficient of performance (COP) of the chilled water system increases with the refrigerant mass flow rates. The highest value of COP is about 3.1 which is obtained when the refrigerant mass flow rate is about 0.08 kg/s and after that the COP slightly decreases. For the ice storage cycle, the cycle COP also depends on the compressor speed. Lower the compressor speed results in higher the COP. However, However, there is a limitation. The low compressor speed will shift the condensing temperature down. In the case of 7.1 rps compressor speed, the condensing temperature is approximately 21°C which is lower than the

average ambient temperature in Thailand, thus, 7.1 rps of the compressor speed is not acceptable. The refrigerant mass flow rate affects only slightly in the COP for higher compressor speed. The results are shown in Fig. 9.

To operate the appropriate conditions of chilled water cycle and the ice storage cycle, the recommended refrigerant mass flow rates are 0.07 – 0.09 kg/s for chilled water system and 0.08 – 0.09 kg/s which causes a short period of time to produce ice in the ITES. The compressor speed for the ITES system should be 9.5 rps due to the high value of COP.

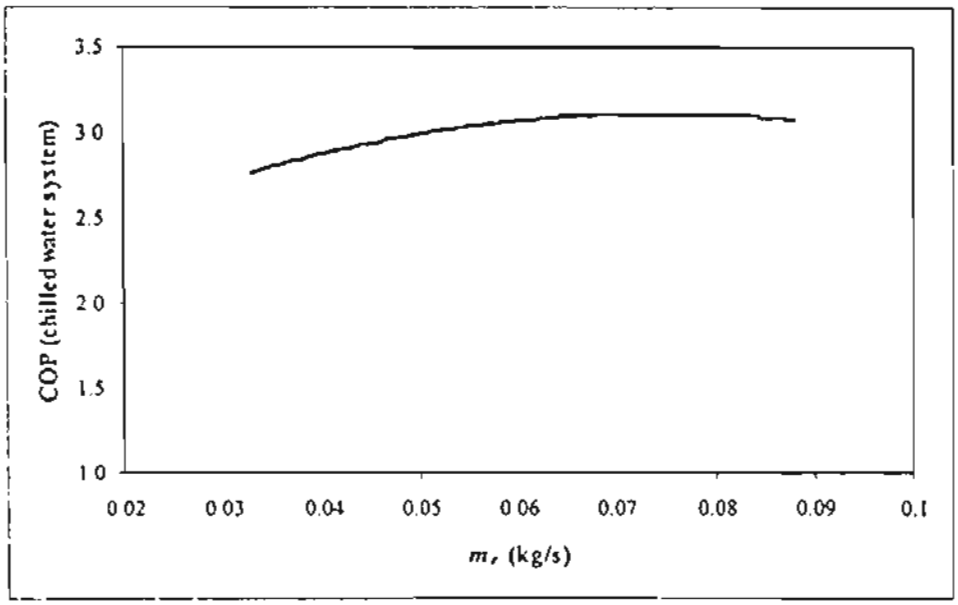

Fig. 8. COP of the chilled water system.

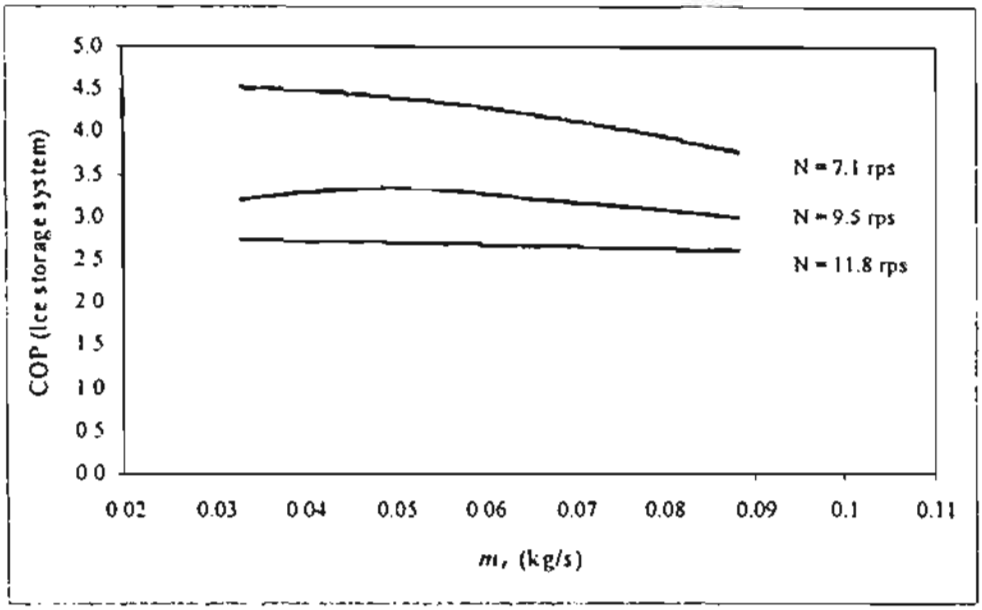

Fig. 9. COP of the ice storage system.

4. APPROPRIATE DESIGN OF THE ITES

In this section, the peak electrical energy demand (kW), energy consumption (kW-hr) and the electricity charge (Baht) for air conditioning system of each category are considered under the assumptions that

(1) The ice storage system is operated at 0.088 kg/s of refrigerant mass flow rate and 9.5 rps of compressor speed.

(2) The sufficient amount of the ice is produced and completely used in each day.

(3) The chilled water cycle is operated at full compressor speed. The refrigerant mass flow rate of the cycle is varied from 0.03 – 0.09 kg/s to support the base cooling load in each case.

The peak energy demand of the air conditioning system during on-peak period as shown in Table 3 is decreased when using the ITES unit assisted with the chilled-water cycle. As the cooling load is more supported by the ITES cycle, the peak energy demand is more reduced.

For categories 5 and 7, the time required for generating ice is longer than that of the off-peak period, therefore there is a load due to the compression mode of ITES cycle added up in the on-peak period. Higher energy consumptions are obtained compared with the conventional system(category 1).

Table 4 shows the electrical energy consumption of the air conditioning system in each category. Comparing to the conventional system (category: no storage), even the total energy consumed is nearly the same or higher, the energy consumed in the chilled-water system operating during the daytime is reduced by shifting the cooling load to the ITES system operating in the nighttime. The load factor will be more uniform.

Table 3. The peak energy demand at various categories on the design day.

Category	Peak energy demand caused by cooling and non-cooling system					Total peak demand of the office (kW)
	Chilled water system (kW)		ITES system (kW)		Non-cooling system (kW)	
	Off-peak (8 a.m. – 9 a.m.)	On-peak (9 a.m.- 5 p.m.)	Off-peak (10 p.m. – 8 a.m.)	On-peak	On-peak (1 p.m. – 4 p.m.)	On-peak (1 p.m. – 4 p.m.)
1	9.7	9.7	0	0	15	24.7
2	7.0	7.0	3.7	0	15	22.0
3	5.3	5.3	3.7	0	15	20.3
4	3.8	3.8	3.7	0	15	18.8
5	2.2	2.2	3.7	3.7 (8 am. – 9 a.m.)	15	17.2
6	3.3	3.3 (9 a.m.- 1 p.m.)	3.7	0	15	15.0
7	0	0	3.7	3.7 (8 a.m. – 10 a.m.)	15	15.0

Table 4. Energy consumed in air conditioning system during the year in each category.

Category	Energy consumption (kW-hr)		
	Chilled water system	ITES system	Total
1 (no storage)	13044.17	0	13044.17
2 (partial design, 25%)	12469.53	610.17	13079.71
3 (partial design, 40%)	10695.55	2965.58	13661.13
4 (partial design, 60%)	7838.09	7157.28	14995.37
5 (partial design, 80%)	4625.70	12152.30	16778.00
6 (demand-limited)	7046.39	6322.71	13369.10
7 (full storage)	0	16371.63	16371.63

The electricity charges of the office in both of the cooling system and non-cooling system are shown in Table 5. They includes the charge counted on the average maximum electricity used in kW over 15 minutes in each month (demand charge), the charge counted on the total amount of power consumed in kW-hr during each month (energy charge) and the service charge as shown in Table 1. As the peak demand reduced and the cooling load is more supported by the ITES system during the off-peak period, the demand charge and the energy charge of the office are reduced. However, due to the overlapped compressor load of the ITES in the on-peak period in the case of categories 5 and 7, the energy charge of the office is slightly increased. The load does not occur at the same time as the peak demand of the office, therefore, there is no effect on the demand charge.

The lowest total charge is obtained when the ITES system is designed as demand-limited in category 6.

Table 5. Electricity charge during the year in each category

Category	Electricity charge (Baht/year)			Total (Baht/year)
	Demand charge	Energy charge	Service charge	
1 (no storage)	30469.9	27301.1	4800	62571.0
2 (partial design, 25%)	27139.2	26878.4	4800	58817.6
3 (partial design, 40%)	25042.1	25579.0	4800	55421.1
4 (partial design, 60%)	23191.7	23750.9	4800	51742.6
5 (partial design, 80%)	21966.4	25782.2	4800	52548.6
6 (demand-limited)	18504.0	18099.1	4800	41403.1
7 (full storage)	18504.0	26297.88	4800	49703.4

The feasibility of using the ITES system with direct contact evaporator in this work is based on an adequate economic return of each storage option (partial, demand-limited and full storage) which has different investment and the maintenance costs. The profit of the ITES system is the decreased electricity charge comparing to the conventional system (1st category). The total electricity charges of all categories are also shown in Fig. 10. The payback periods of the ITES system of all categories are shown in Table 7. The discount rate is assumed to be 8% annually with 2.5% inflation. The most appropriate ITES in this study is the demand-limited storage design of which the limited peak demand is equal to maximum non-cooling demand of the office. In this case, the peak demand during the daytime from 24.7 kW in case of the conventional system could be reduced to 15 kW (39.3% decreased). The electricity charge of the office is reduced from 62,571 baht/year for conventional system to 41,403 baht/year resulting in 33.8% reduction. The payback period is 4.8 years which is the lowest in all categories.

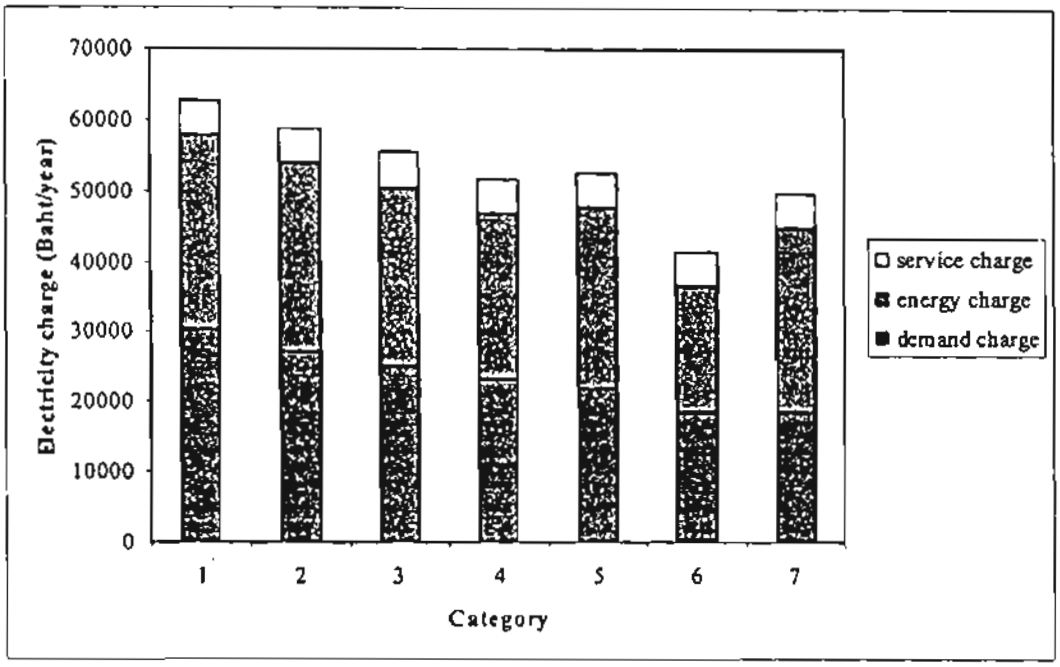

Fig. 10. Electricity charge during the year in each category.

Table 6. Incremental investment cost of the ITES system

Component Lists	Cost (Baht)
Compressor	15,000
Condensing unit	10,000
Direct contact evaporator tank	35,000
Nozzle	3,000
Compressor control motor	5,000
Piping and accessories for full storage design	3,000
Piping and accessories for partial storage design	3,500
Piping and accessories for demand-limited design	6,500
Control circuit for full storage design	1,500
Control circuit for partial storage design	2,500
Control circuit for demand-limited storage design	5,000
Salvage value of the conventional system for full storage design	-3,000
Total (full storage design)	69,500
Total (partial storage design)	74,000
Total (demand-limited storage design)	79,500

Table 7. Payback period of the ITES system at various categories.

Category	Incremental investment cost (Baht)	Decreasing electricity cost including maintenance cost (Baht/year)	Payback period (years)
1	0	0	0
2	74000	1753	More than 20 yrs.
3	74000	5150	More than 20 yrs.
4	74000	8828	11.4
5	74000	8022	13.1
6	79500	19168	4.8
7	69500	12970	6.0

CONCLUSION

The mathematical models of the main components in both of the chilled water system and the ice thermal energy storage with direct contact evaporator are formulated at various mass flow rates and compressor speed and the system performance has been simulated. The estimated values from the simulation program are in good agreement to the experimental results. The results from the simulation shows that the appropriate storage option of the ITES system for the selected office located in Chiang Mai University is the demand-limited design which could reduce the peak electricity demand of the office from 24.7 kW to 15 kW. The electricity charge of the office is also reduced from 62,571 baht/year for conventional system to 41,403 baht/year with the payback period is less than 5 years.

Acknowledgement – The authors gratefully acknowledge the support provided by Thailand Research Fund and the Joint Graduate School of Energy and Environment for carrying out this study.

REFERENCES

1. Electricity Generating Authority of Thailand (EGAT) (1997), *Thailand power development plan PDP 1997-01*. System Planning Department. Bangkok, Thailand.
2. Subbaiyer, S., Andhole, T.M. and Helmer, W.A. (1991), Computer Simulation of a Vapor-Compression Ice Generator with a Direct Contact Evaporator, *ASHRAE Transactions*, part 1, pp. 118-126, paper number 3448.
3. Wendland, R.M. (1990), Commercial Cool Storage, *Energy Engineering*, Vol. 87, No. 6, pp. 18-22.
4. Kiatsiriroat, T. and Maneechote, T. (1996). Formation and Melting of Ice with Direct contact Heat Exchange, paper presented in the *Tri-University International Joint Seminar & Symposium*, Jianxu University of Science & Technology, China.
5. Chatakanonda, T. and Na Bangchang, P. (1998), *A R22 Refrigeration Unit with Direct Contact Evaporator*. Senior Project, Mechanical Engineering, Chiang Mai University, Thailand.
6. Kiatsiriroat, T., Siriplubpla P. and Nuntaphan, A. (1998), Performance Analysis of a Refrigeration Cycle Using a Direct Contact Evaporator, *International Journal of Energy Research*, 22, pp. 1179-1190.
7. Kiatsiriroat, T., Chowcheun, K. and Wibulswas, P. (1994), Simulation of Standard Vapor Compression System, *ASEAN Journal on Science & Technology for Development*, 11(1), pp. 167-180.
8. Stoecker, W.F. (1982). *Refrigerant and Air Conditioning*. McGraw-Hill Book Company, New York, USA.
9. Mayhew, Y.R. and Rogers, G.F.C. (1972). *Thermodynamic and Transport Properties of Fluids*, Basil Blackwell, Oxford, U.K.

NOMENCLATURES

C_P	specific heat capacity (kJ/kgK)
h	specific enthalpy (kJ/kg)
k	polytropic index
L	latent heat (kJ/kgK)
m	mass flow rate (kg/s)
M	mass (kg)
N	compressor speed (rps)
P	pressure (MPa)
Q	heat transfer rate (kW)
T	temperature (°C)
Δt	period of time (s)
UA	overall heat transfer coefficient (kW/K)

Subscripts

a	air
amb	ambient
cd	condenser
ch	chiller
cp	compressor
ev	evaporator
ex	expansion valve
i	inlet
o	outlet
r	refrigerant
w	water

OUTPUT OF THE STUDY

1. Two Master Theses entitled:
    - An Ice Storage System Using a Direct Contact Evaporator for an Air – Conditioned Room, M.Eng Thesis, Department of Mechanical engineering, Chiang Mai University, 2000.
    - Development of a prototype of an ice thermal energy storage with direct contact evaporator, M.Phil Thesis, Joint Graduate School of Energy and Environment (JGSEE), King Mongkut's University of Technology, 2000.

2. Three published papers:
    - Energy Analysis of an Ice Thermal Energy Storage Prototype with Direct Contact Evaporator, Energy-The International Journal, Submitted.
    - Heat Transfer Model of a Direct a Direct Contact Evaporator, Applied Energy, Submitted.
    - Feasibility of Using Ice Thermal Energy Storage with Direct Contact Evaporator in an Office Building, Energy Research-The International Journal, Submitted.